DSPACE

https://dspace.org/

Vertical tropospheric ozone structure and associated atmospheric transport over the South African Highveld region

Phahlane,Agnes Ngwanakgari.

2008-08-29T07:59:52Z
http://hdl.handle.net/10539/5578

Downloaded from a DSpace repository. https://dspace.org/



VERTICAL TROPOSPHERIC OZONE STRUCTURE AND ASSOCIATED ATMOSPHERIC TRANSPORT OVER THE SOUTH AFRICAN HIGHVELD REGION

School of Geography, Archaeology and Environmental Studies

Climatology Research Group

Student Number: 0218515T

Ngwanakgari Agnes Phahlane

A dissertation submitted to
the Faculty of Science, University of the Witwatersrand,
in fulfilment of the requirements
for the degree of
Master of Science in Environmental Sciences

March, 2008

ABSTRACT

Tropospheric ozone plays an important role in the atmosphere especially towards climate change and air quality. In this study, characteristics of tropospheric ozone over the South African Highveld are investigated using the ozonesonde data collected at Irene weather station (25.9°S, 28.2°E, and 1523 m asl) for the period 1990 to 1993 and 1999 to 2003. It was found that synoptic systems have an effect on the vertical distribution of tropospheric ozone. Ozone stratification appeared during anticyclonic conditions as displayed by a continental high ozone profile. During the ridging high, low ozone concentrations are observed with a strong ozone gradient between 10 and 12 km. Ozone enhancement appeared in the lower altitudes, <4 km, in both the ridging high and the westerly disturbance ozone profiles. Ozone profiles exhibited higher ozone concentrations during the westerly wave conditions. Tropospheric ozone over the South African Highveld region follows a clear annual cycle with lower ozone concentrations observed during autumn and higher ozone concentrations during spring. Summer ozone profiles had high ozone concentrations from the earth's surface up to 9 km compared to winter ozone profiles. However, winter ozone profiles exhibited higher ozone concentrations than summer ozone profiles and they were characterised by a strong ozone gradient at 12 km. Ozone profiles obtained during the Southern African Fire-Atmosphere Research Initiative conducted in 1992 (SAFARI-92) displayed lower ozone concentrations than ozone profiles from the Southern African Regional Science Initiative conducted during 2000 (SAFARI-2000). Therefore, it is apparent tropospheric ozone over the South African Highveld has increased over the past decade.

KEY WORDS:

Anticyclonic, atmospheric, concentration, continental, enhancement, Highveld, ozonesonde, photochemical, profile, trajectories, tropospheric, tropopause, stratosphere, synoptic, systems.

DECLARATION

I declare that this dissertation is my own, unaided work except where acknowledged. It is being submitted for the Degree of Master of Science in the University of the Witwatersrand, Johannesburg. It has not been submitted before for any degree or examination in any other University.

_____

Ngwanakgari Agnes Phahlane

March 2008

Psalm 37:4-5

Take delight in the Lord, and He will give you your heart's desires.
Commit everything you do to the Lord.
Trust Him, and He will help you.

PREFACE

The work described in this thesis forms part of the World Meteorological Organisation (WMO) Global Atmosphere Watch (GAW) programme in ozone measurements at the South African Weather Service. The ozonesonde programme was initiated for the first time in 1990 and formed part of the Southern African Fire-Atmosphere Research Initiative conducted during 1992 (SAFARI-92). The ozonesonde programme was terminated in early 1994 and reinstated in November 1998 as part of the National Aeronautics and Space Administration (NASA) Southern Hemisphere ADditional Ozonesondes (SHADOZ) programme, with Dr Anne Thompson as the principal investigator. The ozonesonde programme also formed part of the Southern African Regional Science Initiative conducted during 2000 (SAFARI-2000) field campaign. Ozone ascents have been launched at Irene weather station (25.9°S, 28.2°E, and 1523 m asl) fortnightly since 1998. The trajectory analysis results used in this research were obtained from SHADOZ deduced from the kinematic trajectory model.

The aim of this research study is to characterise and define vertical distribution of ozone over the South African Highveld, and to establish the source of tropospheric ozone over this region, with the following goals:

(a) To determine the vertical tropospheric ozone behaviour over the South African Highveld.

(b) To establish the effects of synoptic circulations on the vertical structure of tropospheric ozone over this region.

(c) To investigate the temporal and seasonal variations of ozone over the South African Highveld.

The thesis is divided into six chapters. **Chapter 1** consists of detailed background information regarding tropospheric ozone. **Chapter 2** contains a description of ozonesonde data, tropopause data and methods used to analyse the data, including a kinematic trajectory model. **Chapter 3** presents ozone vertical structures that occurred over the South African Highveld determined from Self-Organising Maps analysis. In **Chapter 4**, the effects of synoptic systems on ozone vertical distribution are discussed; and evidence supporting the temporal and seasonal changes of tropospheric ozone over the South African Highveld is presented. **Chapter 5** consists of a summary and discussion around the findings of this research study. The main findings of the research are highlighted in **Chapter 6**.

ACKNOWLEDGEMENTS

- My supervisor, Dr Stuart Piketh for his guidance, support and above all for his patience and time to make this possible.
- Dr A M Thompson, for her guidance in this study.
- Ms J C Witte, for the trajectory analysis available on the SHADOZ website.
- Mr G J R Coetzee, D J Esterhuyse for their understanding and support and for their assistance in launching the ozone ascents for my research.
- Irene weather station observers, for their help when needed during the launching of the ozonesondes.
- Dr W J Tennant, for supplying the model for the Self-Organising Maps and for his assistance in using it.
- All my colleagues and friends, for their support in one way or the other, especially Ms Modjadji and Ms Ndabambi of the South African Weather Service for administrative assistance.
- South African Weather Service for financial support and the opportunity to study.
- My family, especially my mom and my brother, for the guidance, love and support they have always shown me during my studies.
- Given, my husband, and my kids – Palesa, Naledi and Itumeleng – thank you for your love, patience and support during my studies.
- Jeannette Menasce is acknowledged for her assistance in proof-reading and correcting this research report.

CONTENTS

ABSTRACT ..... **i**

KEY WORDS: ..... **ii**

DECLARATION ..... **iii**

PREFACE ..... **v**

ACKNOWLEDGEMENTS ..... **vii**

CONTENTS ..... **viii**

LIST OF FIGURES ..... **xi**

LIST OF TABLES ..... **xv**

ABBREVIATIONS, ACRONYMS AND GLOSSARY ..... **xvi**

CHAPTER 1: OVERVIEW **1**

Introduction **1**

Literature Review **3**

- **Ozone in the atmosphere** **3**
  The importance of ozone in the troposphere *4*
- **Origin of tropospheric ozone** **5**
  Tropospheric ozone chemistry *6*
  Stratospheric-tropospheric exchange *8*
- **Definition of tropopause height** **11**
- **Transport of air over southern Africa** **14**
  Types of synoptic systems *14*
  Air transports associated with synoptic fields over southern Africa *16*
  Vertical structure of the atmosphere over southern Africa *18*
- **Classification of ozone profiles** **20**
- **Objectives of this study** **23**

CHAPTER 2: DATA AND METHODOLOGY 25

Ozonesondes 25

- **Electrochemical concentration cells 26**
  Calculation of ozone concentration 30
- **Uncertainties regarding the electrochemical concentration cell ozonesonde 32**
  Background current 32
  Pump efficiency correction 32
- **SAFARI-92 and SAFARI-2000 ozonesonde data 33**
- **Tropopause height data 34**
- **Meteorological synoptic systems 38**
- **Self-Organising Maps 39**
- **Kinematic trajectory analysis 41**

CHAPTER 3: CLASSIFICATION OF TROPOSPHERIC OZONE PROFILES OVER THE SOUTH AFRICAN HIGHVELD REGION 45

Investigation of Tropospheric Ozone Patterns 45

- **Classification of ozone profiles using Self-Organising Maps 46**
- **Results from the Self-Organising Maps 49**
  Group (a) 49
  Group (b) 52
  Group (c) 54
  Group (d) 56
  Group (e) 58
  Group (f) 60

CHAPTER 4: CHARACTERISATION OF TROPOSPHERIC OZONE OVER THE SOUTH AFRICAN HIGHVELD 64

The Effects of Synoptic Systems on the Vertical Distribution of Ozone 64

Ozone profiles associated with continental high systems 67
Ozone profiles associated with ridging high systems 69

Ozone profiles associated with westerly disturbance systems *71*

Ozone profiles associated with easterly wave systems *73*

- **Vertical tropospheric ozone structures over the South African Highveld** **75**
- **Comparison with TWINSPAN and SPSS derived vertical ozone structures.** **81**
- **Tropopause height variations and ozone distribution in the upper troposphere** **87**
- **Seasonal variability of tropospheric ozone over the South African Highveld** **89**

Seasonal variations of tropospheric ozone at different altitudes *94*

- **Temporal variations of tropospheric ozone** **97**

CHAPTER 5: SUMMARY **99**

Vertical Tropospheric Ozone Distribution over the South African Highveld **99**

Low-level enhancement ozone profile *100*

Westerly disturbance ozone profile *100*

Uniformly enhanced ozone profile *101*

Ridging high ozone profile *102*

Easterly wave ozone profile *103*

Continental high ozone profile *103*

Seasonal and Temporal Variations of Ozone over the South African Highveld **104**

CHAPTER 6: CONCLUSIONS **106**

Vertical Distribution of Tropospheric Ozone over the South African Highveld **106**

Effects of Synoptic Systems on the Vertical Distribution of Ozone **107**

Seasonal and Temporal Ozone Changes over the South African Highveld **107**

REFERENCES 110

LIST OF FIGURES

Figure 1.1: Dynamical aspects of stratosphere-troposphere exchange 10

Figure 1.2: Major circulation types affecting southern Africa and their frequency of occurrence over the period 1988-1992 (bottom right) 15

Figure 1.3: Major transport associated with different circulation types over southern Africa 17

Figure 1.4: Occurrence of absolutely stable layers 19

Figure 1.5: Ozone profiles classified using aircraft data from the MOZAIC campaign over Johannesburg 22

Figure 2.1: Balloon-borne ECC ozone sensor 27

Figure 2.2: Detailed construction of the ECC ozone sensor 27

Figure 2.3: An example of a temperature profile displaying a tropopause height over Irene weather station 35

Figure 2.4: Occurrence frequencies of the first thermal tropopause height over the South African Highveld..... 36

Figure 2.5: Occurrence frequencies of the second thermal tropopause height over the South African Highveld..... 37

Figure 2.6: Seasonal variability of the first and second tropopauses over the South African Highveld..... 37

Figure 2.7: A typical example of a synoptic chart at 850 hPa on 11 October 2000 from Irene weather office. 38

Figure 2.8: SOM training procedure 39

Figure 2.9: The three dimensional grid cube, showing the parcel position 43

Figure 3.1: Six tropospheric ozone profiles classified by SOMs for the period 1990 to 1993..... 47

Figure 3.2: Six tropospheric ozone profiles classified by SOMs for the period 1999 to 2003 48

Figure 3.3: Average ozone profiles and trajectories of Group (a) for the periods 1990 to 1993, and 1999 to 2003 51

Figure 3.4: Average ozone profiles and trajectories of Group (b) for the periods 1990 to 1993, and 1999 to 2003 53

Figure 3.5: Average ozone profiles and trajectories of Group (c) for the periods 1990 to 1993, and 1999 to 2003 55

Figure 3.6: Average ozone profiles and trajectories of Group (d) for the periods 1990 to 1993, and 1999 to 2003 57

Figure 3.7: Average ozone profiles and trajectories of Group (e) for the periods 1990 to 1993, and 1999 to 2003 59

Figure 3.8: Average ozone profiles and trajectories of Group (f) for the periods 1990 to 1993, and 1999 to 2003 61

Figure 3.9: Typical ozone structures normally observed from the two data sets, as identified by SOMs 62

Figure 4.1: Frequencies of occurrence of meteorological fields during the ozone ascents launch, for the period 1990 to 1993 66

Figure 4.2: Frequencies of occurrence of meteorological fields during the ozone ascents launch, for the period 1999 to 2003 66

Figure 4.3: Average ozone profiles corresponding to continental high conditions and trajectories for the periods 1990 to 1993, and 1999 to 2003 68

Figure 4.4: Average ozone profiles corresponding to a ridging high conditions and trajectories for the periods 1990 to 1993, and 1999 to 2003 70

Figure 4.5: Average ozone profiles corresponding to westerly disturbance conditions and trajectories for the periods 1990 to 1993, and 1999 to 2003 72

Figure 4.6: Average ozone profiles corresponding to easterly wave conditions and trajectories for the periods 1990 to 1993, and 1999 to 2003 74

Figure 4.7: Vertical ozone profiles (a) identified by SOMs (b) westerly disturbance associated ozone profile 76

Figure 4.8: Vertical ozone profiles (a) identified by SOMs (b) associated with the ridging high system 77

Figure 4.9: Vertical ozone structures (a) identified by SOMs (b) associated with the easterly wave system 78

Figure 4.10: (a) and (b) Vertical ozone structures identified by SOMs, and (c) continental high associated ozone profile 79

Figure 4.11: Vertical tropospheric ozone structures over the South African Highveld derived from SOMs and synoptic systems 80

Figure 4.12: Vertical ozone profiles (a) identified by SOMs (b) TWINSPAN (Diab *et al*., 2003) 81

Figure 4.13: Vertical ozone profiles (a) identified by SOMs (b) TWINSPAN (Diab *et al*., 2003) and (c) SPSS (Diab *et al*., 2004) 83

Figure 4.14: Vertical ozone profiles (a) associated with the ridging high system (b) SPSS (Diab *et al*., 2004) 84

Figure 4.15: Vertical ozone profiles (a) identified by SOMs (b) TWINSPAN (Diab *et al*., 2003) and (c) SPSS (Diab *et al*., 2004) 85

Figure 4.16: Vertical ozone structures (a) Continental high profile (b) Westerly wave profile 86

Figure 4.17: Occurrence frequencies of the tropopause heights below and above average value (~15.8 km) over the South African Highveld region 88

Figure 4.18: Average ozone profiles associated with the tropopause below and above average value (~15.8 km) over the South African Highveld region 88

Figure 4.19: Seasonally averaged tropospheric ozone profile and average relative humidity over the South African Highveld for 1990 to 1993 92

Figure 4.20: Seasonally averaged tropospheric ozone profile and average relative humidity over the South African Highveld for 1999 to 2003 93

Figure 4.21: Seasonal variation of tropospheric ozone at different altitudes for the period 1990 to 1993 95

Figure 4.22: Seasonal variation of tropospheric ozone at different altitudes for the period 1999 to 2003 96

Figure 4.23: Average tropospheric ozone profiles during SAFARI-92 and SAFARI-2000 97

LIST OF TABLES

Table 2.1: Preparation of ECC sensor solutions 28

Table 4.1: The number of synoptic systems occurred during the study periods 65

ABBREVIATIONS, ACRONYMS AND GLOSSARY

ECC(s)	Electrochemical Concentration Cell(s)
GAW	Global Atmosphere Watch
hPa	hectopascal
MOZAIC	Measurements of Ozone and Water Vapour by Airbus In-service AirCraft
mPa	millipascal
NASA	National Aeronautics and Space Administration
NCEP	National Centre for Environmental Prediction
NOAA	National Oceanic and Atmospheric Administration
ppbv	parts per billion by volume
PUV	Potential Vorticity Units
SAFARI-92	Southern African Fire-Atmosphere Research Initiative conducted during 1992
SAFARI-2000	Southern African Regional Science Initiative conducted during 2000
SAST	South African Standard Time
SHADOZ	Southern Hemisphere ADditional Ozonesondes
SOM(s)	Self-Organising Map(s)
SPSS	Statistical Package for the Social Science
TWINSPAN	Two Way Indicator Species Analysis
UT	Universal Time
WMO	World Meteorological Organisation

CHAPTER 1:
OVERVIEW

Characteristics of tropospheric ozone, including photochemical production, vertical distribution, and the importance of tropospheric ozone in the atmosphere are described in detail in this chapter. The contribution of stratospheric tropospheric exchange and transport of trace gases from polluted areas to tropospheric ozone budget is discussed. The research goals are outlined.

Introduction

Since the industrialisation, atmospheric ozone has changed from being of interest to only a small scientific group to becoming a global issue of concern because of the increase in chemical constituents including trace gases and ozone precursor gases in the atmosphere from anthropogenic activities (WMO, 1995; Crutzen and Zimmermann, 1991). Atmospheric ozone occurs in varying concentrations from the troposphere to the stratosphere, with ~90% located in the stratosphere where it acts as a blanket to protect the biosphere against harmful ultraviolet radiation (Crutzen *et al*., 1999). The remaining 10% is contained in the troposphere, which is the main focus of this research study.

The production of tropospheric ozone depends primarily on the availability of ozone precursor gases (such as carbon monoxide, methane, oxides of nitrogen, and non-methane hydrocarbons) (Crutzen and Zimmermann, 1991; Kleinman, 2005). Ozone results from photochemical reactions involving these trace gases, therefore the increase in ozone precursor gases result in high photochemical production of tropospheric ozone (Kleinman, 2005; Fishman *et al*., 1979; Crutzen and

Zimmermann, 1991; Crutzen *et al*., 1999; Collins *et al*., 2000; Lelieveld and Dentener, 2000). The increase in tropospheric ozone poses an environmental threat as ozone is a reactive gas that is dangerous to life on earth and contributes to climate forcing (Thompson *et al*., 1997; Leung *et al*., 2004). The South African Highveld, in particular, has the largest number of industrial sources of ozone precursor gases leading to a possible increase of tropospheric ozone production which, as a pollutant, has all the above detrimental effects (Diab *et al*., 2004).

Apart from being a greenhouse gas, tropospheric ozone is required for the production of the hydroxyl radical, which is the most important oxidising agent in the troposphere (Fishman *et al.*, 1979; Crutzen and Zimmermann, 1991; Crutzen *et al*., 1999). The removal rate of atmospheric gases – including greenhouse gases – is regulated by the oxidation capacity of the troposphere, hence contributing to a change in climate (Staehelin *et al*., 2001; Levy, 1972).

Tropospheric ozone over the South African Highveld follows an annual cycle exhibiting a minimum in autumn and a maximum in spring (Thompson *et al*., 1996a). The enhanced ozone concentrations observed during spring coincide with southern Africa's burning season which normally occurs from May to October (Scholes *et al*., 1996, Le Canut *et al*., 1996). During SAFARI-92, scientific investigations found that ~50 % of atmospheric sources of gases (such as hydrocarbons, carbon monoxide, oxides of nitrogen and ozone precursor gases) came from biomass burning (Lacaux *et al*., 1996; Shea *et al*., 1996; Ward *et al*., 1996; Harris *et al.,* 1996). However, it was established that tropospheric ozone variations over the South African Highveld are controlled by both tropical and mid-latitude influences because of its southerly location, and the influence of biomass burning is less compared with other stations on the southern Africa subcontinent (Diab *et al*., 2004).

This study focuses mainly on the vertical structure of tropospheric ozone over the South African Highveld using ozonesonde data collected from the Irene weather

station (25.9°S, 28.2°E, 1523 m asl) for the periods 1990 to 1993 and 1999 to 2003. In addition, an investigation is made on the changes in tropospheric ozone structure due to meteorological phenomena. Analysis of backward trajectories is undertaken to determine the origin of air masses reaching the South African Highveld affecting the concentrations of tropospheric ozone. Data collected during two field campaigns – SAFARI-92 and SAFARI-2000 – are used to investigate temporal variations of tropospheric ozone over this region and lastly; the climatological vertical structure of tropospheric ozone over the South African Highveld is established.

Literature Review

Ozone in the atmosphere

Ozone is one of the atmospheric trace gases showing a large amount of temporal and spatial variation (Collins *et al*., 2000). The amount of ozone in the troposphere at an individual site is influenced by several factors including transport processes (such as advection, convection and dispersion); stratosphere-troposphere exchange; deposition to the earth's surface, and photochemical production and destruction within the troposphere (Collins *et al.*, 2000; Fishman *et al*., 1979; Junge, 1962).

Temporal variation of tropospheric ozone concentration is related to day-to-day variation of the boundary layer, which influences the vertical distribution of trace gases (Zhang and Rao, 1999). Ozone formed in the boundary layer is transported into the free troposphere by convective processes or by turbulent mixing processes (Fishman *et al*., 1992). During the night, due to radiative cooling, a stable layer near the ground is formed (Zhang and Rao, 1999). When the sun rises and starts to heat the earth's surface, convective processes break down the stratification, releasing pollutants which lead to the rapid change in concentration and mixture of pollutants at ground level (Zhang and Rao, 1999; O'Hare, 1997). These pollutants that are produced or emitted at the boundary layer can be transported upward into the middle and upper troposphere by deep convection (Thompson *et al.*, 1997) changing the

chemical composition of the gases throughout the troposphere. Unlike any other pollutants, tropospheric ozone is not directly emitted from sources, but rather is a by-product of a complex set of photochemical reactions involving sunlight and various precursor emissions such as carbon monoxide, methane, oxides of nitrogen and volatile organic compounds (Crutzen and Zimmermann, 1991; Crutzen *et al*., 1999; Collins *et al*., 2000; Lelieveld and Dentener, 2000). Hence its concentration at a particular location depends on the availability of the ozone precursor gases which are mainly trace gases emitted from natural and man-made processes (Black, 1989; Kleinman, 2005).

Meteorological conditions favouring the long-range transport and accumulation of trace gases have previously been investigated. For example, Merrill and Moody (1996) suggested that meteorological phenomena play an important role in the chemistry of atmospheric gases. Transport of these atmospheric constituents depends on the lifetime of that particular substance. Ozone has an atmospheric lifetime of a few weeks in the free troposphere, as compared to the boundary layer where its lifetime is a few days or less (Watson *et al.*, 1990, Fishman *et al.*, 1992). Therefore, tropospheric ozone as a secondary pollutant can be transported thousands of kilometres by the prevailing upper-air winds from source regions (Fishman *et al*., 1991). Therefore using transport information, the chemistry and distribution of tropospheric ozone at any location can be explained (Thompson *et al.*, 2001).

The importance of ozone in the troposphere

Although only a small amount of ozone is contained in the troposphere, it is an important greenhouse gas. Greenhouse gases include gases such as carbon dioxide, methane, nitrous oxide, ozone, and chlorofluorocarbons. As the amount of energy radiated from the sun to the earth's surface equals the amount of energy radiated back into space, greenhouse gases absorb thermal infrared radiation emitted by the earth's surface and the atmosphere, trapping heat and keeping the lower atmosphere warm.

Therefore an increase in tropospheric ozone is crucial because of its contribution to energy balance and its linkage to climate change (Staehelin *et al.*, 2001).

Ozone is important in the troposphere during the production of hydroxyl radicals (Fishman *et al.*, 1979; Levy, 1972). The absorption of solar ultraviolet radiation of wavelengths shorter than ~310 nm (hν) by ozone generates an excited O (^{1}D) atom (Crutzen and Zimmermann, 1991; Crutzen *et al*., 1999). The radical photochemistry involves the destruction of ozone through the following equations (Levy, 1972):

$$O_3 + h\nu \rightarrow O_2 + O\ (^1D) \qquad 1.1$$

The high energy atoms react with water vapour producing hydroxyl radicals

$$O\ (^1D) + H_2O \rightarrow 2\ OH^- \qquad 1.2$$

The hydroxyl radicals determine the oxidising capacity of the troposphere, which controls the tropospheric lifetime of many important greenhouse gases that are emitted into the atmosphere at the earth's surface by natural processes or human activities (Levy, 1972, 1973; Staehelin *et al.*, 2001; Crutzen *et al*., 1999). The main gases which normally react with hydroxyl radicals to produce ozone or to regenerate the hydroxyl radicals are carbon monoxide, methane, and methane oxidation products (Crutzen *et al*., 1999). Therefore, tropospheric ozone is regarded as the major source for hydroxyl radicals in the troposphere, affecting the oxidising capacity of the troposphere, hence controlling the atmospheric cycle of some trace gases released into the atmosphere (Crutzen and Zimmermann, 1991).

Origin of tropospheric ozone

Junge (1962) suggested that the transfer of stratospheric ozone downward into the troposphere was the primary source of tropospheric ozone. However, it was later discovered that most of stratospheric ozone transported into the troposphere is

destroyed when reaching the earth's surface (Fishman and Crutzen, 1978). The input of ozone from the stratosphere is important in the upper levels of the troposphere where ozone plays a crucial role as a greenhouse gas (Collins *et al*., 2003). Therefore, photochemical processes are regarded as important sources of ozone in the troposphere (Fishman *et al*., 1979).

Photochemical production of tropospheric ozone depends on the availability of ozone precursor gases from biogenic emissions, pyrogenic emissions and anthropogenic activities (Kleinman, 2005). Biogenic emissions include hydrocarbons, carbon monoxide, carbon dioxide, nitrogen oxide, and dinitrogen oxide; pyrogenic emissions are associated with biomass burning such as savannah fires, forest fires, agricultural waste combustion, and domestic biofuel combustion (Otter *et al.*, 2001; Marufu *et al.*, 2000). The use of motor vehicles is one of the anthropogenic activities contributing to the concentrations of the precursor emissions by releasing substances such as nitrogen oxides, and volatile organic compounds (Black, 1989).

Tropospheric ozone chemistry

Equations 1.1 to 1.9 describe the production of ozone in the troposphere (Fishman and Crutzen, 1978; Fishman *et al*., 1979; Crutzen *et al.,* 1999; Crutzen and Zimmermann, 1991).

Naturally, ozone is formed by the reaction of atomic oxygen (O) and molecular oxygen (O_2) in the presence of sunlight ($h\nu$). In Equation 1.1 solar ultraviolet radiation of wavelength 340 nm dissociates ozone into atomic oxygen and molecular oxygen. Some of the excited O atoms produced in Equation 1.1 are deactivated to ground-state O atoms, which again form ozone:

$$O + O_2 \rightarrow O_3 + M \qquad 1.3$$

where M is the third body required to carry away the energy released during the reaction. The remaining O atoms have enough energy to react with water vapour to produce hydroxyl radicals as in Equation 1.2.

The hydroxyl radicals can initiate the reaction, leading to either the formation or destruction of ozone, by reacting with a trace gas (such as carbon monoxide, methane or non-methane hydrocarbons) in the presence of oxides of nitrogen or ozone itself:

For example, carbon monoxide (CO) is oxidised by the hydroxyl (OH^-) radical:

$$CO + OH^- \rightarrow CO_2 + H \qquad 1.4$$

$$H + O_2 + M \rightarrow HO_2 + M \qquad 1.5$$

Then HO_2 radicals react with NO:

$$HO_2 + NO \rightarrow OH^- + NO_2 \qquad 1.6$$

followed by

$$NO_2 + h\nu \rightarrow NO + O \qquad 1.7$$

and

$$O + O_2 + M \rightarrow O_3 + M \qquad 1.8$$

with the net result:

$$CO + 2O_2 \rightarrow CO_2 + O_3 \qquad 1.9$$

The net production of ozone strongly depends on the concentration of nitrogen oxides which are emitted mainly from anthropogenic sources – including burning of fossil

fuels and biomass burning (Crutzen *et al*., 1999). In an environment where the concentrations of nitrogen oxide and nitrogen dioxide are low, Equation 1.6 can compete with Equation 1.10:

$$HO_2 + O_3 \rightarrow OH^- + 2O_2 \qquad 1.10$$

leading to the destruction of ozone molecules with the net result:

$$CO + O_3 \rightarrow CO_2 + O_2 \qquad 1.11$$

Hydroxyl radicals can also react with methane in the production of ozone but at a slower rate (Liu *et al*., 1987).

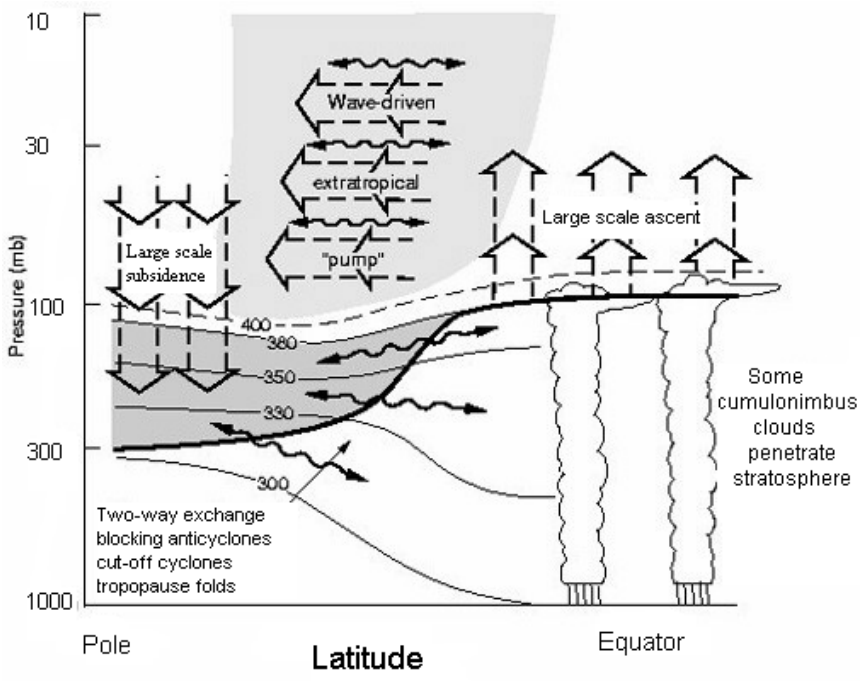
Stratospheric-tropospheric exchange

Although photochemical production of tropospheric ozone has increased due to enhanced emissions of ozone precursor gases, input from the stratosphere is still a significant source of tropospheric ozone (Collins *et al*., 2003) and the same author established that ~40 % of tropospheric ozone originated from the stratosphere. The airflow between the stratosphere and the troposphere is the key component that controls the concentrations and distribution of ozone, water vapour and other compounds, and determines the chemical composition of both stratosphere and troposphere (Appenzeller and Davies, 1992; Seo and Bowman, 2001; Kentarchos and Roelofs, 2003; Cristofanelli *et al.*, 2003, James *et al*., 2003a). Stratospheric-tropospheric exchange of air mass has been discussed for more than three decades, but it is still uncertain as to how this contributes to the tropospheric ozone budget (Kentarchos and Roelofs, 2003; Stohl *et al*., 2003). Stratospheric air has higher potential vorticity and ozone compared to the troposphere, therefore understanding the exchange of air mass between the two layers will improve knowledge of the tropospheric ozone budget (Ancellet *et al.*, 1994; Seo and Bowman, 2001). Upward air transfer from the troposphere to the stratosphere is at a maximum in mid-autumn

and minimum in late spring or early summer in both hemispheres. In contrast, downward transfer of air from the stratosphere into the troposphere is at a maximum in late spring or early summer and a minimum in autumn in both hemispheres (Seo and Bowman, 2001).

Transport of air from the stratosphere into the troposphere on a larger scale is controlled by the Brewer-Dobson circulation which is primarily driven by Rossby waves (Seo and Bowman, 2001; Collins *et al*., 2003). The Brewer-Dobson circulation can be divided into three main processes (summarised in Figure 1.1). Firstly, the rising of air in the tropics from the troposphere to the stratosphere through a Hadley cell. Secondly, whilst in the stratosphere, it is then transported towards mid-latitudes and the poles. Thirdly, in mid-latitude and polar regions, the air descends from the stratosphere into the upper levels of the troposphere where is primarily controlled by smaller-scale processes (such as cut-off low systems, and tropopause folding) (Stohl *et al*., 2003; Collins *et al*., 2003; Seo and Bowman, 2001).

Figure 1.1 illustrates the transfer of stratospheric air mass into the troposphere on a global view. The dry tropical air with low ozone concentrations is lifted from the troposphere into the stratosphere, but the lifting is slow and not all of the rising air is able to penetrate the upper stratosphere due to the high stability of the stratosphere (James *et al.*, 2003b).



Legend: The tropopause is shown by a thick line. Double-headed arrows denote transport by eddy motions including upper tropospheric troughs, and cyclones from cut-off lows.

Source: Holton *et al.* (1995:408); Stohl *et al.* (2003:STA 1-3).

Figure 1.1: Dynamical aspects of stratosphere-troposphere exchange

The uncertainties as to how the tropospheric air enters the stratosphere in the tropics are still under discussion. However, cumulonimbus anvils may penetrate the tropopause and extend well into the stratosphere, stirring up the troposphere and mixing ozone-rich air from the stratosphere and other atmospheric substances between the two layers (Price and Vaughan, 1993; Stohl *et al*., 2003). Whilst in the stratosphere, ozone-rich air is transported poleward and into the extratropics, then into the upper levels of the troposphere governed by smaller scale processes.

On a small scale, major intrusions of stratospheric air into the troposphere occur across the tropopause break during the formation of the tropopause folds associated with the synoptic Rossby wave breaking (Danielsen, 1968), cut-off low systems (Bamber *et al.*, 1984), and during the development of a low-pressure system and cold

front at ground level (Appenzeller and Davies, 1992). During tropopause folding, a channel of stratospheric air into the troposphere is made and the intrusion takes place rapidly, and the principle of dissipation makes sure that the transferred air stays longer in the troposphere (Kim *et al*., 2001; James *et al*., 2003b).

Similar processes can occur in the opposite direction, by transporting air from the troposphere to the stratosphere, but this occurs less frequently than stratosphere-to-troposphere transport (Stohl *et al*., 2003). This is because the troposphere is characterised by strong vertical mixing including convection, which controls the vertical transport of the atmospheric constituents (Staehelin *et al.*, 2001) and the stability of the stratosphere (James *et al*., 2003b).

Transfer and exchange of air containing atmospheric constituents between the troposphere and the stratosphere takes place through the tropopause, therefore clarity on the tropopause height is necessary to understand the cycling of atmospheric constituents between the troposphere and the stratosphere (Kiladis *et al*., 2001). The purpose of this study is to understand the variability of the distribution of tropospheric ozone over the South African Highveld. The definition of the tropopause height over this region is of great importance because of its impacts on the evaluation of the ozone content in the troposphere, as the tropopause generally forms a boundary between the well-mixed, ozone-poor troposphere and the ozone-rich lower stratosphere (Steinbrecht *et al*., 1998).

Definition of tropopause height

Originally, the tropopause was defined as a boundary between the ozone-rich stratosphere and the ozone-poor troposphere. This transition zone is generally marked by an abrupt change in temperature lapse rate from the turbulently mixed troposphere (when the temperature decreases with height), to the stably stratified stratosphere (with temperatures constant or increasing with height) (Hoinka, 1998; Zängl and Hoinka, 2001; Hoerling *et al.*, 1991). The tropopause is not a material, defined

surface but rather a transition layer which freely deforms and is influenced by vertical air motion and thermal advection (Kim *et al*., 2001; Gettelman and Forster, 2002). On average the tropopause height ranges between 9 km in polar regions and 16 km in the tropics (Hoinka, 1999). In order to understand the airflow processes that link the stratosphere and the troposphere, it is important to understand the temporal and spatial variations of the tropopause layer including factors that determine the physical properties of the tropopause height (Hoinka, 1999; Kiladis *et al*., 2001, Reid and Gage, 1981). The height of the tropopause depends upon the criteria used to define it (Kim *et al*., 2001). Two definitions are recognised worldwide to determine tropopause height namely, the thermal definition and the dynamical definition.

According to the WMO, "thermal tropopause" is defined as the lowest level at which the lapse rate decreases to 2°C/km or less, provided the average lapse rate between this level and all higher levels within 2 km does not exceed 2°C/km (WMO, 1986). This transition from the tropospheric lapse rate to stratospheric lapse rate occurs over a depth of several kilometres rather than occurring at a well-defined height (Bethan *et al*., 1996). In addition to the WMO definition, thermal tropopause height is expected to occur at pressures > 400 hPa or <85 hPa (Kiladis *et al.,* 2001).

The definition for "dynamical tropopause" is based on the potential vorticity, *P*, as the tropopause separates the low potential vorticity values in the troposphere from the high vorticity values in the stratosphere (Hoerling *et al*., 1991; Hoinka, 1998; Zängl and Hoinka, 2001; Kim *et al*., 2001). In isentropic coordinates, the potential vorticity is defined by using the equation:

$$P = \frac{1}{\rho}(fk + \nabla \times v).\nabla\theta$$

where

ρ	=	Density
f	=	Coriolis parameter
k	=	unit vector in the vertical
ν	=	(u, ν) horizontal wind vector
θ	=	potential temperature

Additionally, the WMO defines "dynamical tropopause" as the surface where the isentropic potential vorticity value is 1.6 Potential Vorticity Units (PVU) (where 1 PVU = 1×10^{-6} $km^2.kg^{-1}.s^{-1}$) (WMO, 1986).

However, studies comparing tropopause heights obtained from these two definitions have been undertaken and those researchers discovered that tropopause heights derived by using the WMO 1.6 PVU threshold are higher than thermal tropopause heights (Hoerling *et al*., 1991). The same authors investigated the tropopause heights using different potential vorticity thresholds and the results show that tropopause height was overestimated for values <3 PVU and underestimated for values >4 PVU. Therefore, the best agreement was set for threshold values of ~3.5 PVU, assuming positive values in the Northern hemisphere and negative values in the Southern Hemisphere (Hoinka, 1999; Hoinka, 1998).

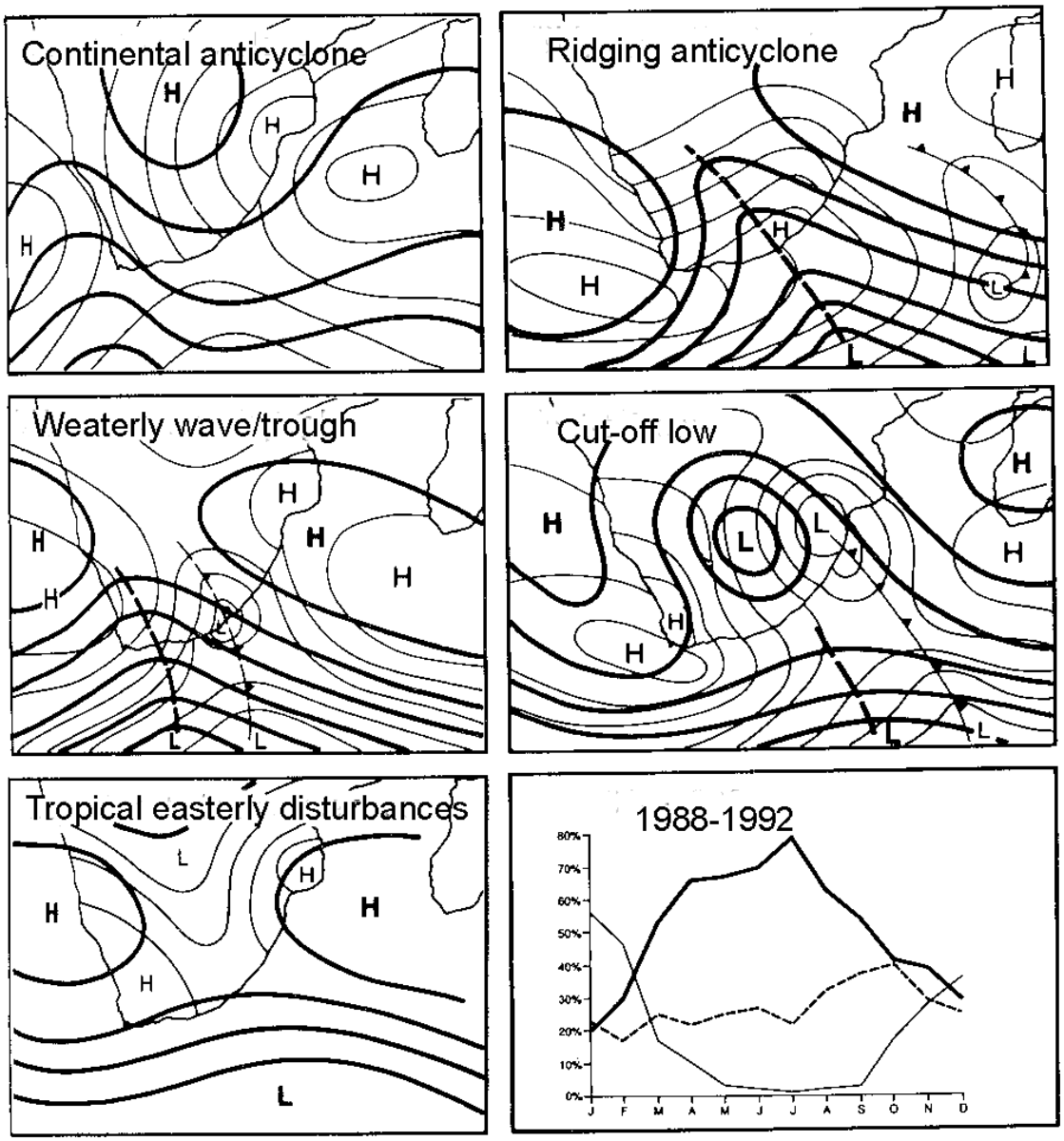
The advantage of using dynamical tropopause is that potential vorticity is unaffected by adiabatic convergence and divergence, whilst the thermal tropopause height can be determined from a single temperature profile (Bethan *et al*., 1996). Hoinka (1998), having analysed the global tropopause, suggested that for latitudes >28° dynamical tropopause should be used; for latitudes <13° the thermal definition is recommended, and for latitudes between 13° and 28° the weighted average of the dynamical and thermal tropopause heights should be considered.

Transport of air over southern Africa

Medium- to long-range transport of pollutants from elsewhere could influence the distribution and the concentrations of ozone and ozone precursor gases at an individual site (Liu *et al*., 1987; Tyson *et al*., 1996; Tyson *et al*., 1997). Thermodynamic structure of the atmosphere plays a significant role in regulating vertical mixing, whilst transport of atmospheric constituents over the subcontinent is controlled by dominant air-flow patterns (Tyson *et al*., 1997; Kirkman *et al*., 2000). In a stable atmosphere, trace gases tend to mix horizontally rather than vertically, and when the atmosphere is unstable, free vertical mixing and transport occur (Cosijn and Tyson, 1996; Zunckel *et al*., 2000).

Types of synoptic systems

Transport of air is primarily controlled by the atmospheric circulation prevailing at any one time (Preston-Whyte and Tyson, 2000). Atmospheric daily synoptic systems prevailing over southern Africa have been reviewed in detail and classified into major predominant circulation types (Garstang *et al.,* 1996; Tyson *et al.,* 1996) (Figure 1.2). These circulation types occur at different frequencies throughout the year, but southern Africa – being located in the subtropical high pressure belt – experiences a mean anticyclonic circulation at 800 hPa for much of the year (Preston-Whyte and Tyson, 1988).



Legend: Heavy lines represent conditions at 500 hPa. Light lines give surface conditions (as sea level isobars over the oceans and contours of the 850 hPa surface over the subcontinent).

Source: Tyson *et al.* (1996:268); Garstang *et al.* (1996:23723).

Figure 1.2: Major circulation types affecting southern Africa and their frequency of occurrence over the period 1988-1992 (bottom right)

Continental highs exhibit a clear annual cycle reaching a maximum in winter (June and July) with a frequency of ~70 % of days, and a minimum in summer (December and January) with a frequency of <20 %. There is little annual variation of ridging anticyclones with a frequency of occurrence of ~10 to 15 %, reaching a slight maximum during the austral spring (September and October). If both these anticyclonic conditions are grouped together, on >80 % of all days in July, a high-pressure system dominates over southern Africa (Tyson *et al*., 1996; Garstang *et al*., 1996).

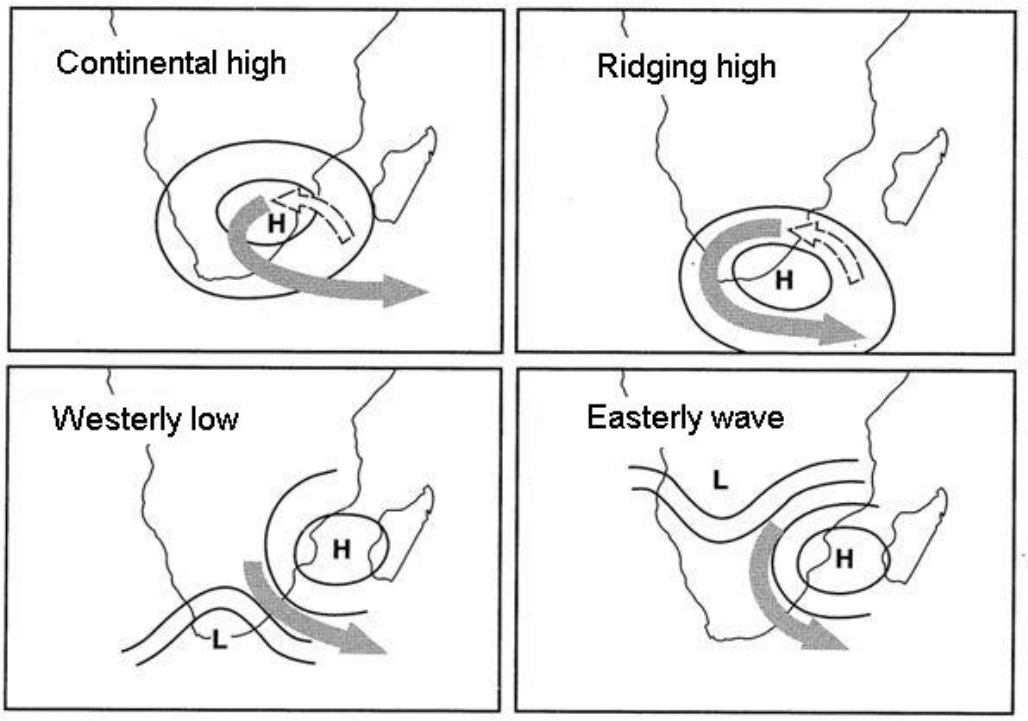
Westerly disturbances occur throughout the year, showing little seasonal variation, with a maximum frequency of occurrence of ~40 % in spring (October). Easterly waves exhibit an annual cycle, reaching a maximum in midsummer (January) with an frequency of occurrence of ~50 to 60 %, and a minimum in midwinter (July) when the daily frequency falls to <5 % (Tyson *et al*., 1996; Garstang *et al*., 1996).

Air transports associated with synoptic fields over southern Africa

Each synoptic circulation type produces different transport fields (Tyson *et al*., 1996) (Figure 1.3). Transport of trace gases and aerosols over southern Africa is primarily controlled and dominated by continental anticyclones and south Indian anticyclones (Zunckel *et al*., 2000). This does not necessarily eliminate transport modes associated with other synoptic systems, but it is because of the high frequency of occurrence of anticyclonic conditions over southern Africa for much of the year (Tyson *et al.,* 1996; Garstang *et al*., 1996; Cosijn and Tyson, 1996).

Continental high systems produce two modes of transport – the first being into the Atlantic Ocean via the Angolan plume and the second into the Indian Ocean via the Natal plume. However, ~75 % of all air is transported over the southern African subcontinent towards the Indian Ocean and beyond; whilst little air is transported over the Atlantic Ocean (Tyson *et al*., 1996; Zunckel *et al*., 2000).

The ridging high conditions favour transport primarily towards the southern Atlantic Ocean, with possible recirculation of air likely to occur as in the case of the continental high conditions. Westerly disturbances, including cut-off low systems, tend to disturb the whole troposphere, and most air is transported into mid-latitudes of the Indian Ocean with little transport over the Atlantic Ocean. When easterly waves prevail, transport of air is over the Atlantic Ocean via Angolan plume rather than over the Indian Ocean via Natal plume (Tyson *et al.,* 1996; Kirkman *et al.*, 2000; Zunckel *et al*., 2000).



Legend: Shaded arrows indicate direct transport; broken arrows show recirculation.
Source: Preston-Whyte and Tyson (2000:289).

Figure 1.3: Major transport associated with different circulation types over southern Africa

Vertical structure of the atmosphere over southern Africa

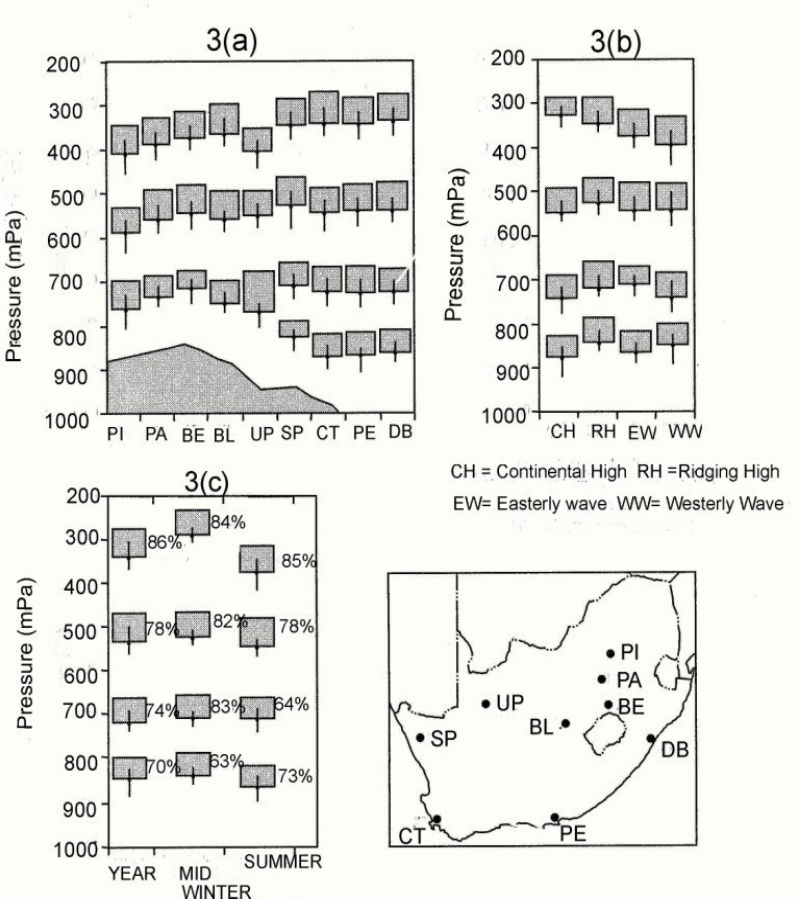
Vertical transport controls the vertical distribution of ozone and is linked to the occurrence of absolutely stable layers (Tyson *et al*., 1997). Kirkman *et al.* (2000) established from airborne ozone measurements that concentrations of ozone over southern Africa exhibit strong stratification with height, due to the presence of absolutely stable layers which prevent vertical mixing in the troposphere. The state of the atmosphere determines the residence times of atmospheric gases; therefore it is important to have a precise knowledge of the thermodynamic structure of the atmosphere to understand the chemistry of various constituents in the atmosphere (Freiman *et al*., 2002).

Anticyclonic conditions normally prevail during winter, resulting in drying and subsidence of air. The predominance of these systems increases the stability of the atmosphere which then becomes more conducive for the development of absolutely stable layers (Cosijn and Tyson, 1996). Absolutely stable layers tend to regulate vertical mixing and allow only horizontal mixing, permitting atmospheric constituents trapped below the absolutely stable layers to react photochemically and be transported away from their sources, depending on their atmospheric lifetimes (Kirkman *et al*., 2000).

Semi-permanent, absolutely stable layers (in which the lapse rate of temperature is less than the saturated adiabatic lapse rate) develop around 700, 500, and 300 hPa with an additional absolutely stable layer occurring at 850 hPa over the coastal regions (Figure 1.4).

The first layer (located at 700 hPa) is associated with the top of the mixing layer; the second layer (located at 500 hPa) is mainly associated with subsidence and has an influence on the vertical and horizontal transport of gases; whilst the third layer (located at 300 hPa) is less effective in horizontal and vertical transport of trace gases over southern Africa (Cosijn and Tyson, 1996; Kirkman *et al*., 2000, Garstang *et al*.,

1996). There are small annual variations in the base heights of absolutely stable layers at 850, 700, 500 hPa. The 700 hPa layer is frequently observed in winter. The 500 hPa layer also occurs in winter (being higher over the eastern areas); whilst in summer it is substantially higher over the western areas (Cosijn and Tyson, 1996).



Legend: (a) over South Africa (b) by circulation type and (c) by time of the year, with percentage frequencies of occurrence, and lower right: the locations of the stations used in the analyses.

Source: Preston-Whyte (2000:189).

Figure 1.4: Occurrence of absolutely stable layers

The 300 hPa layer exhibits seasonal variations in height with the highest being observed in winter and lowest in summer (Cosijn and Tyson, 1996). Absolutely stable layers are not only winter phenomena but occur on average on approximately two days out of three throughout the year. Changing circulation types during rain-free days have little effect on the location or frequency of these absolutely stable layers (Cosijn and Tyson, 1996). Only deep convection can destroy or dissipate absolutely stable layers.

Classification of ozone profiles

Analysis of MOZAIC (Measurements of Ozone and Water Vapour by Airbus In-service AirCraft) data (Diab *et al*., 2003), classified ozone profiles over Johannesburg into six (6) categories (Figure 1.5) using the cluster analysis program, TWINSPAN (Two-Way Indicator Species Analysis). The identified categories are summarised below (Diab *et al*., 2003):

Single mid-tropospheric peak: This ozone profile is characterised by low ozone concentrations near the earth's surface, with a single, well-defined ozone peak at 6 to 8 km and an average maximum of ~70 ppbv. Low ozone concentrations are attributed to the high position of the tropopause, and the convective outflow of ozone-depleted air being lifted from the boundary layer.

Steady tropospheric increase: Ozone profiles in this group occur in summer and sometimes in spring, exhibiting a general steady increase of ozone concentrations. The absence of a tropospheric ozone peak is one of the characteristics of the ozone profiles in this group.

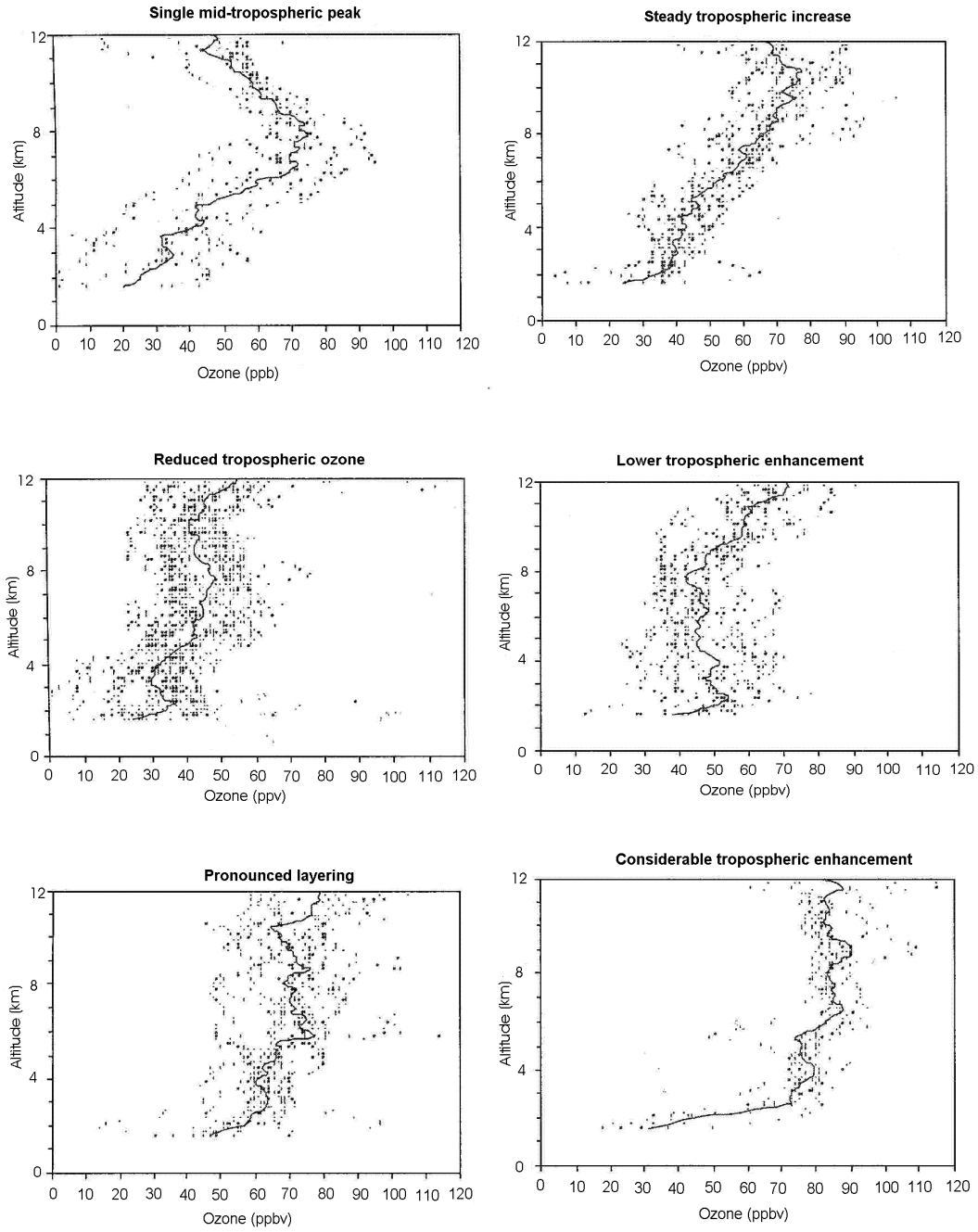
Reduced tropospheric ozone: These ozone profiles are described as having low ozone concentrations throughout the troposphere. The ozone gradient observed in the upper troposphere reflects the lower winter position of the tropopause and the possible penetration of stratospheric air to lower levels. The ozone profiles contained

in this group occur in either autumn or winter, with a mean ozone profile showing values <50 ppbv.

Lower tropospheric enhancement*:* This ozone profile is characterised by the presence of a lower tropospheric enhancement where the mean ozone concentration is >50 ppbv. The peak observed at <5 km above the earth's surface, is the result of the persistent absolutely stable layer which has the great influence on the vertical distribution of trace gases and aerosols over southern Africa (Tyson *et al.,* 1997). These ozone profiles occur in autumn or winter when the absolutely stable layer is most pronounced.

Pronounced layering: Pronounce layering was observed in the ozone profiles contained in this group differing by 50 ppbv, and ozone concentration peaks of up to 110 ppbv. These ozone profiles occur in spring when tropospheric ozone is known to be the highest (Thompson *et al.*, 1996a and Diab *et al.*, 1996).

Considerable tropospheric enhancement: This group is dominated by spring ozone profiles which are characterised by a sharp increase in ozone concentration from the earth's surface to ~2.5 km. These ozone profiles exhibit high ozone concentrations of ~80 to 100 ppbv throughout the troposphere.



Source: Diab *et al.* (2003:3716).

Figure 1.5: Ozone profiles classified using aircraft data from the MOZAIC campaign over Johannesburg

Objectives of this study

Tropospheric ozone over the South African Highveld follows a seasonal cycle displaying a maximum ozone concentration in spring and minimum ozone concentration in autumn (Thompson *et al*., 1996a). These variations of ozone concentration are due to both tropical and midlatitude influences (Diab *et al*., 2004). The possible contribution of stratospheric ozone injection into the troposphere is evident in the upper troposphere especially, during winter and spring. It is during these seasons that South Africa experiences cut-off low systems which lead to the development of tropopause folding, and triggers the transfer of ozone from the stratosphere into the troposphere (Bruintjies *et al*., 1990).

The Irene weather station (25.9°S, 28.2°E, 1523 m asl), being located in the South African Highveld region between the Pretoria and Johannesburg industrial centres, is subjected to industrial influences (Diab *et al*., 2004). The increase of emissions released into the atmosphere due to industrial activities poses an environmental hazard and contributes to climate change. The concern about the environmental issues motivated this research study. The aim of this study is to investigate vertical tropospheric ozone distribution over the South African Highveld using ozonesonde data collected at the Irene weather station. The specific goals of this research are:

(a) To determine the vertical tropospheric ozone behaviour over the South African Highveld.

(b) To establish the effects of synoptic circulations on the vertical structure of tropospheric ozone over this region.

(c) To investigate the temporal and seasonal variations of ozone over the South African Highveld.

(d) To develop the climatology of tropospheric ozone distributions over the South African Highveld.

****

Photochemical production of ozone in the troposphere from atmospheric trace gases has been discussed. A detailed description of other processes contributing to tropospheric ozone budget, vertical distribution and behaviour of tropospheric ozone over southern Africa has been given in this chapter. Typical ozone profiles observed over the South African Highveld from previous studies were outlined.

CHAPTER 2:
DATA AND METHODOLOGY

A detailed description of the ozonesonde instrument is given in this chapter. The location and the behaviour of the tropopause height over South African Highveld were investigated by using the radiosonde data. Methods used for analysing ozonesonde data, including the statistical analysis technique and trajectory model, are discussed.

Ozonesondes

Ozonesonde data used in this study were collected at Irene weather station (25.9°S, 28.2°E, and 1523 m asl) for the periods 1990 to 1993 and 1999 to 2003. Between 1990 and 1993, ozonesonde type 5A electrochemical concentration cells (ECCs) were used. Since 1999, however, ozonesonde type 6A ECCs have been used. Each ECC ozonesonde, containing a 1 % buffered potassium iodide (KI) solution, is coupled and flown with a standard meteorological Vaisala RS 80 radiosonde through an electronic interface (Komhyr and Harris, 1971). Ozone concentrations – as well as meteorological parameters such as atmospheric pressure, temperature, and relative humidity – are recorded at the ground station via Vaisala DigiCORA through metgraph software provided by Vaisala. The ozonesondes are launched fortnightly, with 2000 g or 1200 g rubber balloons. The balloons can reach an altitude of ~30 km.

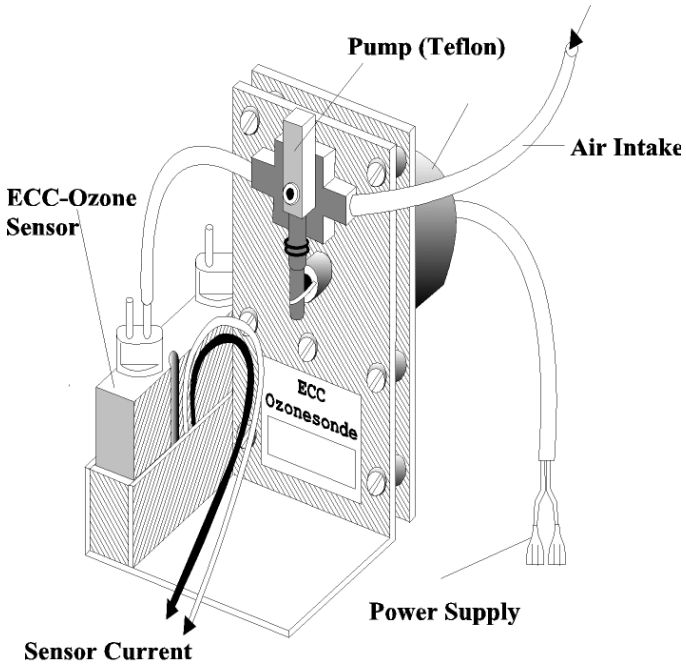
For the period 1990 to 1993, 156 ozone profiles that have no missing values from the earth's surface to 12 km were selected for this research study. Of the ozonesondes launched between 1999 and 2003, only 143 ozone profiles have no missing values and were selected for the study. Ozone data in millipascals (mPa) sampled at 5-second intervals were recorded and converted to parts per billion by volume (ppbv).

The ozone profiles selected for this study were analysed from 1.6 to ~12 km at 0.1 km (100 m) intervals.

Electrochemical concentration cells

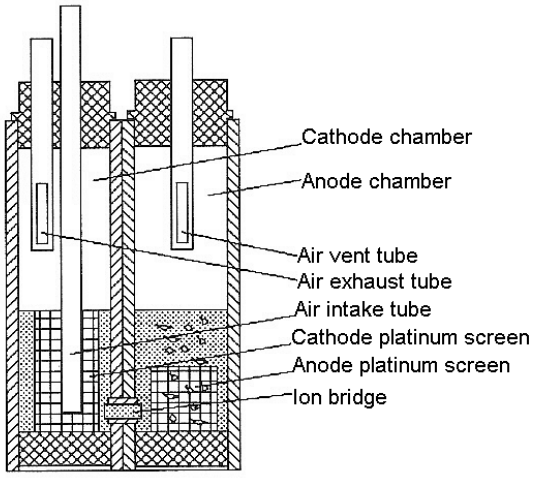
The balloon-borne measurements were introduced by Brewer and Milford (1960) who experimented using an electrochemical detector to measure ozone concentration. Thereafter, Regener (1960), investigated ozone concentration using luminescence of a dry substance in the presence of ozone. The development of the present-day ECCs evolved from an instrument called the carbon-iodide ozonesonde developed for the use of measuring the vertical distribution of ozone (Komhyr, 1964, Komhyr and Harris, 1971). The National Oceanic and Atmospheric Administration (NOAA) Air Resources Laboratory then expanded the work, by developing an ECC ozonesonde that uses KI solutions in measuring the vertical distribution of atmospheric ozone in sampled air (Komhyr, 1986).

An ECC ozonesonde is a simple, balloon-borne instrument used to measure the vertical distribution of ozone concentrations with varying height (Komhyr and Harris, 1971). The schematic ECC ozone sensor and the detailed construction of the ozone sensor as described in Vaisala (1991) are presented in Figures 2.1 and 2.2, respectively.



Source: Vaisala (1991:24(93)).

Figure 2.1: Balloon-borne ECC ozone sensor



Source: Vaisala (1991:25(93)).

Figure 2.2: Detailed construction of the ECC ozone sensor

The ozone sensor consists of two platinum electrodes immersed in buffered KI solutions of different concentrations contained in the cathode and anode chambers as described by Komhyr (1986) (Figure 2.2). The chambers are made of polytetrafluoroethylene and are linked with an ion bridge that serves as an ion pathway and prevents the mixing of the cathode and the anode solutions, preserving their concentrations (Komhyr, 1986). The chemical compositions of the cathode and anode solutions are described in Table 2.1.

Table 2.1: Preparation of ECC sensor solutions

CATHODE SOLUTION	ANODE SOLUTION
10.0 g KI 25.0 g KBr 1.25 g $NaH_2PO_4 * H_2O$ 5.0 g $Na_2HPO_4 * 12H_2O$ or 3.73 g $Na_2HPO_4 * 7H_2O$ These chemicals are dissolved in distilled water up to 1000 ml	The solution is prepared by adding 125 g KI crystals to 100 ml of the prepared cathode solution. The solution must be saturated at all times during its usage
Source: Vaisala (1991:6(93)).	

The ECC ozonesonde does not require external electrical potential for operation since its electromotive force is created from the difference in concentration of the KI solution in the cathode and the anode chambers (Komhyr, 1986). The electromotive force is calculated from the following equation:

$$E = \frac{-0.0591}{2} \log K \qquad 2.1$$

where E is the electromotive force produced within the cell at 25 $^{\circ}$C.

If the circuit is closed, a small potential exists between the electrodes. The activities in the two half cells will change until the following condition is attained:

$$K = \frac{a_1 \times c_1}{c_2 \times a_2} \sim 1 \qquad 2.2$$

where a_1 and a_2 are the initial and resultant activities, respectively, in the anode chamber and c_1 and c_2 are the initial and resultant activities in the cathode, respectively (Zunckel, 1992, and Komhyr, 1986). At equilibrium, $K \approx 1$. As soon as the sampled air containing ozone molecules is forced into the sensing cell by a battery-driven sampling pump, iodine (I_2) is formed in the cathode chamber according to the following equation:

$$2\ KI + O_3 + H_2O \rightarrow 2\ KOH + I_2 + O_2 \qquad 2.3$$

Iodine (I_2) is converted to I^- through the uptake of two electrons causing the flow of current in the cathode chamber,

$$I_2 + 2\ e \rightarrow 2\ I^- \qquad 2.4$$

while, in the anode chamber, I^- is converted to I_2 through the release of two electrons:

$$2\ I^- - 2\ e \rightarrow I_2 \qquad 2.5$$

The production of the iodine in the cathode chamber disturbs the working equilibrium, resulting in the production of an external current. The cell current is hence directly proportional to the concentration of ozone being bubbled through the cathode solution. Since the ion bridge prevents recirculation, the flow of the current will only stop when the iodine in the cathode is all transported to the anode chamber (Zunckel, 1992). One ozone molecule causes two electrons to flow in the external

circuit. This electrical current is directly related to the uptake rate of ozone in the cathode chamber with the total reaction of:

$$3\ I^- + I_2 \rightarrow I_3^- + 2\ I^- \qquad 2.6$$

Calculation of ozone concentration

In the ECC sensor, each molecule of ozone forced through the sensing solution in the electrochemical cell generates an electrical current of approximately two electrons in the external circuit. In other words, the electrical current generated is directly related to the uptake of ozone in the sensing solution and is determined from the equation (Vaisala, 1991):

$$c = \frac{1 \times t}{2F \times 100\ ml} \qquad 2.7$$

where

c = ozone concentration in $m.mol^{-1}$
F = Faraday constant, 9.6485×10^4 °C.mol^{-1}
I = current measured in μA
t = pumping time for 100 ml of air in seconds

The partial pressure of ozone in mPa is calculated by:

$$O_3 = C \times R \times T_{air} \qquad 2.8$$

So that

$$O_3 = \frac{R}{2 \times F \times 100 ml} \times I \times T_{air} \times t$$

where $R = 8.31431$ JK^{-1} mol^{-1}

$$O_3 = 4.307 \times 10^{-4} (I - I_{BG}) \times T_p \times t \times C_{ef} \times C_{ref} \qquad 2.9$$

where

O_3	=	partial pressure of ozone in mPa
I	=	measured ozone current in µA
I_{BG}	=	current caused by oxidant other than ozone mainly O_2 in µA
T_p	=	Air flow temperature measured from pump base in K
t	=	pumping time for 100 ml of air in seconds
C_{ef}	=	correction for the pumping speed due to ambient pressure
C_{ref}	=	1 (if using another method – for example, light absorption for measuring total ozone concentration – but, if not, then $C_{ref} = 1$)

Background current caused by oxidants other than ozone is measured using an ozone destruction filter through which air is pumped, and is calculated from the equation:

$$I_{BG} = \frac{(A_0 + A_1 \times P + A_2 \times P)^2}{(A_0 + A_1 \times P_0 + A_2 \times P_0)^2} \times I_0 \qquad 2.10$$

where

P	=	ambient pressure in hPa
P_0	=	weather station surface pressure in hPa
A_0	=	0.00122504
A_1	=	0.0001241115
A_2	=	-2.687066×10^{-8}

Uncertainties regarding the electrochemical concentration cell ozonesonde

The accuracy and reliability of the ECC ozonesonde depends on several factors, including the care exercised during preparation of the ozonesonde before use. An ECC ozonesonde can be quickly prepared and flown. However, it is best to prepare the instrument at least one week prior to use, and, as present usage has indicated, two (2) to three (3) weeks prior to use might be even better. The consistency of the ozonesonde data can be affected by setting changes in the manufactured instrument and differences in standard operating guidelines (Thompson *et al*., 2003; Johnson *et al*., 2002). The same authors established that the strength of the KI solution and whether the solution was buffered or unbuffered could also introduce uncertainties in the measurements. In addition, there are uncertainties with pressure and temperature determined by the radiosonde at higher altitude (the temperature uncertainties are ~0.5 K) (Thompson *et al.*, 2003). Other factors that may affect ozone concentrations by introducing bias into the measurements are:

Background current

For ECC ozonesondes, the background current (I_{BG}) is measured prior to the balloon launch of each ozonesonde by using an ozone destruction filter so that the resulting current is only generated by other oxidants. This means that the current inside the ozone sensor must be corrected by I_{BG} as in equation 2.10. Measurements are sensitive to the errors related to background current where ozone concentrations are small. For example in the stratosphere, errors associated with background current are small as ozone concentrations are higher.

Pump efficiency correction

Another possible cause of error in ozone measurements is a change in the efficiency of the pump (Komhyr, 1986; De Backer *et al*., 1998). The flow rate of an ozonesonde pump is constant at the surface pressure and remains constant down to level of 300 hPa. Below 300 hPa, the flow rate decreases (Johnson *et al*., 2002) with respect

to the greater effect of resistance from pumping against the cathode solution and perhaps pump leakage. Hence the calculated ozone partial pressure should be corrected for efficiency loss by using the correction curve provided by Komhyr (1986). Vaisala Metgraph software used at the Irene weather station for the calculation of ozone has already been corrected for the efficiency loss.

Despite these limitations, ozonesonde measurements provide high temporal resolution data in the vertical of the atmosphere (Boyd *et al*., 1998; WMO, 1998, 1998b; Johnson *et al*., 2002).

SAFARI-92 and SAFARI-2000 ozonesonde data

The SAFARI projects were formulated to study the impact of biomass emissions, transport, and deposition on aerosols and trace gases over the southern African subcontinent (Lindesay *et al*., 1996). These field campaigns have increased the understanding of the role played by fire in the southern African savannah which affects the status of the atmospheric chemistry. Biomass burning produces radiatively active gases that potentially contribute to enhanced greenhouse effects (Lindesay, 1997). The same author indicated that photochemical reactions involving biomass-burning emissions are responsible for ozone production, leading to an increase in the tropospheric ozone budget. Therefore, any processes that lead to changes in tropospheric ozone are of great importance. SAFARI-92 and SAFARI-2000 were conducted during the dry season: during the end of winter and the beginning of spring (Swap *et al*., 2002). During both field campaigns, the anticyclonic conditions prevailed during most of the days over the subcontinent (Garstang *et al*., 1996; Freiman *et al*., 2002). These conditions are conducive for the existing absolutely stable layers to become more persistent, trapping the products of biomass burning (Cosijn and Tyson, 1996) and increasing the concentrations of trace gases in the troposphere, which will be subjected to the photochemical production of ozone in the troposphere. The South African Weather Service participated in both SAFARI campaigns and ozone ascents were released at Irene weather station during August to

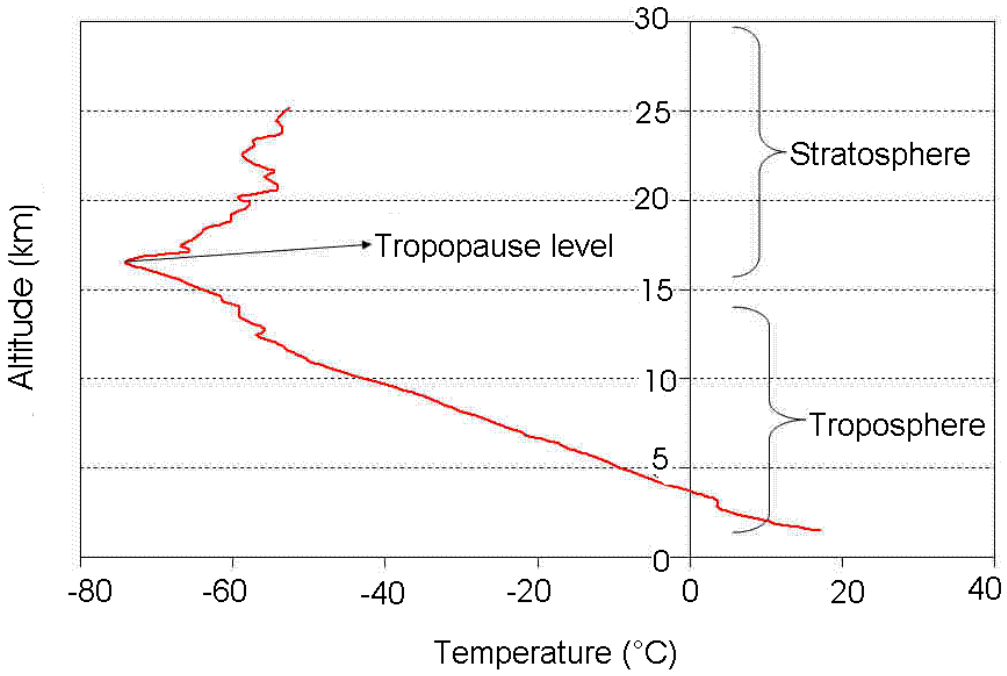
October in 1992 and 2000. In this study, 20 and 15 ozone profiles for 1992 and 2000, respectively, were available for analysis.

Tropopause height data

Since the tropopause forms a boundary between the well-mixed, ozone-poor troposphere and the ozone-rich lower stratosphere (Steinbrecht *et al*., 1998), an alternative way to understand the dynamics of ozone in the upper troposphere and the lower stratosphere is to investigate the relative position of the tropopause height (Varotsos *et al*., 2004).

The tropopause height data used in this research study were obtained from the South African Weather Service collected at Irene weather station (25.9°S, 28.2°E, and 1523 m asl). The South African Weather Service has been launching radiosonde ascents at this station since 1974. The radiosonde ascents are launched twice daily at 00:00 and 12:00 UT and the data are received at the observing station by Vaisala DigiCora. Only radiosondes launched from 07:00 to 15:00 SAST for the period 1974 to 2003 were used in this analysis. The data are then used to obtain information on the vertical distribution of temperature and pressure. The tropopause marks the boundary layer between the troposphere where temperature decreases with height and the stratosphere where temperature increases with height (Figure 2.3). The location of the tropopause was determined for all upper-air sondes by applying standard WMO thermal definition criteria, as the lowest level at which the lapse rate decreases to 2 °C/km or less, provided that the average lapse rate between this level and all higher levels within 2 km does not exceed 2 °C/km.

The first and the second thermal tropopause heights were extracted from the radiosonde data and displayed in Figures 2.4 and 2.5. Only the first tropopause height will be used in this study because, if more than one tropopause height occurs, the lowest altitude tropopause should be taken as the correct tropopause height (Newchurch *et al*., 2003).



Legend: Obtained from the Irene radiosonde data on 12 August 2003 at 11:00.
Source: Data obtained from the South African Weather Service.

Figure 2.3: An example of a temperature profile displaying a tropopause height over Irene weather station

There are large height differences displayed between the first and the second thermal tropopauses (Figures 2.4 and 2.5). The first thermal tropopause ranges between 6 and 19 km and is distributed between 16 and 17 km, with a maximum appearing at ~16.7 km. The first thermal tropopause shows seasonal dependence, with the maximum occurring in summer and minimum in winter (Figure 2.6). The second thermal tropopause appears to be more concentrated at ~17 to 18 km and have a wider range of heights (between 8 and 26 km), with a maximum height at ~17.6 km. It is interesting to note that the second tropopause height does not follow a clear annual cycle but still has a maximum in summer and a minimum in winter and spring.

The results have shown that the distribution of the first thermal tropopause over the South African Highveld has an average height of ~15.8 km. It was established that the definition of the tropopause height affects the proportion of tropospheric ozone (Bethan *et al*., 1996). Since this study concentrates only on the tropospheric ozone up to an altitude of 12 km, the tropospheric ozone was not over-estimated.

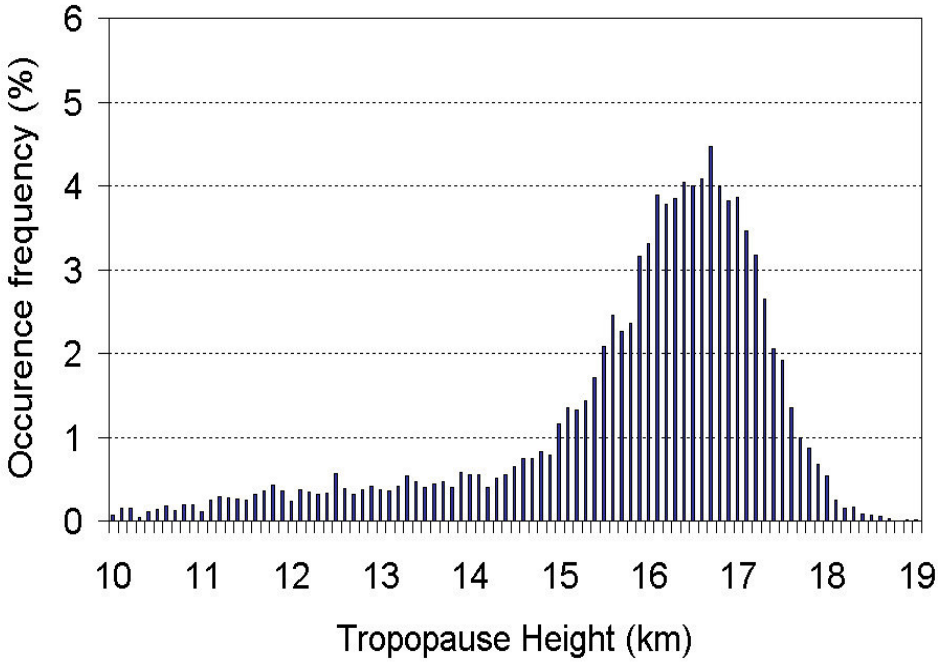


Figure 2.4: Occurrence frequencies of the first thermal tropopause height over the South African Highveld

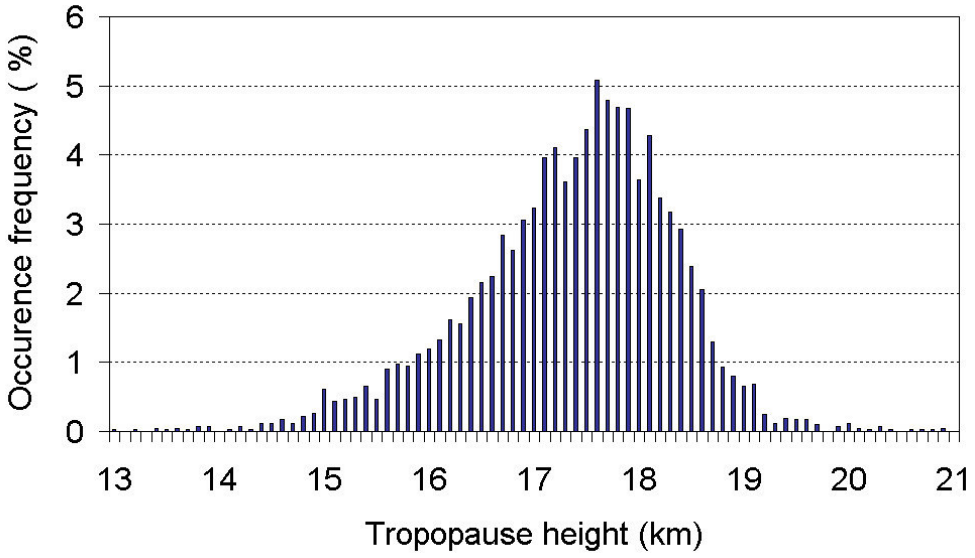


Figure 2.5: Occurrence frequencies of the second thermal tropopause height over the South African Highveld

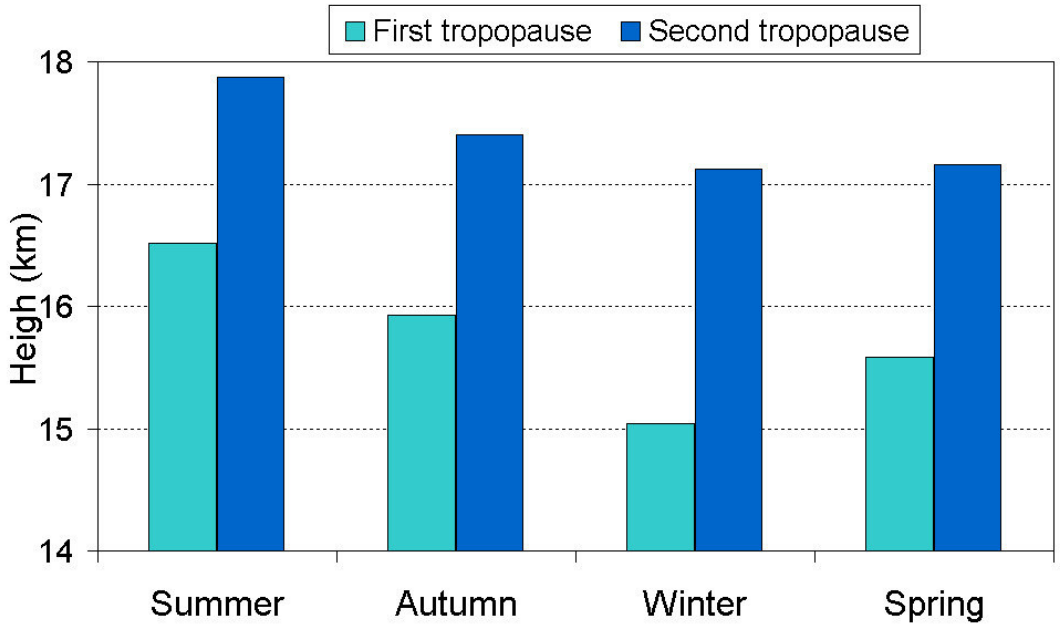


Figure 2.6: Seasonal variability of the first and second tropopauses over the South African Highveld

Meteorological synoptic systems

South African Weather Service 00:00 UT and 12:00 UT synoptic charts at 850 and 500 hPa over the periods 1990 to 1993, and 1999 to 2003 were used to determine synoptic fields that prevailed during the days when ozonesondes were launched. The surface synoptic system and the upper-air systems are then used to classify a predominant synoptic system for a particular day based on the major circulation types described given in Chapter 1 (Garstang *et al., 1996*; Tyson *et al*., 1996). An example of an 850 hPa synoptic chart is given in Figure 2.7.

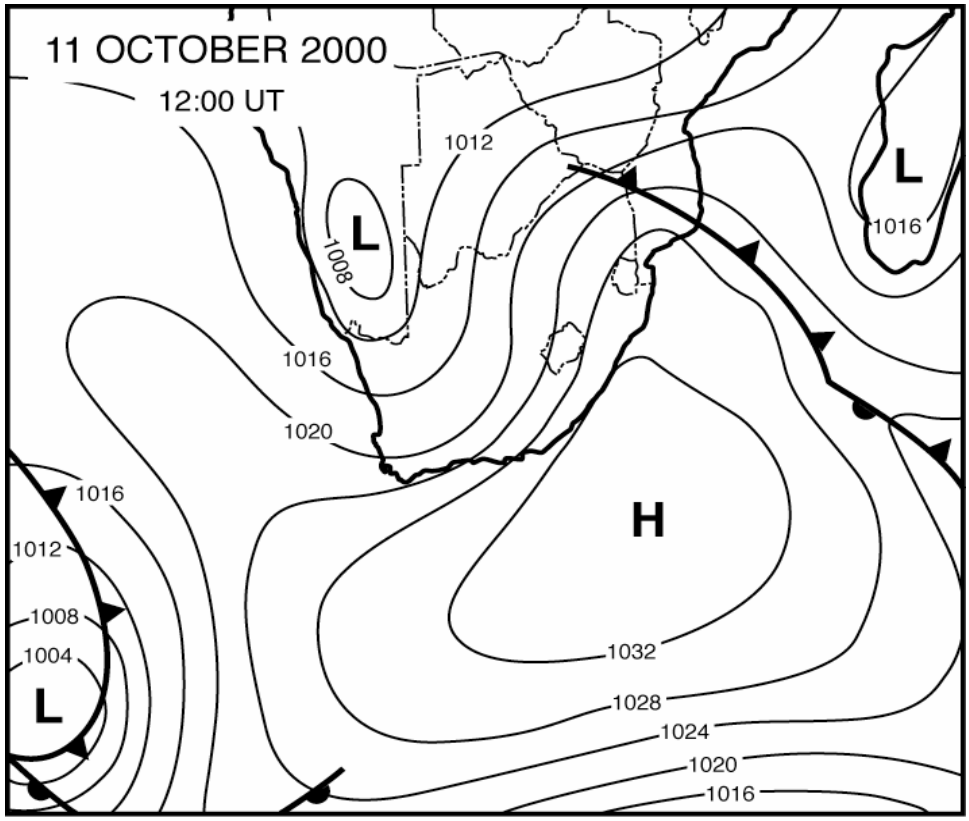
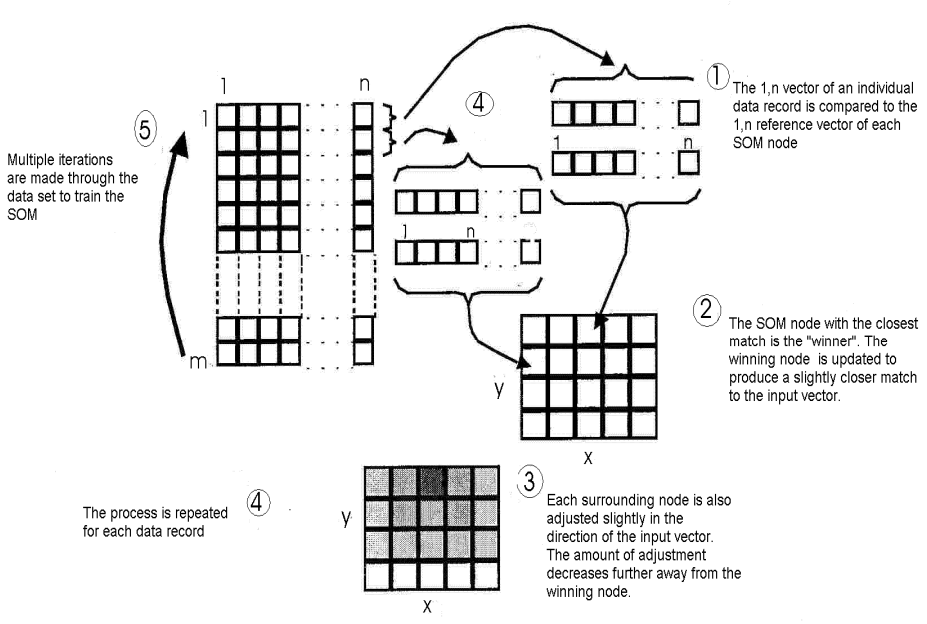


Figure 2.7: A typical example of a synoptic chart at 850 hPa on 11 October 2000 from Irene weather office.

Self-Organising Maps

Initially developed by Prof Teuvo Kohonen in 1995, Self-Organising Maps (SOMs) are a data visualisation technique that identifies the dominant modes within the given data space, such that the distribution of the nodes represents the observed distribution (Tennant and Hewitson, 2002; Tennant, 2003). SOMs can also be regarded as a cluster analysis that reduces the data by grouping similar items together (Germano, 1999). Observations that are similar to each other define nodes that are close together on the SOM, while observations that are noticeably different are located further apart on the SOM (Crane and Hewitson, 2003). Figure 2.8 outlines the SOM process described by Crane and Hewitson (2003).



Source: Crane and Hewitson (2003:96).

Figure 2.8: SOM training procedure

The process in constructing a SOM begins with initialising the reference vectors or patterns using random numbers (Tennant and Hewitson, 2002). The number of nodes in a map is chosen according to the amount of generalisation required, that is, the size

ranges from an array of two (2) horizontal by three (3) vertical nodes to six (6) horizontal by eight (8) vertical nodes (Tennant and Reason, 2005; Tennant, 2003). In this study, the rectangular array of two (2) horizontal nodes by three (3) vertical nodes was chosen. The input data are then presented and each input data record is competitively matched against the SOM node reference vectors in trying to find the best matching node ((Tennant and Reason, 2005). The best matching node is determined as the one having the least difference or having the shortest distance (Crane and Hewitson, 2003), calculated as a measure of Euclidean distance given by the following equation (Marsland, 2003):

$$d_j = \sum_{i=0}^{N-1} (v_i(t) - w_{ij}(t))^2 \qquad 2.11$$

where $v_i(t)$ is the input to node i at the time t, and w_{ij} is the strength of the element of the weight vectors between input i, and neuron j. The node with the shortest distance is chosen as the winner (Germano, 1999). This winning node is adjusted toward the input vector by using the equation (Marsland, 2003):

$$w_{ij}(t+1) = w_{ij}(t) + \eta(t)(v_i(t) - w_{ij}(t)) \qquad 2.12$$

where j is the index of a neighbouring node, and η is the learning rate ($0 \leq \eta(t) \leq 1$). Not only is the winning node adjusted, but each of the adjacent nodes is also updated (Crane and Hewitson, 2003). The final process of this stage is developing finer aspects of the SOM array such that only nodes in the immediate vicinity of the best matching node are updated (Tennant, 2003). Once the SOM is trained, the process is repeated for each input data sample and any other that can be associated with the best matching node as part of the algorithm output (Tennant, 2003; Tennant and Reason, 2005).

Self Organizing Maps was used in this study because it was more inclusive as a large number of profiles were used as compared to other techniques in the previous studies. For example of the 165 profiles launched over the period 1999-2003, a total of 143 with no missing values between the surface and 12 km, were selected for the classification.

As with any other methods, SOMs have their advantages and disadvantages explained below as described by Germano (1999). These include the ability to classify the data well and they are easily evaluated for their own quality. SOMs are simple methods to use and easy to interpret. The data selected should not have any missing values. SOMs organise sample data so that, in the final product, the samples are surrounded by similar samples. However, similar samples are not always near each other. Sometimes the clusters will be split and there will be two groups of similar data. Those two groups in reality are similar but, with most data, those two clusters will look totally unrelated. Therefore, many SOMs need to be constructed in order to generate one final good map.

SOMs are regarded as a cluster analysis which groups similar ozone profiles together. Ozone profiles were classified according to ozone concentrations from the earth's surface up to 12 km, resulting in six (6) different categories. Some of the groups identified contain ozone profiles displaying low ozone concentrations, whilst others contain ozone profiles having higher ozone concentrations.

Kinematic trajectory analysis

The backward trajectory analysis used in this study was provided by Southern Hemisphere ADditional Ozonesondes (SHADOZ), using a kinematic trajectory model provided by the Goddard Space Flight Centre of the National Aeronautics and Space Administration (NASA). This method has been used to evaluate synoptic-scale transport of pollutants and trace gases (Tyson *et al.,* 1996; Garstang *et al*., 1996). The

model uses vertical velocities to trace three-dimensional movement of an air parcel (D'Abreton, 1996).

In this study, the National Centre for Environmental Prediction (NCEP) 12:00 UT wind field data are used as input data to trace back parcels of air reaching the South African Highveld. The point of origin (SP) within a 2.5°× 2.5°× 100 hPa volume (Figure 2.9) is calculated in degrees and hPa, and designated ΔX, ΔY, ΔZ, and the reference point (ir, jr, kr) is defined as the lowest level at the western corner of the grid. The NCEP wind data are linearly interpolated to determine the values of the, *u, v*, and *w* wind components using the following equations:

$$AM = A1 + \Delta Z \times (A2 - A1) \qquad 2.13$$

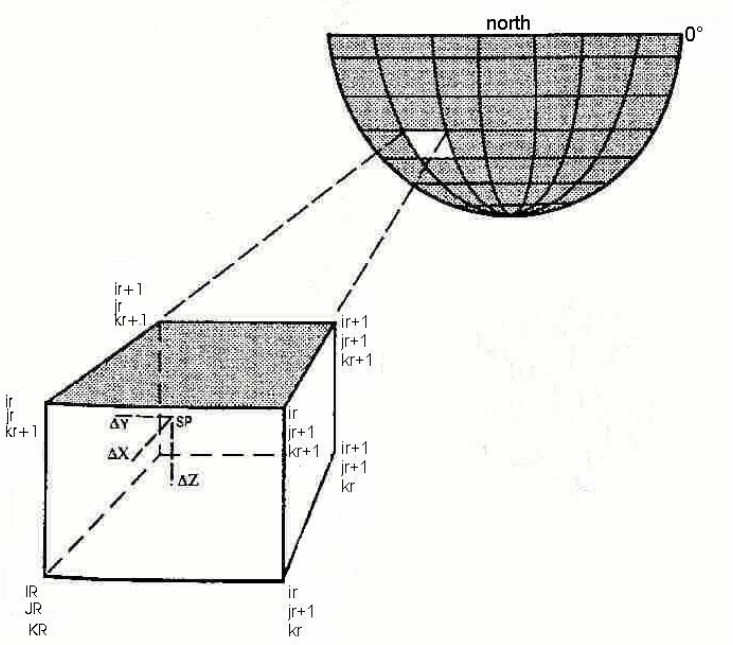
where

$$\begin{aligned} A1 = {} & [A(ir, jr, kr) + \Delta X \times (A(ir + 1, jr, kr) \\ & - A(ir, jr, kr))] + [\Delta Y \times \{(A(ir, jr + 1, kr) \\ & + \Delta X \times (A(ir + 1, jr + 1, kr) - A(ir, jr + 1, kr)) \\ & - A(ir, jr, kr) + \Delta X \times (A(ir + 1, jr, kr) \\ & - A(ir, jr, kr)))\}] \end{aligned} \qquad 2.14$$

$$\begin{aligned} A2 = {} & [A(ir, jr, kr + 1) + \Delta X \times (A(ir + 1, jr, kr + 1) \\ & - A(ir, jr, kr + 1))] + [\Delta Y \times \{(A(ir, jr + 1, kr + 1) \\ & + \Delta X \times (A(ir + 1, jr + 1, kr + 1) \\ & - A(ir, jr + 1, kr + 1)) - A(ir, jr, kr + 1) \\ & + \Delta X \times (A(ir + 1, jr, kr + 1) - A(ir, jr, kr + 1)))\}] \end{aligned} \qquad 2.15$$

ir, jr, kr is defined as the reference point, ΔX, ΔY, ΔZ is the distance of the parcel from the reference point, and A is the variable to be interpolated. The parcel is then advected for 15 minutes with a new position fixed and the components *u, v*, and *w* at the new location are redetermined by interpolation. The new positions are then

determined by using the components at the new locations to calculate the next position and so on. The new reference point ir, jr, kr will be selected at the lower south-western corner of the new cube once the parcel is advected out of the 2.5°× 2.5°× 100 hPa grid cube. This procedure is repeated for the required time and days. The boundary condition at the surface of zero vertical motion, and atmospheric stability permits air parcels to go around obstacles at the surface (Garstang *et al*., 1996), thus if the parcel hits the ground it will continue at that level until negative vertical velocity transports the parcel to higher levels (Piketh, 2000; D'Abreton, 1996).



Legend: **SP** indicates the parcel position to be interpolated at the distance ΔX, ΔY, ΔZ from the reference point ir, jr, kr**.**
Source: D'Abreton (1996:157).

Figure 2.9: The three dimensional grid cube, showing the parcel position

Air parcels are advected using the equation:

$$x(t + \Delta t) = x(t) + V[x(t)]\,\Delta t \qquad 2.16$$

where $x(t + \Delta t)$ is the new three-dimensional parcel position at time $(t + \Delta t)$; $x(t)$ is the parcel's previous position; $V(t)$ is the velocity vector of the parcel, and Δt is the time step (Piketh, 2000; D'Abreton, 1996, D'Abreton and Tyson, 1996). The time step (Δt) used in this analysis is 15 minutes.

The 5-day backward trajectories at 750 hPa, 500 hPa, 300 hPa, and 200 hPa were determined using the Irene weather station (25.9°S, 28.2°E, 1523 m asl) as a point of origin to trace the paths of atmospheric constituents back in time and space to their origin, but only trajectories at 750 hPa and 500 hPa are used in this study. The trajectories at 750 hPa, and 500 hPa for different categories produced by the SOM tool, were constructed on separate diagrams to determine the collective transport patterns produced by each group at a prescribed pressure surface.

****

Techniques and tools used in the collection of data were discussed in the above chapter. The accuracy and uncertainties in the data are supported by the description of the instrument and the procedures involved. The SOM and kinematic trajectory model used in analysing the data were described in detail.

CHAPTER 3:
CLASSIFICATION OF TROPOSPHERIC OZONE PROFILES OVER THE SOUTH AFRICAN HIGHVELD REGION

Ozone profiles for the periods 1990 to 1993 and 1999 to 2003 are classified into different categories using the statistical tool, SOMs. Final vertical ozone structures over the South African Highveld, together with related trajectories, are presented in this chapter.

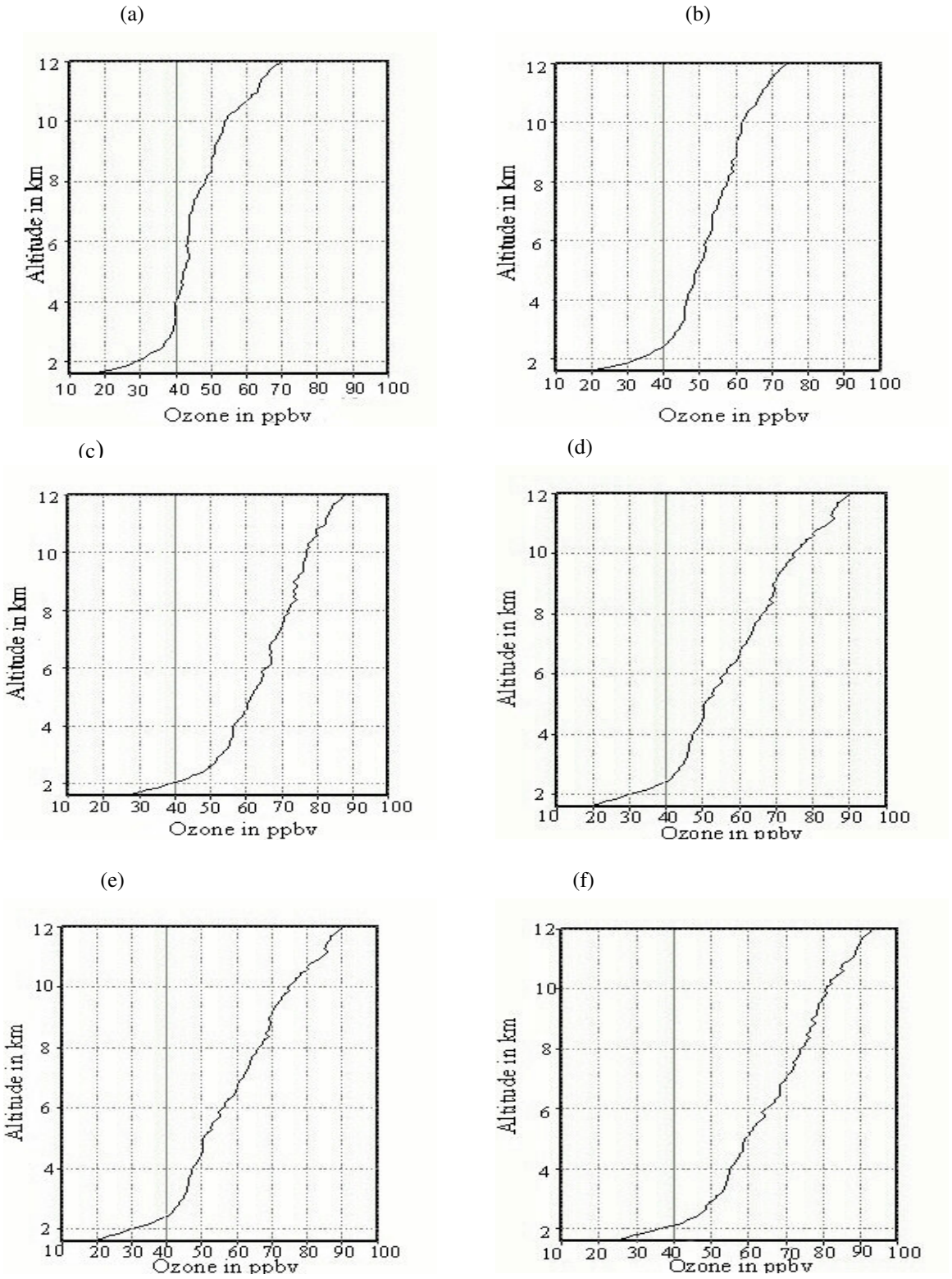
Investigation of Tropospheric Ozone Patterns

At any individual site, the variability of ozone concentration at a given time produces a unique vertical ozone structure which is of great importance in understanding photochemical and dynamical processes operating in the troposphere contributing to the tropospheric ozone budget (Diab *et al*., 2003). Each observation station has a different climatological ozone distribution in response to various factors experienced by that particular station (Collins *et al.*, 2000; Fishman *et al*., 1979). In this study different vertical ozone structures observed over the South African Highveld are investigated using two procedures: SOMs and synoptic systems. Different techniques have been used previously to group ozone profiles. For example, Diab *et al*. (2003) identified six categories of ozone profiles over Johannesburg area using TWINSPAN (Two-Way INdicator SPecies ANalysis). This chapter deals with the classification of ozone profiles using SOMs. Classification of ozone profiles based on meteorological phenomena will be investigated in the next chapter.

Classification of ozone profiles using Self-Organising Maps

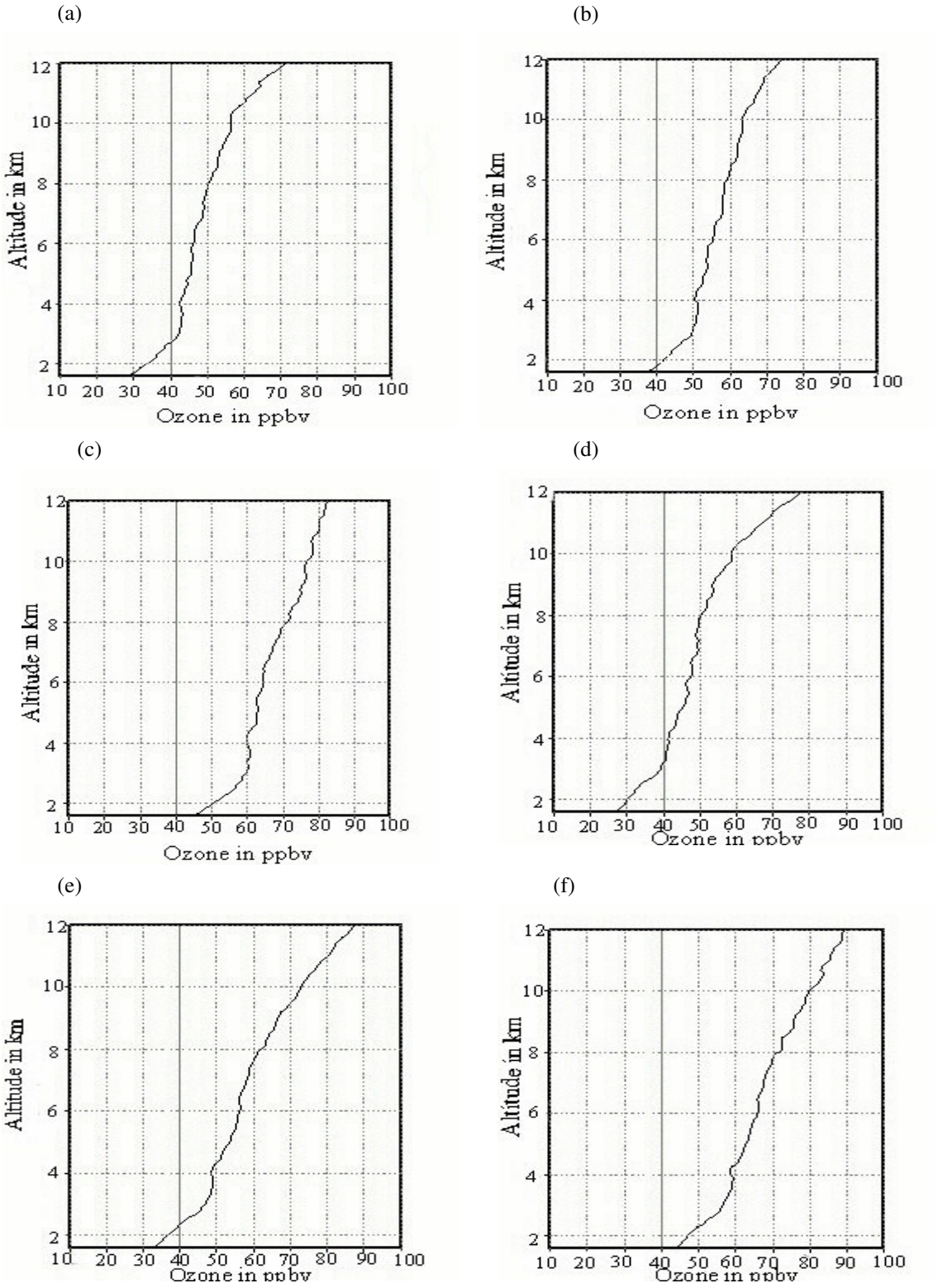
As was mentioned in Chapter 2, an array of two (2) horizontal and three (3) vertical nodes has been chosen for the SOMs. Six (6) different categories of vertical distribution of tropospheric ozone over the South African Highveld have been identified for the study periods 1990 to 1993 and 1999 to 2003 (Figures 3.1 and 3.2). Ozone profiles that belong to these six categories were grouped together and average ozone profiles for each group were constructed. In the next sections, these average ozone profiles, together with the trajectories describing the point of origin and the paths travelled by air masses reaching the South African Highveld, are presented and discussed in detail.

Ozonesondes launched between 1990 and 1993 exhibited low tropospheric ozone concentrations (a minimum of <30 ppbv) as compared to ozone profiles from the period of 1999 to 2003 (for which the minimum value ranges between 30 to 45 ppbv). It is clear that tropospheric ozone over the South African Highveld has increased in recent years (by ~10 to 15 ppbv) as was corroborated by Diab *et al*. (2004). This increase is more evident in the lower altitudes of the troposphere especially near the earth's surface. The groups contain ozone profiles from low ozone concentrations to ozone profiles displaying higher ozone concentrations, clearly highlighting the extremes (Figures 3.1 and 3.2).



Legend: The solid vertical line at 40 ppbv serves as a reference value.

Figure 3.1: Six tropospheric ozone profiles classified by SOMs for the period 1990 to 1993



Legend: The solid vertical line at 40 ppbv serves as a reference value.

Figure 3.2: Six tropospheric ozone profiles classified by SOMs for the period 1999 to 2003

Results from the Self-Organising Maps

Group (a)

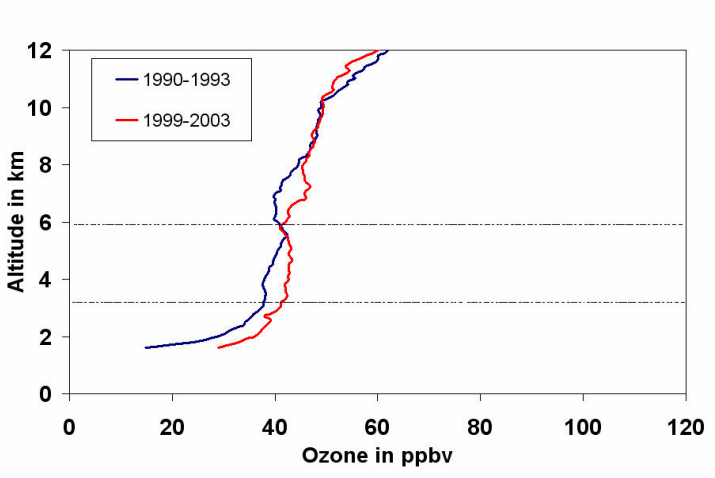
Group (a) contains 49 ozone profiles for the period 1990 to 1993 and 30 ozone profiles over the period 1999 to 2003. The group was dominated by autumn ozone profiles (20 ozone profiles in each period). However, some of these structures were also observed regularly in winter and occasionally in summer (Figure 3.3(a)). Low ozone concentrations were observed near the earth's surface (an average of <20 ppbv over the period 1990 to 1993 and 30 ppbv over the period 1999 to 2003), reaching a maximum of ~60 ppbv. Individual ozone profiles contained in this group did not exceed a maximum of 90 ppbv, except in one case (where 109 ppbv was reached). A noticeable ozone enhancement was exhibited by average ozone profiles at <6 km for both study period. In addition, an ozone enhancement was also exhibited at ~7 km over the period 1999 to 2003.

Low ozone concentrations throughout the troposphere are explained by the upper-air data, which showed an unstable atmosphere for almost all days (except for one day with conditional stability), allowing free mixing and vertical transport of trace gases and other atmospheric constituents throughout the troposphere. Ozone enhancement observed at <6 km could be linked to the possible existence of absolutely stable layers at 700 hPa and 500 hPa. Trace gases trapped below these layers then become available for photochemical production of ozone, leading to the increase in concentrations of ozone as observed between these altitudes (Kirkman *et al*., 2000).

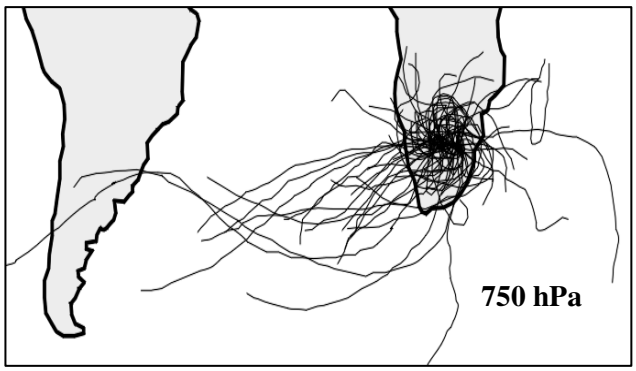
Trajectory analysis showed air masses reaching the South African Highveld at 750 hPa were mainly continental air masses (57 %) originating locally and from other African countries (such as Namibia, Zimbabwe, and Zambia), and a few from South America, contributing to the enhancement observed at <6 km (Figure 3.3(b)). However, some of the trajectories at this level originated from the Indian and Atlantic Oceans (43 %). This contribution was responsible for low ozone concentrations near

the earth's surface. At 500 hPa (Figure 3.3(c)) air masses were predominantly maritime air from the west Atlantic Ocean (66 %), explaining the decrease in ozone concentrations observed at ~6 km. The remaining trajectories (34 %) were of continental origin (South America and other African countries (such as Zimbabwe, Angola)). The overall low ozone concentrations exhibited by both ozone profiles was due to the lack of anthropogenic activities (such as biomass burning) over southern Africa during autumn.

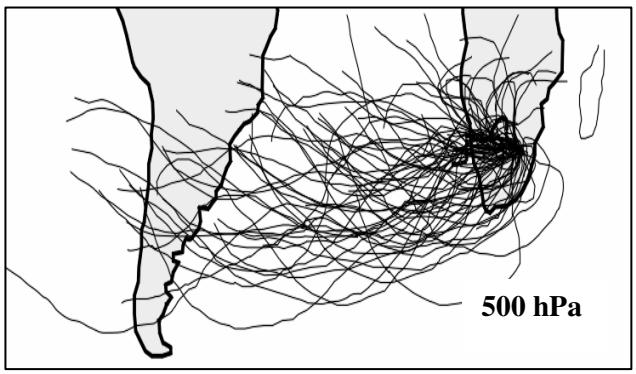
(a)



(b)



(c)



Legend: The profiles in (a) correspond to Figure 3.1(a) and Figure 3.2(a) as identified by SOMs. (b) and (c) are 5-day backward trajectories reaching South African Highveld at 750 hPa and 500 hPa levels, respectively.

Figure 3.3: Average ozone profiles and trajectories of Group (a) for the periods 1990 to 1993, and 1999 to 2003

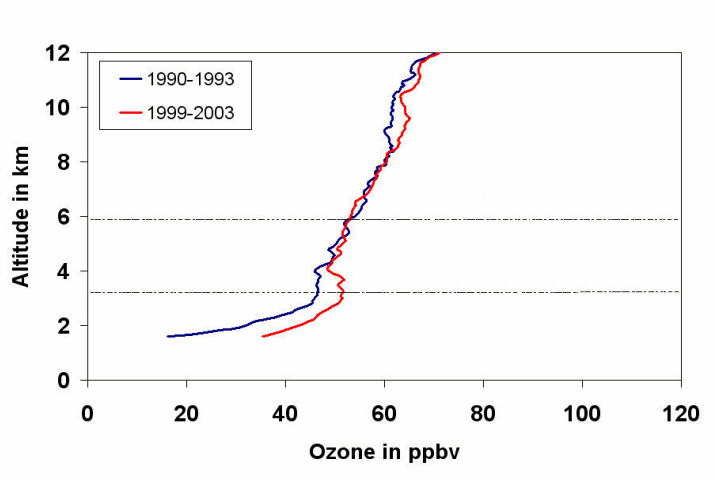
Group (b)

There were a total of 18 ozonesondes over the period 1990 to 1993 and 22 ozonesondes over the period 1999 to 2003, predominantly launched during winter. However, a few ozonesondes were also launched during summer and autumn, with fewer in spring. Group (b) displayed low ozone concentrations near the earth's surface, with an average value of ~16 ppbv and 35 ppbv over the period 1990 to 1993 and 1999 to 2003, respectively (Figure 3.4(a)). Ozone concentrations increased steadily with height between 4 and 12 km (reaching a maximum of ~70 ppbv) but did not exceed a maximum of 90 ppbv in the individual ozone profiles. Ozone enhancement at <4 km was also evident in both average ozone profiles.

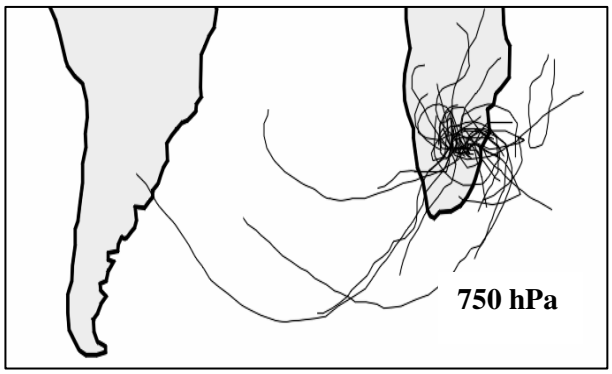
Upper-air data showed temperature inversions occurred at altitudes between 2 and 4 km during most days. The enhancement of ozone observed at <4 km could be linked to the contribution of trace gases being trapped below the 700 hPa absolutely stable layer.

The enhancement in ozone concentrations at <4 km was also due to continental air masses (58 %) mainly originating from other African countries (such as Mozambique and Botswana) and local sources reaching the South African Highveld at 750 hPa (Figure 3.4(b)). Fewer trajectories originated from the adjacent Atlantic and Indian Oceans (42 %), contributing to low ozone concentrations near the earth's surface. At 500 hPa moist maritime air dominated trajectories from the west and south Atlantic Ocean (58 %) (Figure 3.4(c)), with a few trajectories originating locally and from other African countries (42 %).

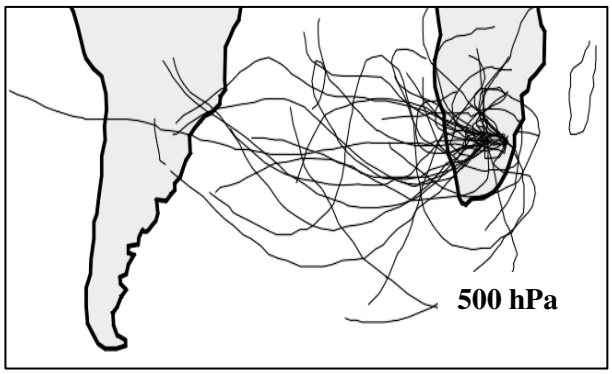
(a)



(b)



(c)



Legend: The profiles in (a) correspond to Figure 3.1(b) and Figure 3.2(b) as identified by SOMs. (b) and (c) are 5-day backward trajectories reaching South African Highveld at 750 hPa and 500 hPa levels respectively.

Figure 3.4: Average ozone profiles and trajectories of Group (b) for the periods 1990 to 1993, and 1999 to 2003

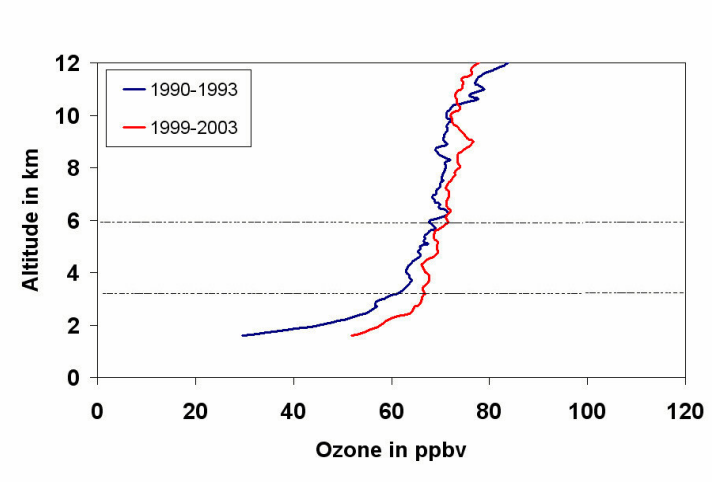
Group (c)

Group (c) were dominated by spring ozone profiles. For the period 1990 to 1993, 16 out of 26 ozonesondes, and 15 out of 25 ozonesondes for the period 1999 to 2003 were launched in spring. High ozone concentrations were displayed near the earth's surface, reaching as high as 55 ppbv in the individual ozone profiles over the period 1990 to 1993, and 89 ppbv over the period 1999 to 2003. Relatively high ozone concentrations were uniformly distributed throughout the troposphere, with ozone concentrations increasing slowly up to 12 km and having an average maximum of ~80 ppbv during both periods (Figure 3.5(a)).

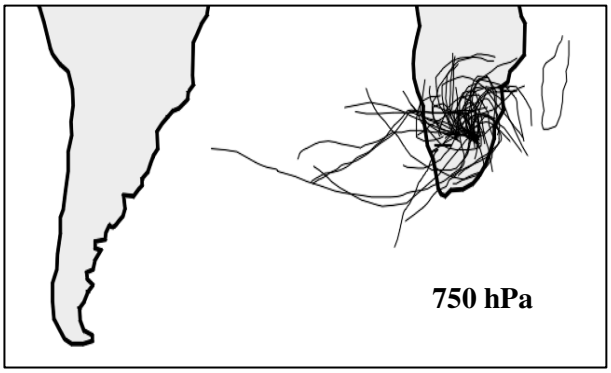
The upper-air data showed that during most of the days the troposphere was characterised by subsidence (downward movement of air within the troposphere). Therefore, trace gases will build up and become available for production of tropospheric ozone, contributing to the high ozone concentrations observed in the ozone profiles contained in this group. There is no sign of persistent absolutely stable layers, meaning free vertical mixing occurred as ozone concentrations appeared to be uniformly distributed throughout the troposphere.

Movement of continental air parcels (57 %) reaching the South African Highveld at 750 hPa (Figure 3.5(b)) originated locally as well as from other African countries (such as Botswana, and Mozambique), and was responsible for the high ozone concentrations exhibited by individual ozone profiles. However, the remaining trajectories originated from the adjacent Atlantic and Indian Oceans (43 %). These high concentrations of ozone observed coincide with the southern African burning season which normally occurs from May to October (Scholes *et al*., 1996, Le Canut *et al*., 1996). At 500 hPa, continental air masses (37 %) reached the South African Highveld also contributing to high ozone concentrations observed but the trajectories mainly originated from the west Atlantic Ocean (63 %) bringing in moist air with low ozone concentrations (Figure 3.5(c)).

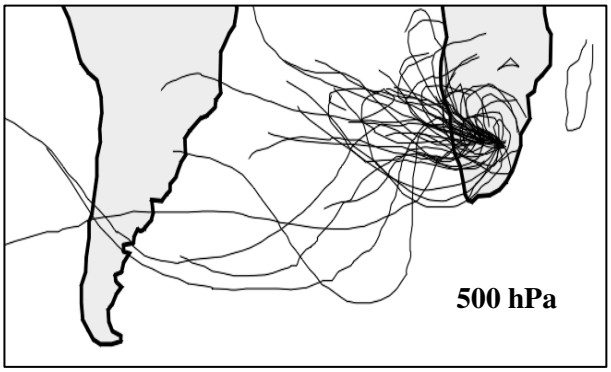
(a)



(b)



(c)



Legend: The profiles in (a) correspond to Figure 3.1(c) and Figure 3.2(c) as identified by SOMs. (b) and (c) are 5-day backward trajectories reaching South African Highveld at 750 hPa and 500 hPa levels respectively.

Figure 3.5: Average ozone profiles and trajectories of Group (c) for the periods 1990 to 1993, and 1999 to 2003

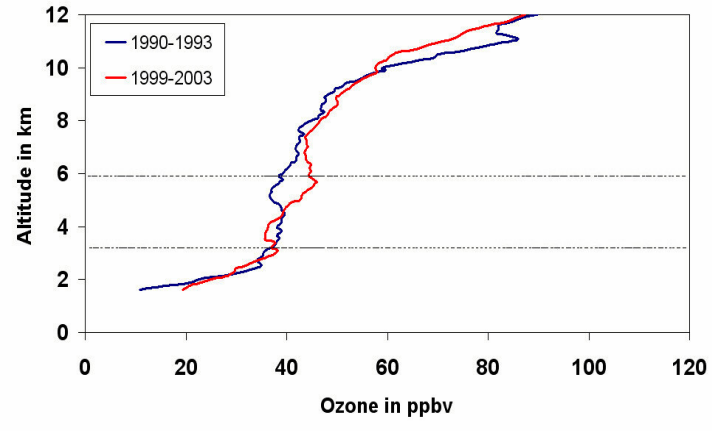
Group (d)

This group contains ozonesondes mainly launched during winter and autumn. For the period 1990 to 1993, there were 16 ozone ascents, of which eight (8) were launched in winter and five (5) in autumn. For the period 1999 to 2003, there were 22 ozone ascents, of which 10 were launched in winter and eight (8) in autumn. The average ozone profiles displayed ozone concentrations increasing steadily with height and there was a strong ozone gradient between the 10 and 12 km (Figure 3.6(a)). Ozone enhancement was observed between 2 and 5 km for the period 1990 to 1993. Significant ozone peaks were observed at 3 and 6 km for the period 1999 to 2003. Low ozone concentrations occurred near the earth's surface (with an average minimum of <20 ppbv) during both periods, reaching an average maximum of ~90 ppbv.

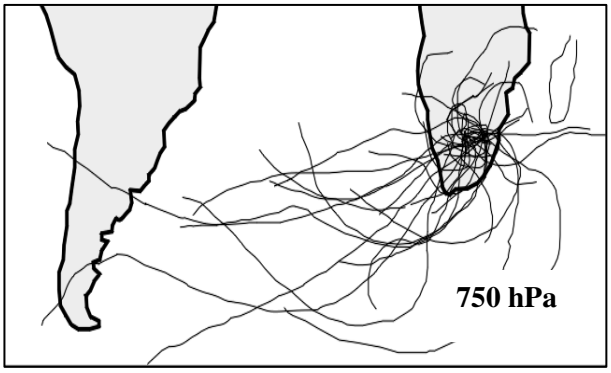
The upper-air data analysis showed the appearance of inversions at 3 and 6 km during most of the days. There was an indication of persistent absolutely stable layers at 700 hPa and 500 hPa as of ozone enhancement was observed between 2 and 5 km, and at 3 and 7 km. This is supported by findings from previous studies that, it is during this period when absolutely stable layers are more pronounced (Cosijn and Tyson, 1996).

Air masses reaching the South African Highveld (62 %) at 750 hPa (Figure 3.6(b)) primarily originated from the south and west Atlantic Ocean, contributing to low concentrations of ozone near the earth's surface. However, the remaining trajectories (38 %) originated locally and from other African countries (such as Angola), contributing to the enhancement in ozone concentrations observed at <4 km. At 500 hPa (Figure 3.6(c)) air masses originated from South America (32 %) and some from other African countries (11 %) (such as Zimbabwe and Zambia). But, at this level, air masses were predominantly from the west Atlantic Ocean (57 %) bringing in moist maritime air with low ozone concentrations.

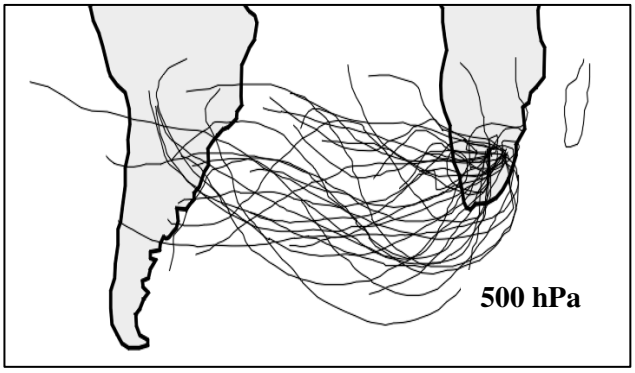
(a)



(b)



(c)



Legend: The profiles in (a) correspond to Figure 3.1(d) and Figure 3.2(d) as identified by SOMs. (b) and (c) are 5-day backward trajectories reaching South African Highveld at 750 hPa and 500 hPa levels respectively.

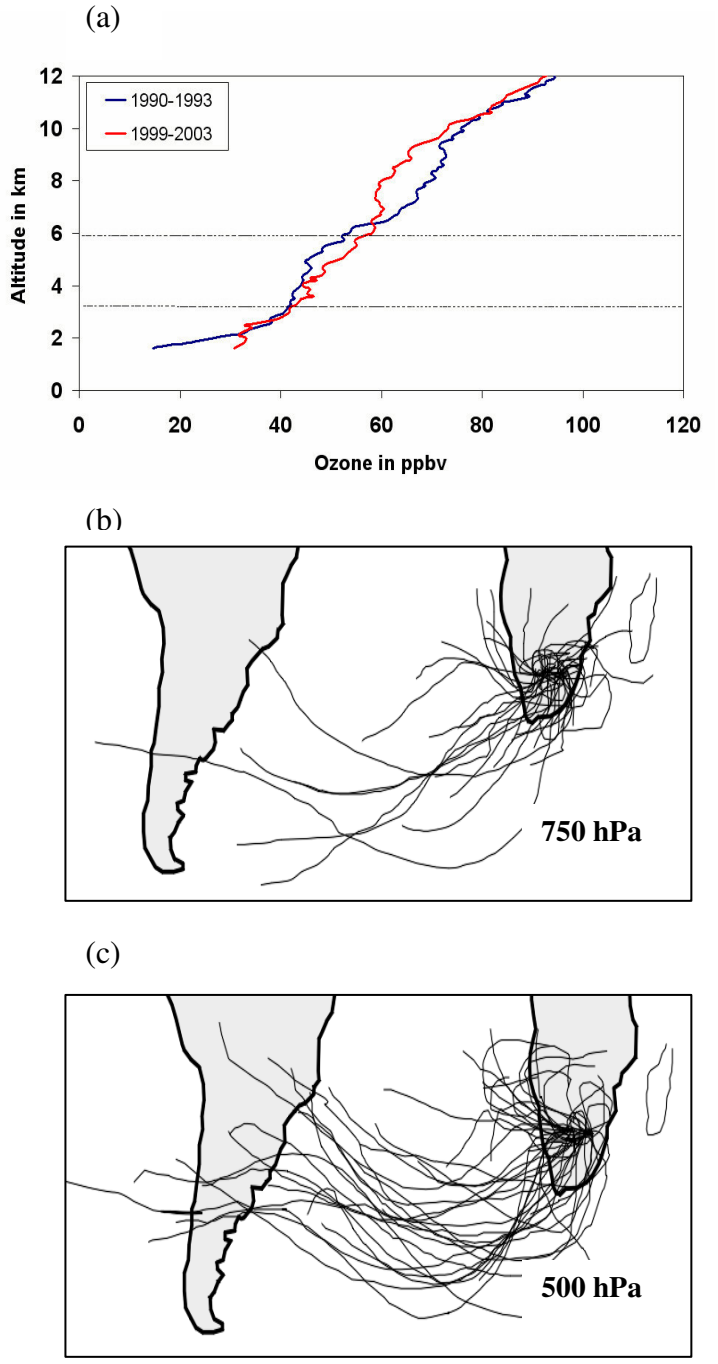
Figure 3.6: Average ozone profiles and trajectories of Group (d) for the periods 1990 to 1993, and 1999 to 2003

Group (e)

This group did not display a clear seasonal dependence as it contains ozonesondes launched throughout the year with 24 ozone profiles and 21 ozone profiles for the periods 1990 to 1993 and 1999 to 2003, respectively. Both average ozone profiles showed a steady increase of ozone concentrations with height from the earth's surface up to 6 km and from 10 to 12 km (Figure 3.7(a)). Between 6 and 9 km, the ozone profile for the period 1999 to 2003 displayed a decrease in ozone concentrations, whilst the ozone profile for the period 1990 to 1993 exhibited an enhancement in ozone concentrations. In addition, there was a strong ozone gradient (with an average maximum of ~95 ppbv) displayed by both ozone profiles at 12 km.

A steady increase of ozone concentrations with height is an indication of an unstable troposphere where vertical movement occurs at <6 km and at >10 km. However, between 6 and 9 km, the ozone enhancement over the period 1990 to 1993 could be linked to the possibility of trace gases being trapped below an absolutely stable layer at 350 hPa.

Trajectory analysis showed that trajectories reaching the South African Highveld at 750 hPa (Figure 3.7(b)) were primarily from the west Atlantic Ocean (56 %), responsible for low ozone concentrations near the earth's surface, with the remaining air parcels (44 %) originating from local sources and from other African countries (such, as Mozambique and Zimbabwe). At 500 hPa (Figure 3.7(c)) trajectories were mainly dominated by maritime air from the west Atlantic Ocean (56 %) contributing to low ozone concentrations. The few trajectories of continental origin emanate from South America (18 %), other African countries (such as Botswana), and local sources (26 %).



Legend: The profiles in (a) correspond to Figure 3.1(e) and Figure 3.2(e) as identified by SOMs. (b) and (c) are 5-day backward trajectories reaching South African Highveld at 750 hPa and 500 hPa levels respectively.

Figure 3.7: Average ozone profiles and trajectories of Group (e) for the periods 1990 to 1993, and 1999 to 2003

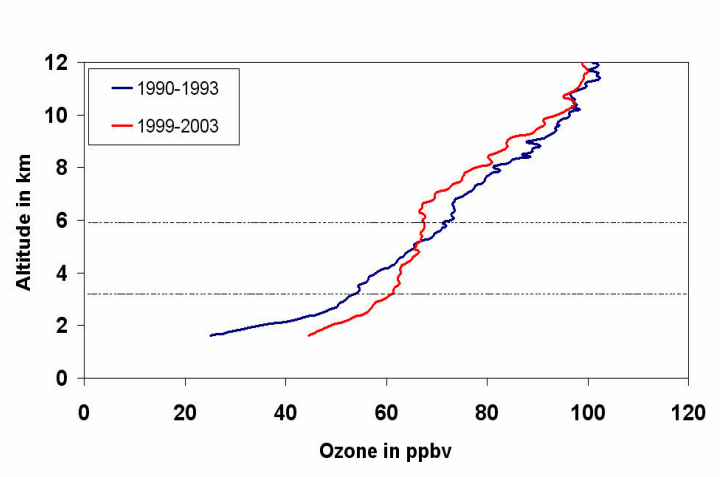
Group (f)

This is another spring-dominated group, with 17 out of 23 ozone profiles and 15 out of 23 ozone profiles for the study periods 1990 to 1993 and 1999 to 2003, respectively. The difference between this group (Figure 3.8(a)) and the other spring-dominated group (Figure 3.5(a)) is that ozone concentration was increasing steadily with height throughout the troposphere. Higher ozone concentrations were displayed by the individual ozone profiles reaching up to 45 ppbv and 70 ppbv near the earth's surface over the two periods, respectively. There was an average maximum ozone concentration of ~100 ppbv with higher ozone concentrations up to 170 ppbv being exhibited by a few individual ozone profiles. There was noticeable ozone enhancement observed between 3 and 6 km for the period 1999 to 2003.

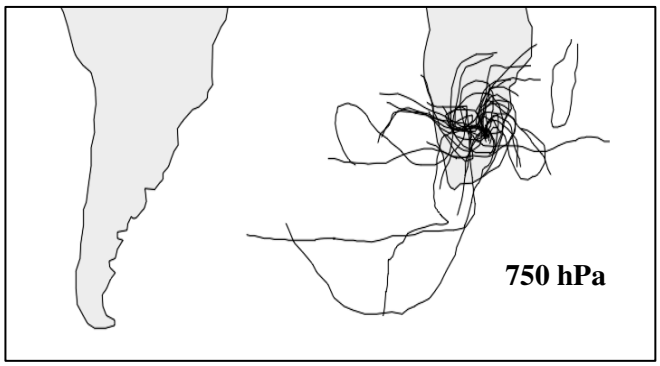
Upper-air data had shown that the atmosphere was unstable during most of the days, which allows atmospheric constituents to be mixed throughout the troposphere. However, ozone enhancement between 3 and 6 km for the period 1999 to 2003 could be the result of the existence of absolutely stable layers at 700 hPa and 500 hPa.

The high ozone concentrations displayed in the individual ozone profiles were due to a predominance of continental air masses (57 %) originating from local sources and other African countries (such as Mozambique, Namibia and Botswana) reaching the South African Highveld at 750 hPa (Figure 3.8(b)). This coincides with the southern African burning period, normally occurring during winter to spring, bringing burning emissions to this region. The remaining air masses (43 %) at this level originated from the adjacent Atlantic and Indian Oceans. At 500 hPa (Figure 3.8(c)) maritime air from the west Atlantic Ocean dominated (59 %) with few continental air masses (41 %) from local sources, other African countries (such as Namibia and Botswana) and South America.

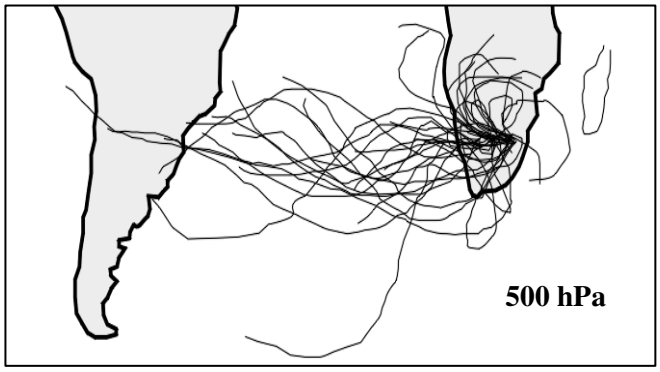
(a)



(b)

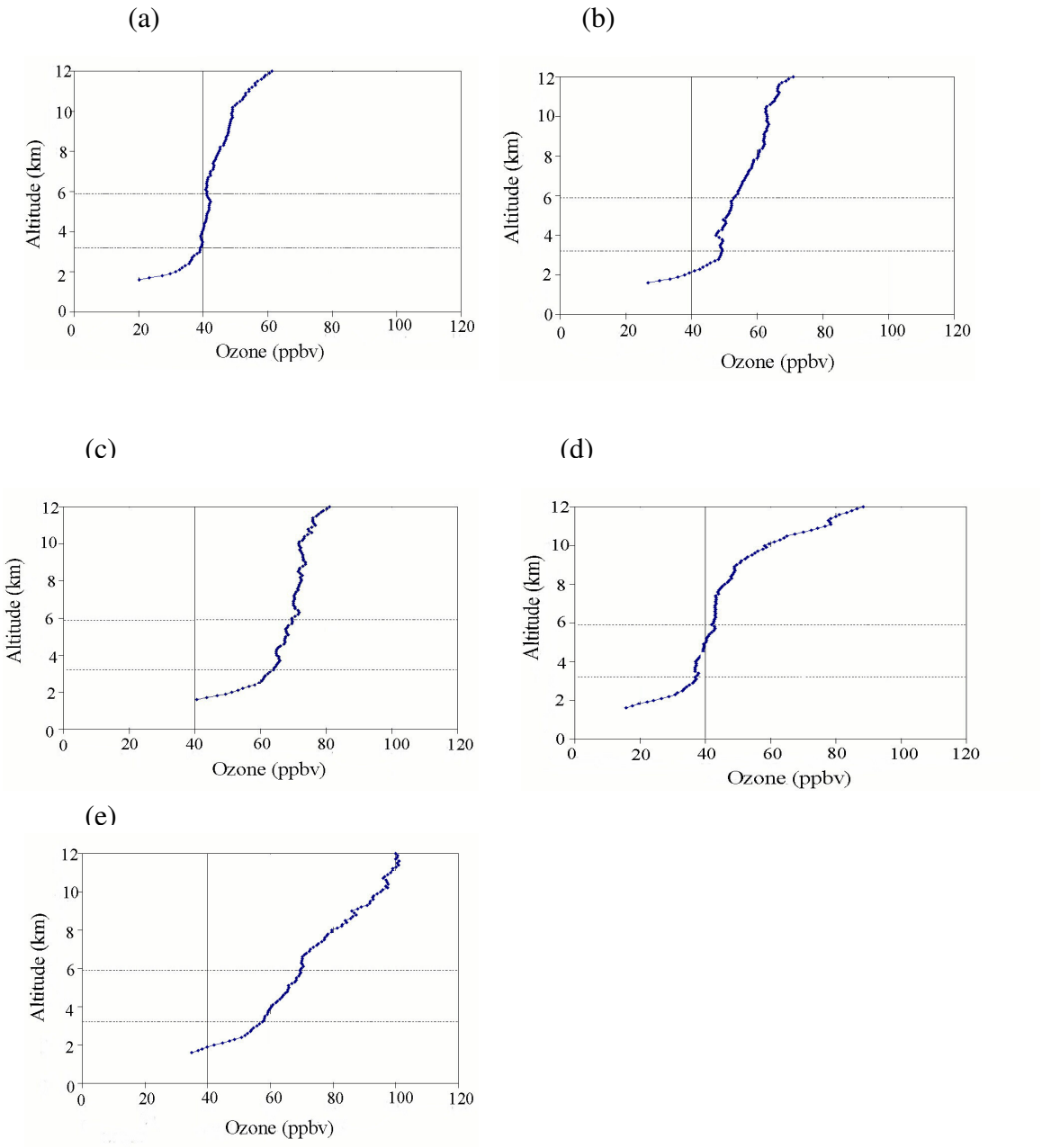


(c)



Legend: The profiles in (a) correspond to Figure 3.1(f) and Figure 3.2(f) as identified by SOMs. (b) and (c) are 5-day backward trajectories reaching South African Highveld at 750 hPa and 500 hPa levels respectively.

Figure 3.8: Average ozone profiles and trajectories of Group (f) for the periods 1990 to 1993, and 1999 to 2003



Legend: The vertical solid line at 40 ppbv serves as a reference value, and dotted horizontal lines represent the absolutely stable layers at 700 hPa and 500 hPa.

Figure 3.9: Typical ozone structures normally observed from the two data sets, as identified by SOMs

From the above classification, Group (e) and Group (f) (Figures 3.7(a) and 3.8(a)), can be regarded as one group as they have similar features displayed in their vertical ozone structures. Except for the lower ozone enhancement displayed in the average ozone profiles, ozone concentrations appear to be increasing steadily with height, displaying a strong ozone gradient at 12 km. Group (e) is not seasonally dependent, whilst Group (f) is spring-dominated. Therefore, this steady increase ozone profile is observed throughout the year, with a higher ozone concentration during spring. In conclusion, SOMs identified five ozone vertical structures normally observed over the South African Highveld (Figures 3.9(a) to 3.9(e)).

****

Ozone structures normally observed over the South African Highveld were determined using SOMs. Similar structures were discovered from the two study periods (1990 to 1993 and 1999 to 2003). Trajectories from SHADOZ were used to identify the point of origin of air masses arriving at the South African Highveld at 750 hPa and 500 hPa levels.

CHAPTER 4:
CHARACTERISATION OF TROPOSPHERIC OZONE OVER THE SOUTH AFRICAN HIGHVELD

The influence of synoptic systems on the vertical distribution of tropospheric ozone is investigated in this chapter. A comparison between ozone structures obtained from SOMs and synoptic systems is presented. Final ozone structures are compared with the structures from previous studies. An investigation of the strong ozone gradient displayed in some of the ozone profiles using the tropopause data is given. Evidence to support seasonal variations of tropospheric ozone over the South African Highveld is presented. Data collected during the SAFARI-92 and SAFARI-2000 field campaigns are used to investigate the temporal variations of tropospheric ozone over this region.

The Effects of Synoptic Systems on the Vertical Distribution of Ozone

Studies have shown that specific meteorological variables have an influence on ozone concentrations (Davies *et al*., 1992), although the response of ozone profiles – especially their vertical structure – to meteorological phenomena is less well known (Halenka *et al*., 1994). In this section, attempts are made to investigate the influence of atmospheric circulation systems on vertical distribution of tropospheric ozone over the South African Highveld.

The ozonesonde data for the two study periods, 1990 to 1993 and 1999 to 2003 were grouped into different categories according to the major synoptic circulation systems prevailing for the day on which the ozonesonde was launched. The synoptic classification consisted of continental highs, ridging highs, westerly disturbances and

easterly waves. The synoptic system summaries available for the study periods are summarised in Table 4.1. The frequencies of occurrence of these major synoptic systems are plotted in Figures 4.1 and 4.2.

Table 4.1: The number of synoptic systems occurred during the study periods

SYNOPTIC SYSTEM	STUDY PERIOD	
	1990 to 1993	1999 to 2003
Continental high	69	22
Ridging high	28	36
Westerly disturbance	22	26
Easterly wave	29	50
TOTAL	**148**	**134**

Continental high conditions prevailed throughout the year (Figures 4.1 and 4.2) for both periods except for November (1990 to 1993) and March (1999 to 2003). The distribution had a maximum in April (1990 to 1993) and in May, and June (1999 to 2003).

Ridging high systems occurred throughout the year except in April (1990 to 1993), and February and October (1999 to 2003). They reached a maximum in January and March (1990 to 1993) and May (1999 to 2003).

Westerly disturbances during 1990 to 1993 appeared mainly during late winter to spring, with a maximum in October. During 1999 to 2003, these systems occurred throughout most of the year (except for May, October, November and December), whilst they reached a maximum in September.

Easterly waves occurred throughout the year (except for June during 1990 to 1993, and May to July during 1999 to 2003). The first maximum occurred in February and another maximum in December over the period 1990 to 1993. During the period 1999 to 2003, a maximum occurred in October.

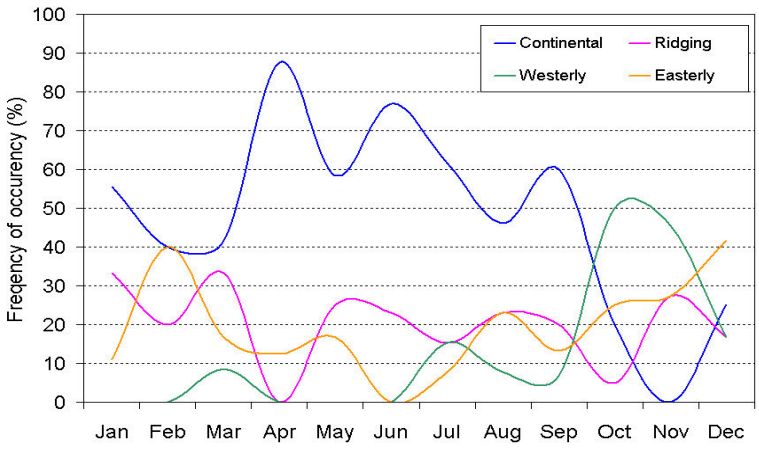


Figure 4.1: Frequencies of occurrence of meteorological fields during the ozone ascents launch, for the period 1990 to 1993

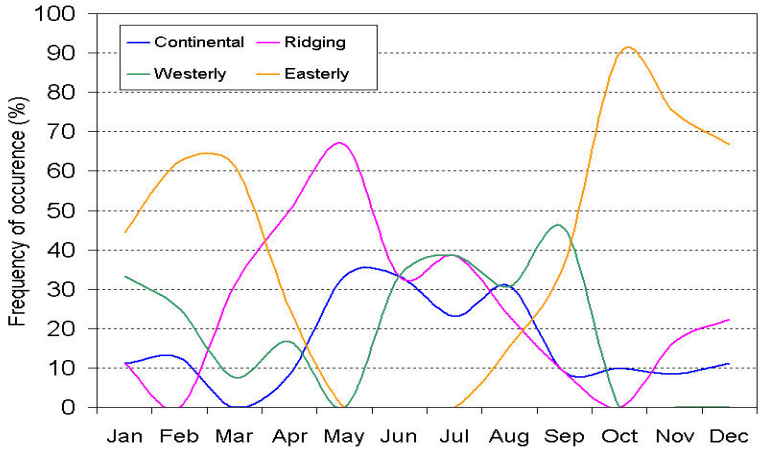


Figure 4.2: Frequencies of occurrence of meteorological fields during the ozone ascents launch, for the period 1999 to 2003

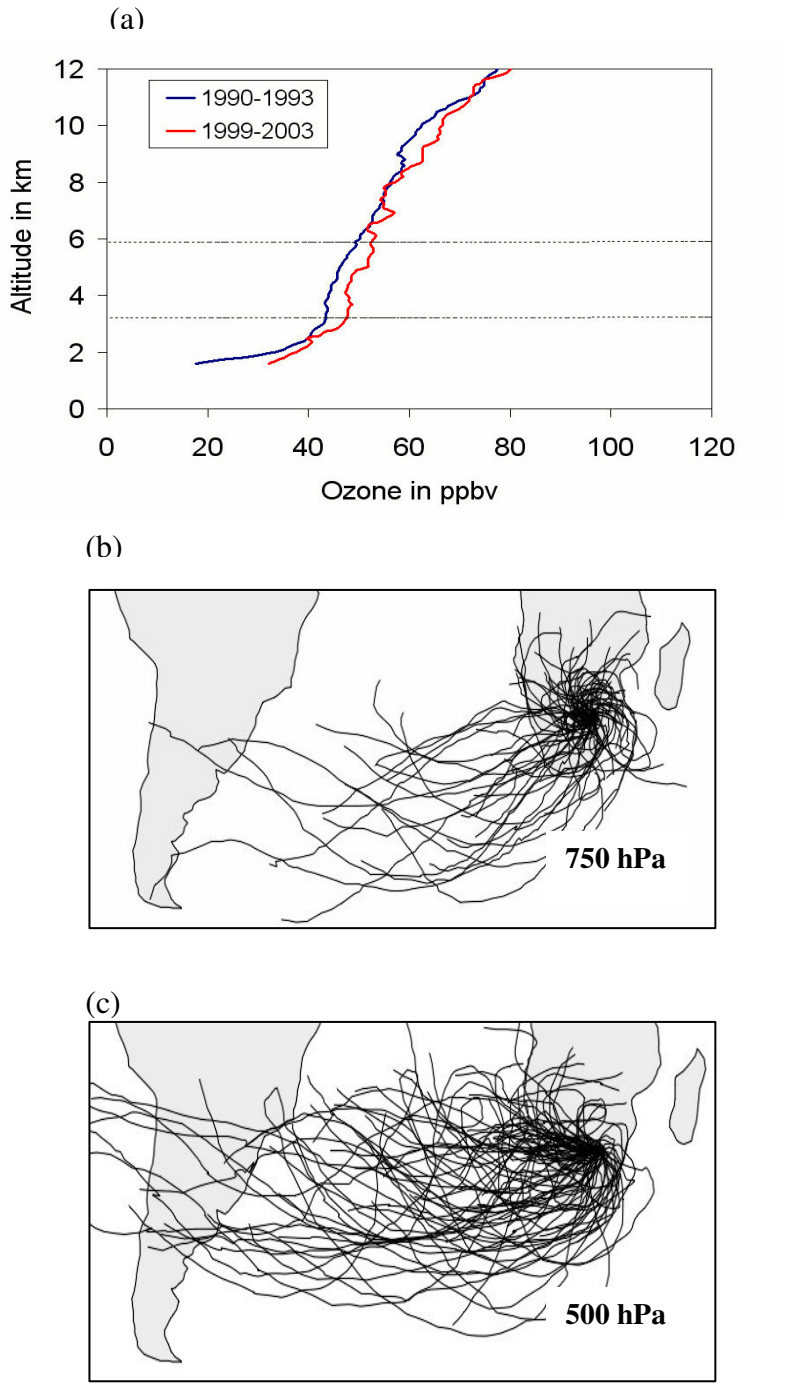
Ozone profiles associated with these major circulation types were averaged to obtain the mean vertical ozone distribution for that meteorological field and plotted together with trajectories reaching the South African Highveld.

Ozone profiles associated with continental high systems

The two average ozone profiles in Figure 4.3(a) showed ozone concentrations increasing steadily from 4 up to 12 km reaching a maximum value of ~80 ppbv. Generally both ozone profiles exhibited a noticeable ozone enhancement between 2.5 and 4 km. The 1999 to 2003 average ozone profile displayed strong stratification, indicating the existence of absolutely stable layers (Kirkman *et al*., 2000).

Continental high systems are more pronounced during winter (Tyson *et al*., 1996). These systems are associated with subsidence of air, and increase the stability of the troposphere to a point where absolutely stable layers – especially at 700 hPa and 500 hPa – could become persistent and inhibit vertical mixing of atmospheric constituents (Cosijn and Tyson, 1996). This explains the ozone stratification observed – especially in the 1999 to 2003 average ozone profile – and ozone enhancement at <4 km exhibited by the ozone profiles for both study periods.

The enhancement at <4 km is also explained by trajectories of continental air masses (52 %) reaching the South African Highveld at 750 hPa (Figure 4.3(b)), but some were maritime air from the adjacent Atlantic and Indian Oceans (48 %). At the 500 hPa level, air masses primarily originated from the west and south Atlantic Ocean (65 %) and South America (24 %). A few (11 %) were of continental origin (Figure 4.3(c)).



Legend: (a) Ozone profiles. (b) and (c) are 5-day backward trajectories reaching South African Highveld at 750 hPa and 500 hPa levels respectively.

Figure 4.3: Average ozone profiles corresponding to continental high conditions and trajectories for the periods 1990 to 1993, and 1999 to 2003

Ozone profiles associated with ridging high systems

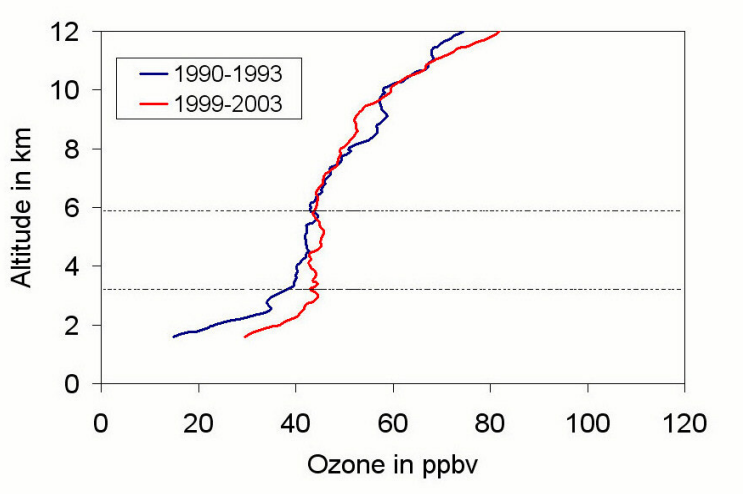
Low level ozone enhancement was evident in the average ozone profiles, located between 3 and 6 km for the period 1990 to 1993 and between 3 to 4 km and 5 to 6 km for the period 1999 to 2003 (Figure 4.4(a)). A small ozone peak was observed in both ozone profiles but is more noticeable during 1990 to 1993 at ~9 km. There was also a peak at ~11 km. At altitudes of >6 km, ozone concentrations increase sharply with a strong ozone gradient from 10 to 12 km. Generally, the average ozone profiles displayed low ozone concentrations throughout the troposphere, reaching an average maximum of 80 ppbv.

The ridging high systems, also associated with subsidence and the presence of absolutely stable layers at 700 hPa and 500 hPa, are reflected noticeably in both average ozone profiles as ozone peaks are observed from 3 to 6 km for the period 1990 to 1993; and from 2 to 4 km, and 4 to 6 km for the period 1999 to 2003 as a result of the stratified troposphere.

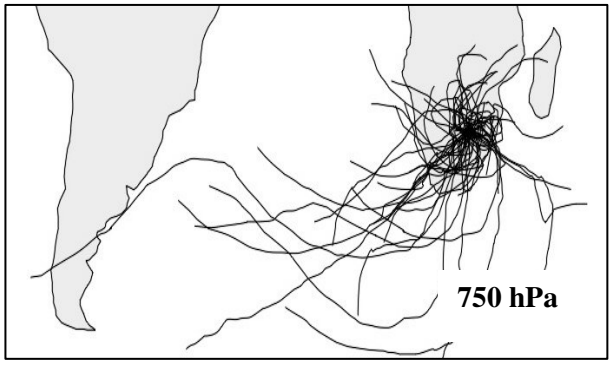
At 750 hPa, continental air (52 %) originated locally, and from other African countries (such as Zimbabwe and Botswana) (Figure 4.4(b)), and was responsible for the enhancement observed at the lower levels of the troposphere as displayed by both average ozone profiles. The remaining trajectories (48 %) originated from the adjacent Atlantic and Indian Oceans.

The ridging high is associated with the westerly wave at 500 hPa, which advects moist unstable air over the land. This was supported by trajectories at 500 hPa mainly originating from the west Atlantic Ocean (50 %), explaining the overall low ozone concentrations observed. The remaining trajectories originated from South America (30 %) and from continental sources (20 %) (Figure 4.4(c)),

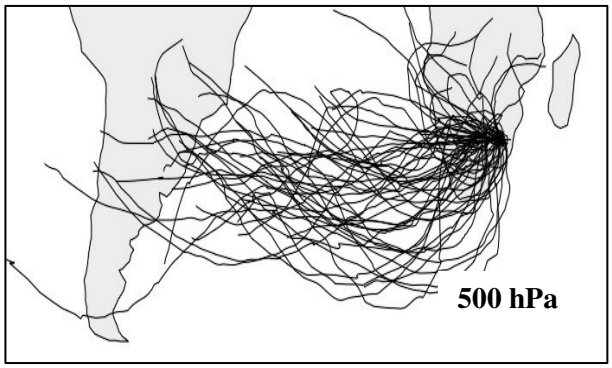
(a)



(b)



(c)



.

Legend: (a) Ozone profiles. (b) and (c) are 5-day backward trajectories reaching South African Highveld at 750 hPa and 500 hPa levels respectively.

Figure 4.4: Average ozone profiles corresponding to a ridging high conditions and trajectories for the periods 1990 to 1993, and 1999 to 2003

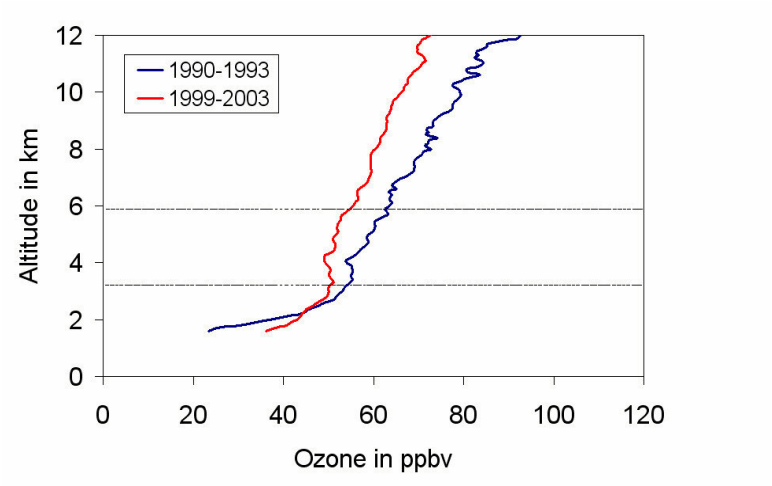
Ozone profiles associated with westerly disturbance systems

The two average ozone profiles have similar features: enhancement in ozone concentrations at <4 km. A steady increase of ozone concentrations from 4 to 12 km reaching an average maximum of 90 ppbv for the period 1990 to 1993 and 70 ppbv for the period 1999 to 2003 (Figure 4.5(a)).

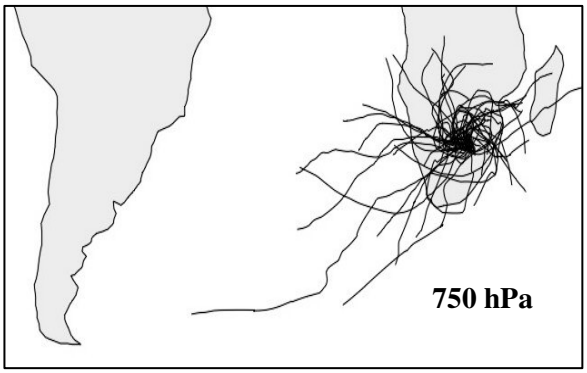
The occurrence frequencies (Figures 4.1 and 4.2) showed that the westerly disturbances were more of a winter to spring phenomenon, with a maximum in October for 1990 to 1993 and July to September for 1999 to 2003, coinciding with the burning season in southern Africa. Westerly disturbances are associated with strong convergence at the earth's surface and upper-air divergence, which are ideal conditions for uplifting of air. Strong uplifting of air results in vertical mixing of ozone throughout the troposphere as indicated by a steady increase of ozone with height at altitudes of >4 km.

The enhancement at <4 km is explained by air masses which reached the South African Highveld at 750 hPa originating from Madagascar, other African countries (such as Zambia), and local sources (40 %). The remaining air masses emanated from the adjacent Atlantic and Indian Oceans (60 %) (Figure 4.5(b)). At 500 hPa air masses originated from other African countries (37 %) (such as Botswana and Zambia) and South America (23 %). The remaining air masses (40 %) originated from the west Atlantic Ocean (Figure 4.5(c)). The overall tropospheric ozone enhancement is due to biomass-burning emissions originating from African countries and South America, as these products can be transported at high altitudes via westerlies near 25°S latitude to the tropical south Atlantic Ocean, then deep convection near the earth's surface transport these particles to the upper levels of the troposphere (Piketh and Walton, 2004).

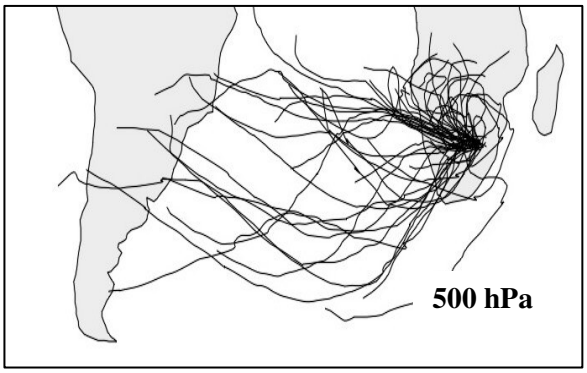
(a)



(b)



(c)



Legend: (a) Ozone profiles. (b) and (c) are 5-day backward trajectories reaching South African Highveld at 750 hPa and 500 hPa levels respectively.

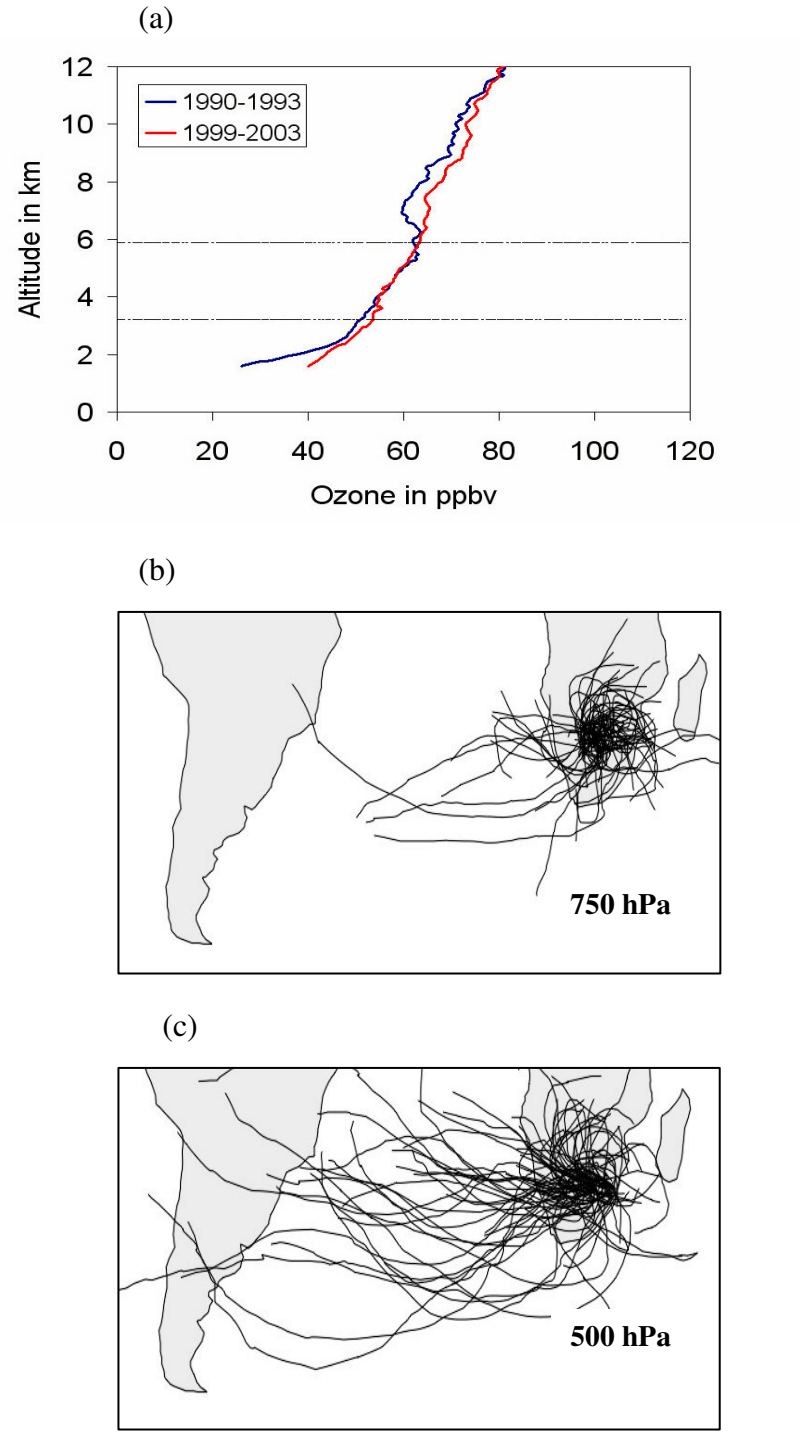
Figure 4.5: Average ozone profiles corresponding to westerly disturbance conditions and trajectories for the periods 1990 to 1993, and 1999 to 2003

Ozone profiles associated with easterly wave systems

On close inspection, the two average ozone profiles in Figure 4.6(a) exhibit similar features. Both ozone profiles displayed ozone enhancement between 4 and 7 km which was more pronounced during 1990 to 1993 than during 1999 to 2003. Individual ozone profiles associated with easterly wave systems exhibited high ozone concentrations near the earth's surface (up to 90 ppbv during the 1999 to 2003 study period).

Occurrence frequencies have shown that easterly waves occurred throughout the year. Easterly waves reached a maximum between late spring to early summer (October to December) for both periods (Figures 4.1 and 4.2). This coincides with the biomass-burning season in southern Africa. The easterly wave system generates convection, therefore, warm and humid air flows from the Inter-Tropical Convergence Zone to the subtropics. This could result in biomass-burning emissions being transported to the South African Highveld.

The easterly wave transports air rich in ozone from the tropics as was evident in both average ozone profiles which exhibited high ozone concentrations. Trajectory analysis showed air masses (42 %) reaching the South African Highveld at 750 hPa (Figure 4.6(b)) from local sources and other African countries (such as Namibia and Mozambique). Maritime air from the adjacent Atlantic and Indian Oceans accounted for 58 % of the air masses at this level. However, at 500 hPa air masses predominantly originated from west Atlantic Ocean and South America (66 %) (Figure 4.6(c)) with the remaining (34 %) air masses coming from local sources and other African countries (such as Angola and Botswana).



Legend: (a) Ozone profiles. (b) and (c) are 5-day backward trajectories reaching South African Highveld at 750 hPa and 500 hPa levels respectively.

Figure 4.6: Average ozone profiles corresponding to easterly wave conditions and trajectories for the periods 1990 to 1993, and 1999 to 2003

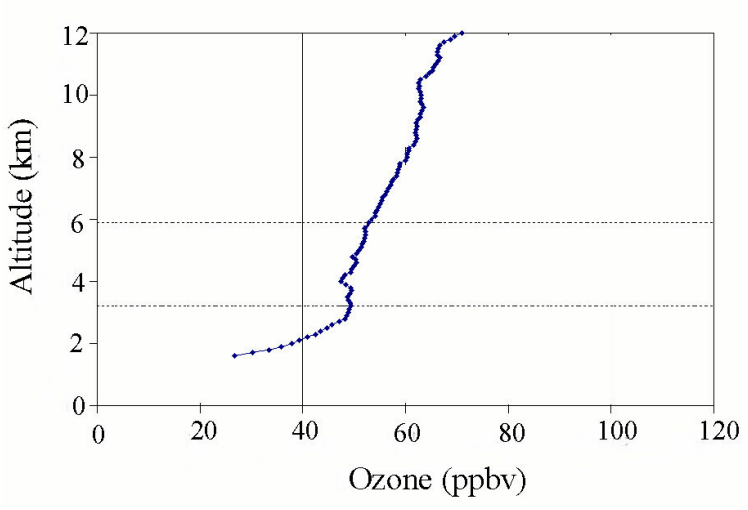
Average ozone profiles associated with the ridging highs, continental highs, and westerly disturbances exhibited ozone enhancement in the lower levels of the troposphere. In some cases, high ozone concentrations were displayed (for example associated with easterly waves) throughout the troposphere. Investigation to link these high ozone episodes with the occurrence of La Niña or El Niño events, showed no conclusive results.

Vertical tropospheric ozone structures over the South African Highveld

Two methods were employed in this study, namely SOMs and meteorological synoptic systems, to investigate vertical tropospheric ozone structures that normally occur over the South African Highveld. These two methods managed to identify similar ozone structures which will be discussed.

Average ozone profiles (Figures 4.7(a) and (b)) exhibited low surface ozone concentrations with ozone enhancement at <4 km. This ozone structure was associated with the westerly disturbance, and SOMs identified it as an ozone profile normally observed during winter, but less frequently in autumn, summer and spring.

(a)



(b)

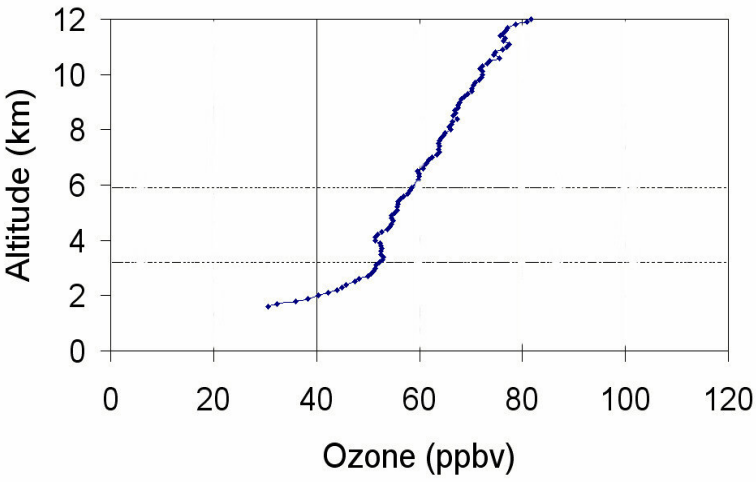


Figure 4.7: Vertical ozone profiles (a) identified by SOMs (b) westerly disturbance associated ozone profile

SOMs identified this ozone structure as being more pronounced during the autumn and winter seasons, during which ridging high conditions showed the highest frequency (Figure 4.8(a) and (b)). The ozone profiles exhibited low ozone concentrations near the earth's surface with ozone enhancement displayed at <4 km and a strong ozone gradient between 10 and 12 km.

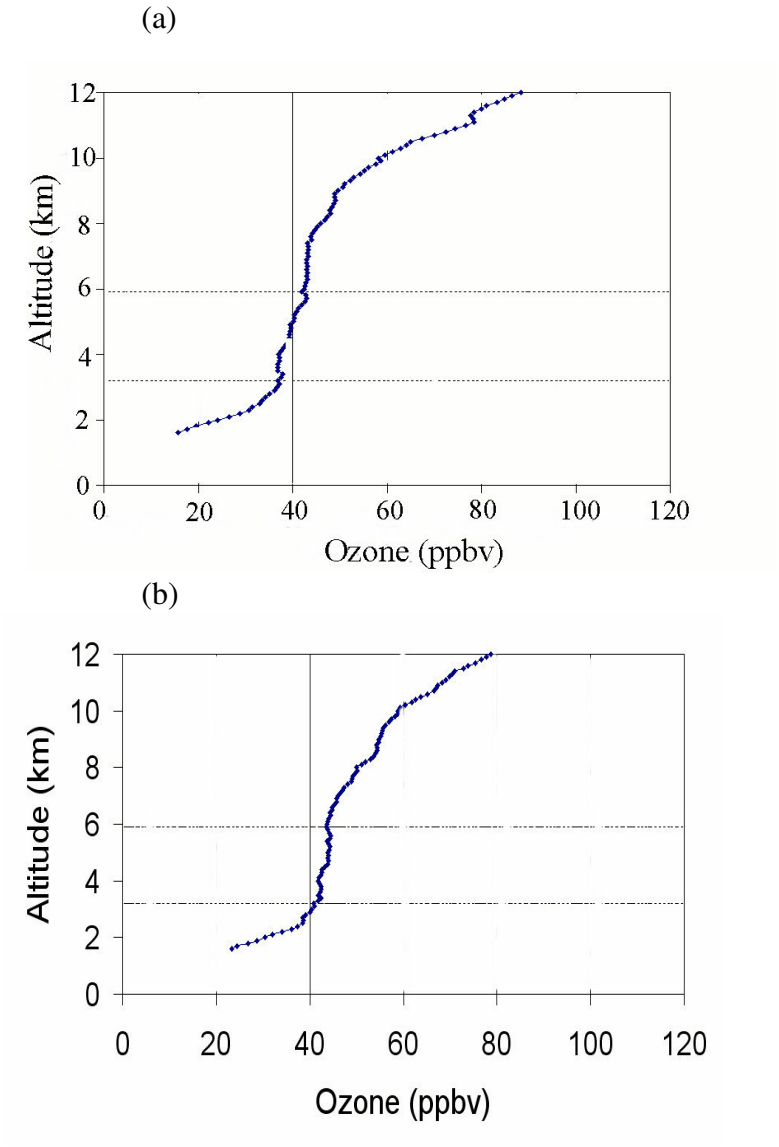
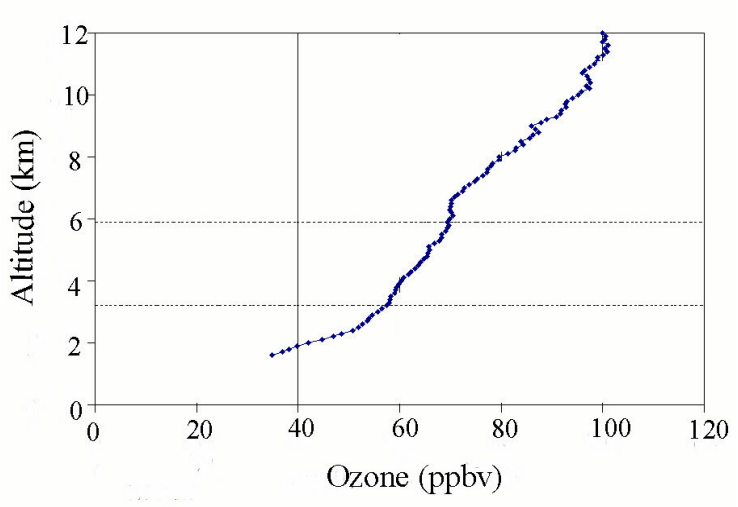


Figure 4.8: Vertical ozone profiles (a) identified by SOMs (b) associated with the ridging high system

In Figures 4.9(a) and (b), this ozone structure was identified by SOMs as independent of the season, and was associated with easterly wave systems. High ozone concentrations were displayed and ozone concentrations increasing steadily with height.

(a)



(b)

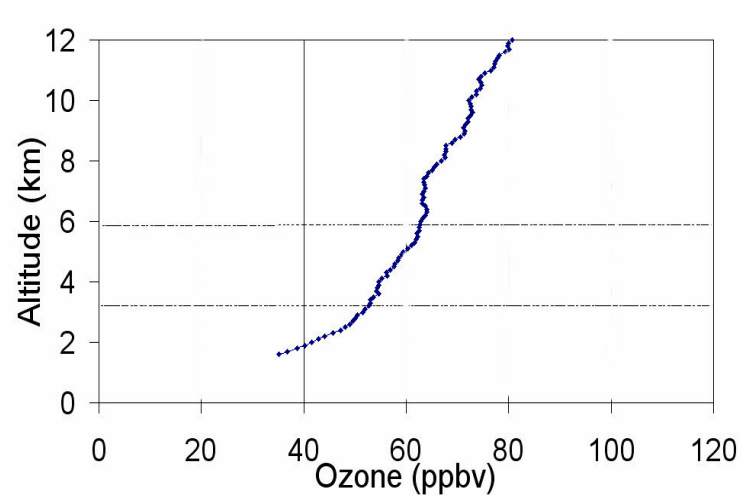


Figure 4.9: Vertical ozone structures (a) identified by SOMs (b) associated with the easterly wave system

The three ozone profiles remaining from the classifications are presented in Figures 4.10(a), (b) and (c). A typical spring ozone profile (Figure 4.10a) was characterised by ozone enhancement and uniform distribution of ozone throughout the troposphere. The autumn-dominated ozone profile (Figure 4.10b) exhibited low overall tropospheric ozone. The continental high ozone profile (Figure 4.10c) showed a steady increase of tropospheric ozone, with noticeable ozone enhancement at 3km.

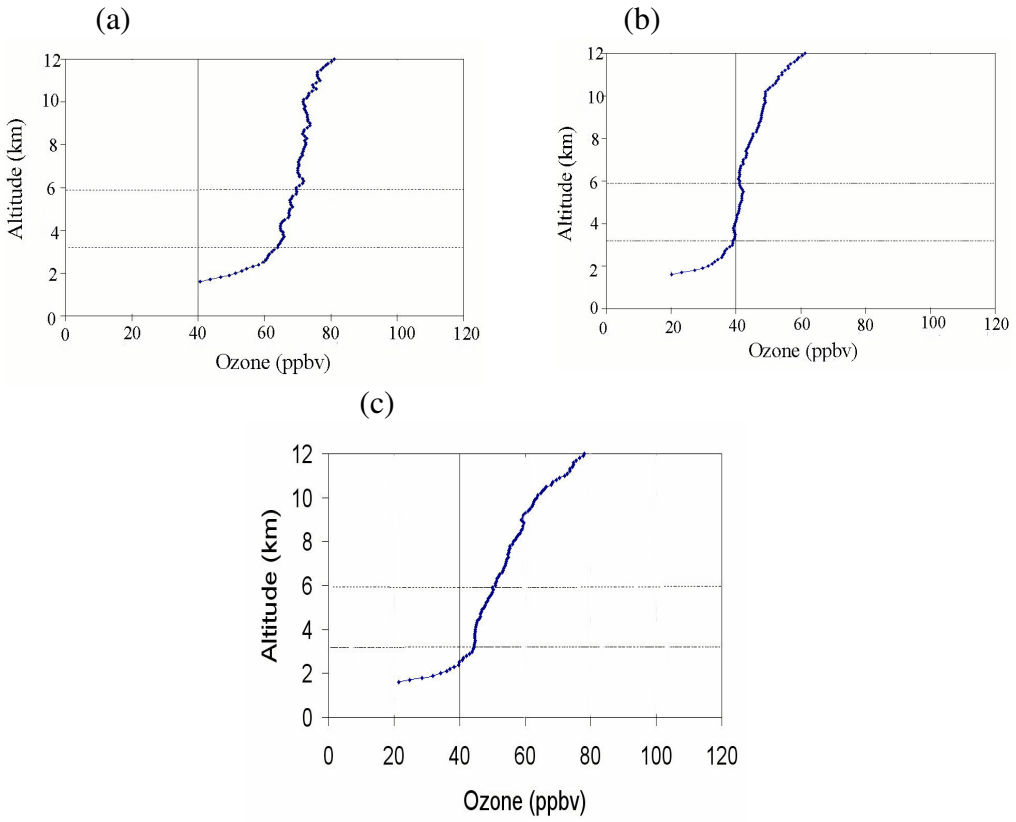


Figure 4.10: (a) and (b) Vertical ozone structures identified by SOMs, and (c) continental high associated ozone profile

Six categories of vertical tropospheric ozone structures that normally occur over the South African Highveld were identified using SOMs and synoptic systems (Figures 4.11(a) to (f)).

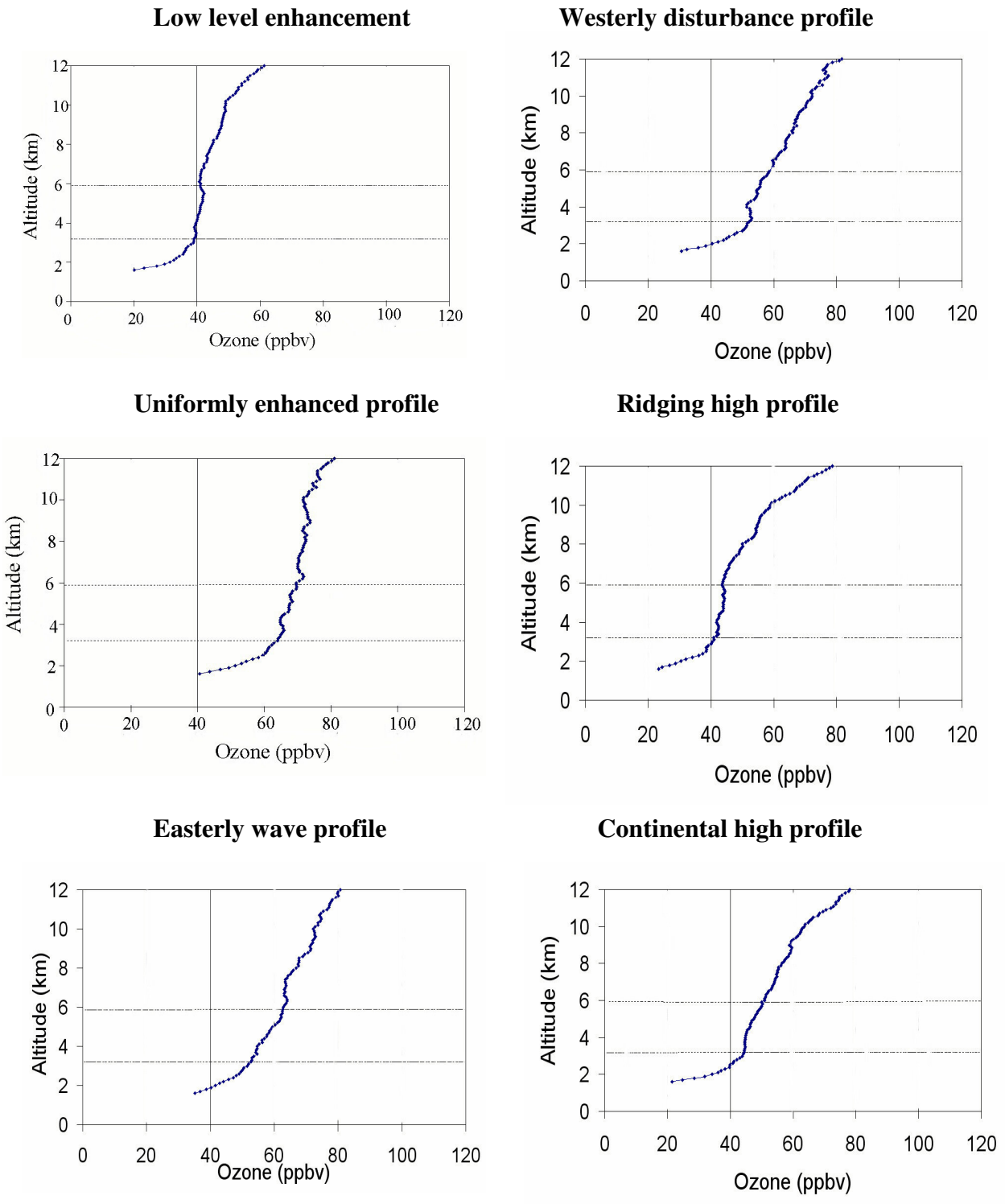


Figure 4.11: Vertical tropospheric ozone structures over the South African Highveld derived from SOMs and synoptic systems

Comparison with TWINSPAN and SPSS derived vertical ozone structures.

Previous studies have determine tropospheric ozone patterns over Johannesburg and Irene in South Africa using TWINSPAN (Two-Way Indicator Species Analysis) and SPSS (Statistical Package for the Social Science, version 11, 2001) respectively (Diab *et al*., 2003; Diab *et al*., 2004). The analyses in this study were more inclusive as a large number of profiles were used as compared to the TWINSPAN technique which was very selective, using 10 % of the available profiles in the classification. In all classifications, the data between the surface and 12 km were utilized. Even though the methods of analysis were different, the results of the analyses give fairly similar ozone structures (Figures 4.12 – 4.15). However, this study identified some structures which were not identified by Diab *et al*. (2003) and Diab *et al*. (2004) ((Figures 4.16 (a) and (b)) because of the large number of profiles used in this classification.

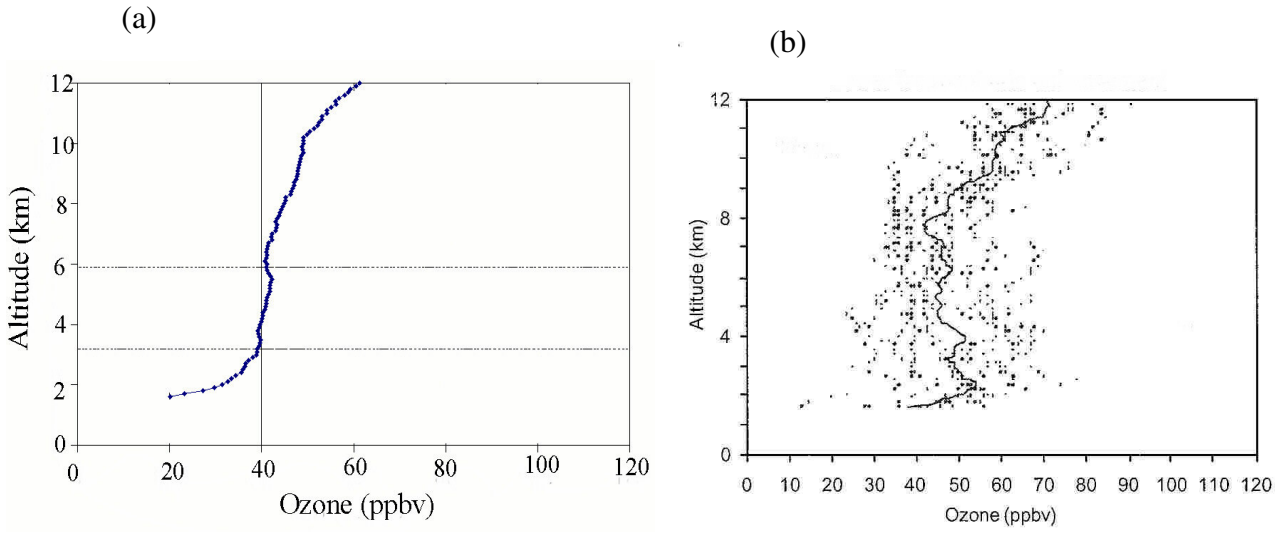


Figure 4.12: Vertical ozone profiles (a) identified by SOMs (b) TWINSPAN (Diab *et al*., 2003)

This structure ((Figures 4.12(a) and (b)) is similar to the one referred to as "lower tropospheric enhancement" by Diab *et* al. (2003) which is characterized by the presence of the lower tropospheric ozone enhancement reaching the average maximum of ~70 ppbv. The difference between these two profiles is the location of the tropospheric enhancement and the levels at which low ozone concentrations were observed. For the profile identified in this study, the enhancement appears at <6 km and low ozone concentrations at 6km. However in Diab *et al*. (2003) the enhancement appears <5 km, exhibited low ozone concentrations between 5 and 8 km. They both display ozone steady increase between 8 and 12 km. These profiles are normally observed during autumn or winter months when absolutely stable layers are more pronounced, which explain the build-up of ozone in the lower troposphere. Trajectory analysis in both studies indicated the that at 750 hPa indicated that air masses primarily originated from African countries (such as Namibia and Zambia) whereas at 500 hPa were dominated by the strong westerly flow from the west Atlantic Ocean bringing in clean maritime air.

A spring time profile ((Figures 4.13(a), (b) and (c)) was identified by all techniques discussed above. High ozone concentrations occur near the earth's surface (~40 ppbv). This type of profile was referred to "Considerable tropospheric enhancement" and represented polluted atmospheric conditions (Diab *et* al., 2003 and Diab *et* al., 2004) respectively. Profiles in this study and Diab *et* al. (2004) exhibited ozone concentrations between 70 and 80 ppbv, whereas in Diab *et* al. (2003) ozone concentrations between 80 and 100 ppbv were observed throughout the troposphere. Trajectory analysis in this study showed that continental air masses from southern Africa dominated at 750 hPa, whereas in Diab *et* al. (2004) continental air masses from southern Africa dominated at 500 hPa. High concentrations of ozone observed coincide with southern Africa burning season which occurs from May to October, suggesting that biomass burning is one of the major contributions of precursor gases.

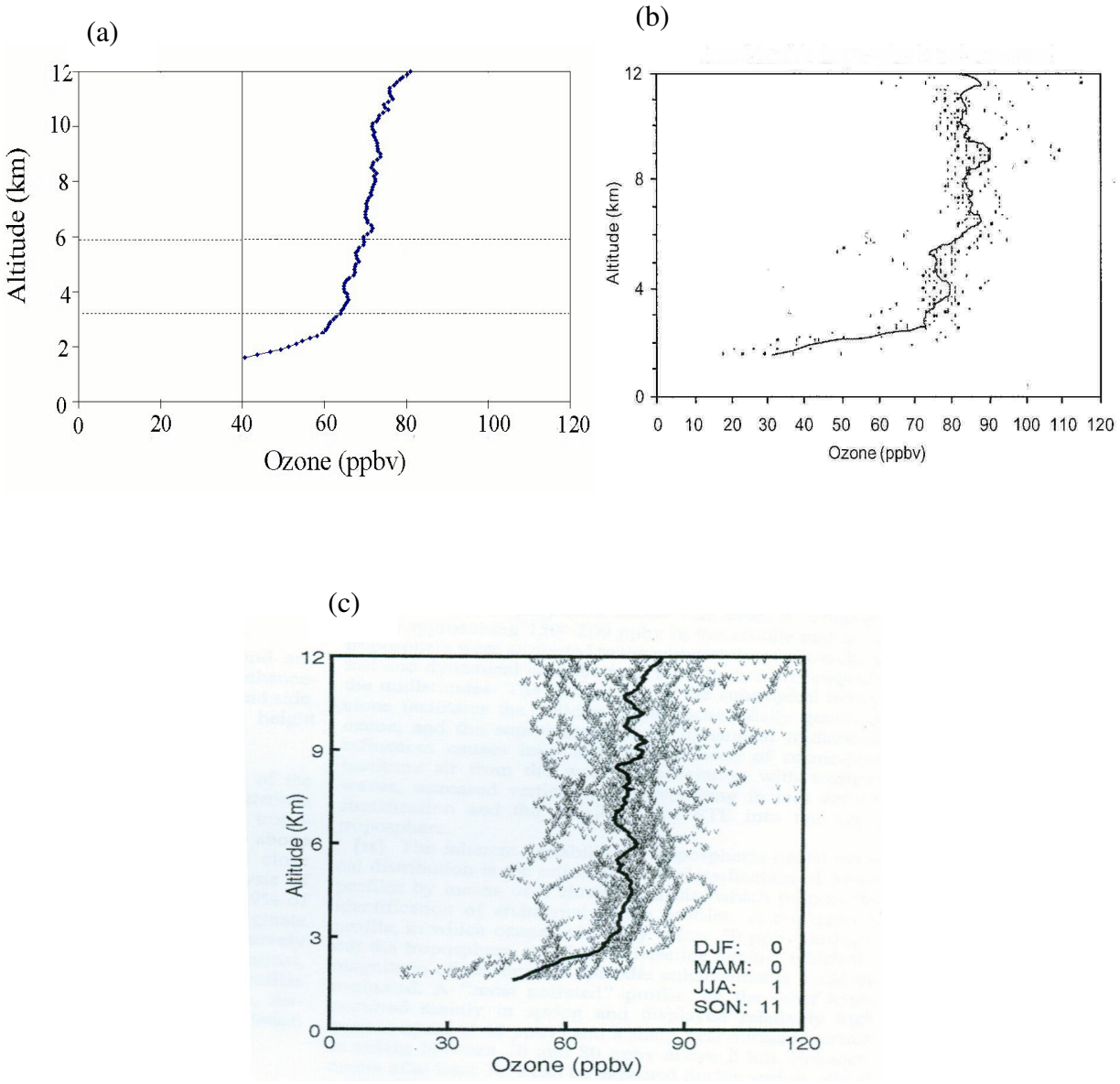


Figure 4.13: Vertical ozone profiles (a) identified by SOMs (b) TWINSPAN (Diab *et al*., 2003) and (c) SPSS (Diab *et al*., 2004)

The profile (Figures 4.14(a) and (b)) was identified is this study as associated with the ridging high systems and referred to "Ridging High Profile" and is similar to the one identified by Diab *et al*. (2004). Ozone enhancement lies at <6 km and <8 km for the profiles observed in this study and Diab *et al*. (2004) study. The profile identified in this study showed a sharp increase of ozone concentrations at ~8 km, whereas in

Diab *et al*. (2004) study an increase was observed at 9 km. This type of ozone profile is predominantly observed during winter and autumn but not exclusively as some profiles where observed during summer and fewer in spring (<5 %). The profiles exhibited strong ozone gradient which suggests the possible stratospheric tropospheric ozone transfer. Air masses at 500 hPa primarily originated from the west Atlantic Ocean. Even though at 750 hPa air masses predominantly originated from the west Atlantic Ocean, some (38 %) originated over southern Africa contributing to low level ozone build-up observed.

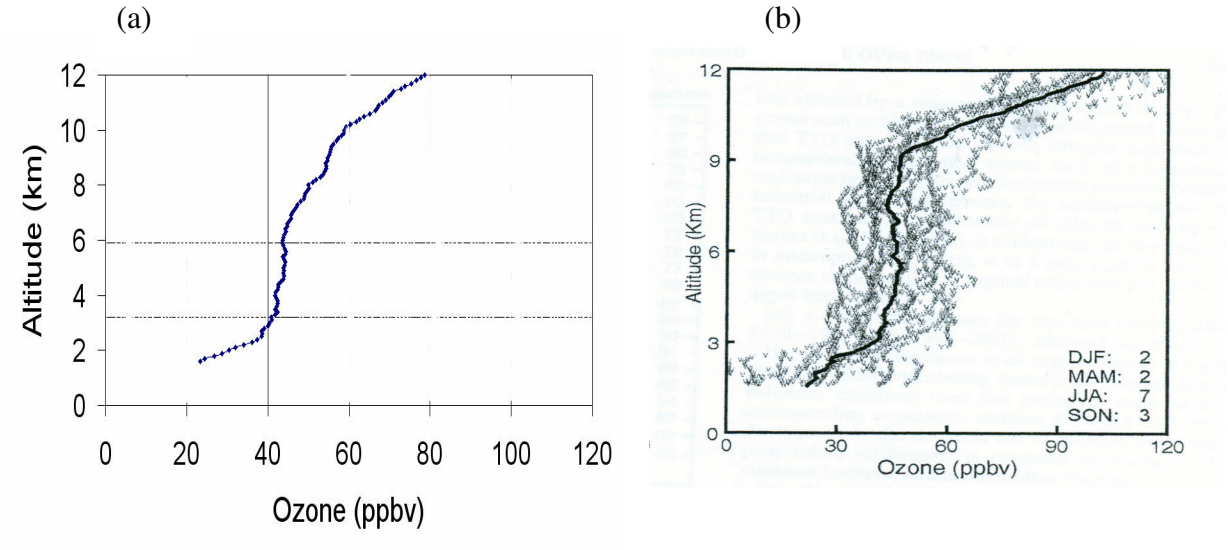


Figure 4.14: Vertical ozone profiles (a) associated with the ridging high system (b) SPSS (Diab *et al*., 2004)

All the above techniques have indicated that, this pattern ((Figures 4.15(a), (b) and (c)) shows no seasonal dependence as it occurs throughout the year. Diab *et al*. (2003) referred to this profile as Steady tropospheric increase". Generally ozone concentrations steadily increase from the average surface concentration of ~30 ppbv to an average concentration of the order 70 and 80 ppbv at 12 km. However, in Diab

et al. (2003) study there is a slight decrease of ozone concentrations between 10 and 12 km. Trajectories in all studies showed air masses originated primarily from the west Atlantic Ocean bringing with fewer of continental origin.

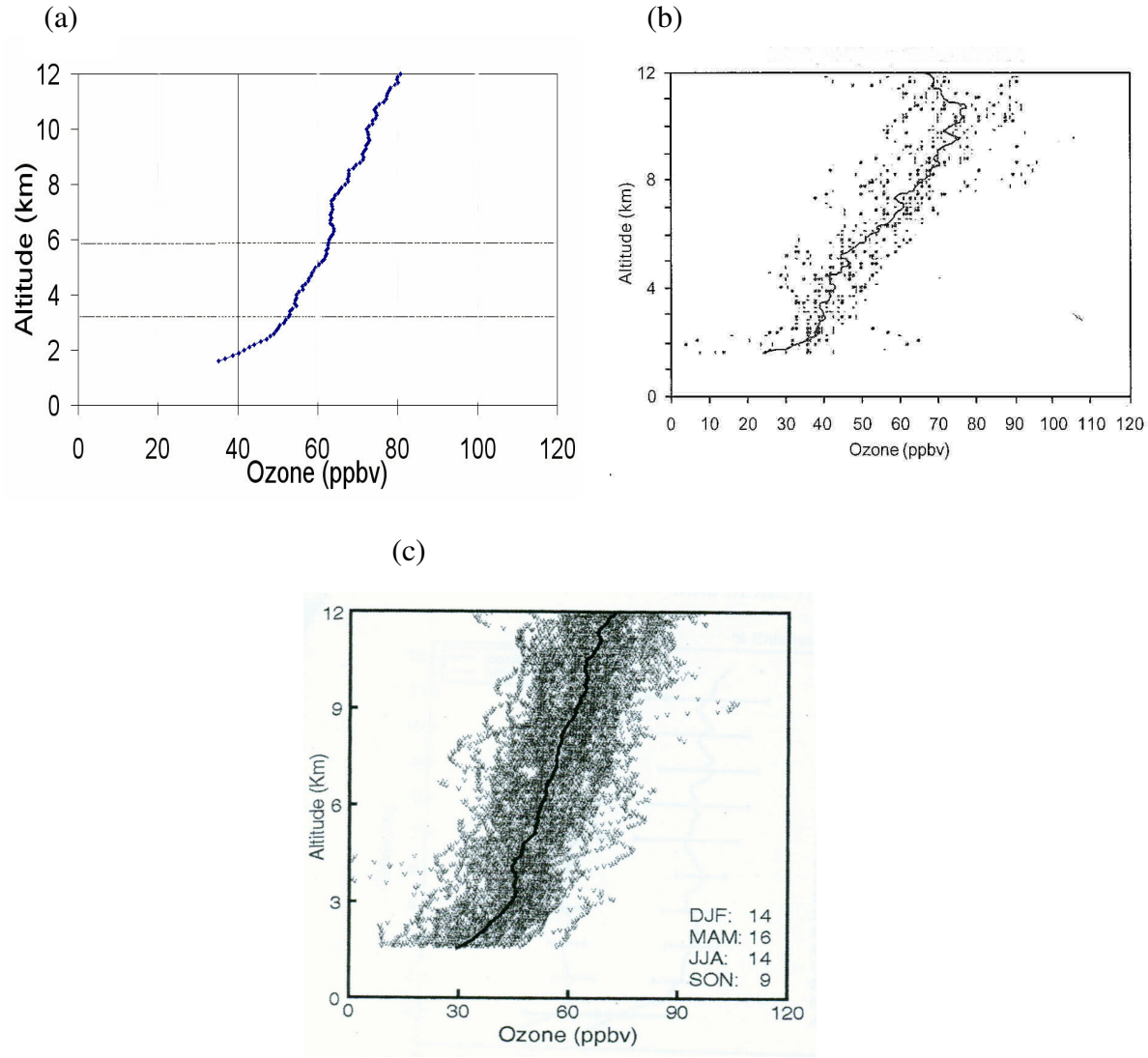


Figure 4.15: Vertical ozone profiles (a) identified by SOMs (b) TWINSPAN (Diab *et al*., 2003) and (c) SPSS (Diab *et al*., 2004)

The remaining two profiles identified in this study but were not identified by Diab *et al*. (2003) and Diab *et al*. (2004) (Figures 4.16 (a) and (b)). These two profiles are associated with the continental high conditions (Figure 4.16a) and westerly disturbance conditions (figure 4.16b) respectively. Ozone profiles associated with continental high conditions display ozone stratification and noticeable ozone enhancement above 4 km. Steady increase of ozone concentrations were observed in some of the profiles. These types of profiles are more pronounced during winter months. Westerly wave associated profiles generally have higher ozone values near the earth's surface and ozone concentrations steadily rise from between 4 and 10 km.

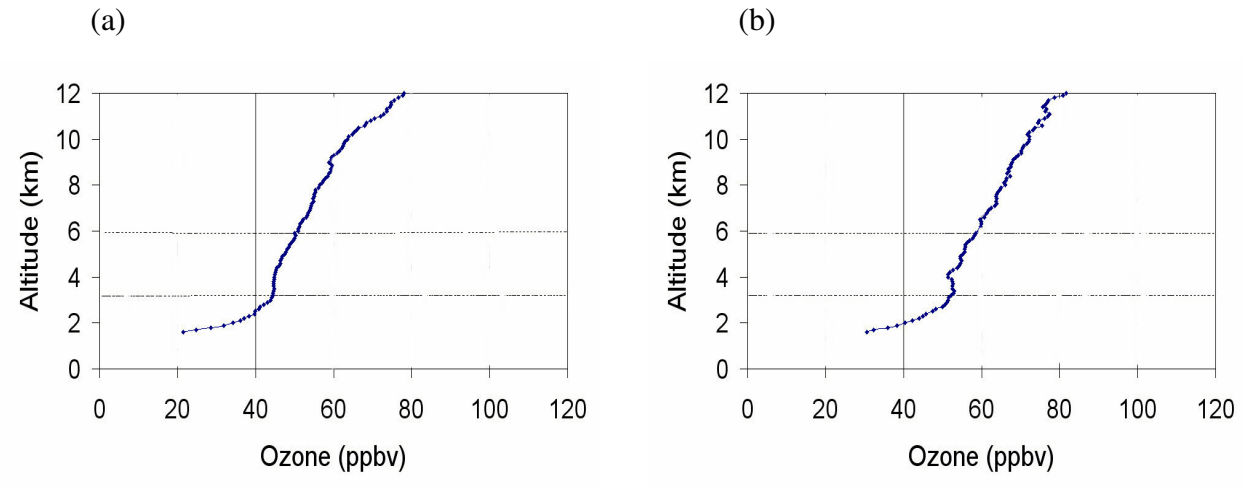


Figure 4.16: Vertical ozone structures (a) Continental high profile (b) Westerly wave profile

The three techniques are in agreement as the results of the analysis gave similar ozone structures except for the few identified in this study due to the large number of profiles used in this classification.

Tropopause height variations and ozone distribution in the upper troposphere

In the previous sections, some of identified vertical ozone structures (for example, a ridging high ozone profile) displayed a deep and strong ozone gradient between 10 and 12 km. This could have been the result of a transfer of ozone from the lower levels of the stratosphere into the upper levels of the troposphere. Ozone-rich air descends from the stratosphere into the troposphere and the transfer is primarily controlled by smaller-scale processes (such as cut-off low systems, and tropopause folding) (Stohl *et al*., 2003; Collins *et al*., 2003; Seo and Bowman, 2001). It was established that the South African Highveld experiences cut-off low systems, with the highest frequency of occurrence between April and September (Taljaard, 1985). When these systems become well-developed and mature, tropopause folding occurs which results in ozone being transported downward into the upper levels of the troposphere (Zunckel, 1992).

Ozonesonde data for the two study periods were divided into two groups: the first group contains all ozone profiles with tropopause heights above the average value of ~15.8 km, whilst the second group contains ozone profiles with tropopause heights below ~15.8 km. Occurrence frequencies and average ozone profiles for both groups were constructed (Figure 4.17 and 4.18, respectively).

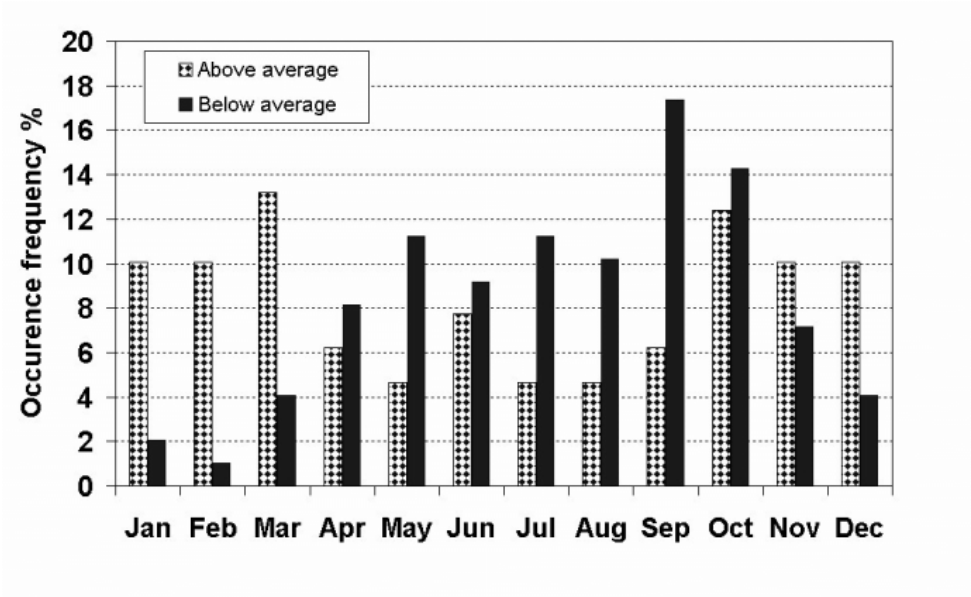


Figure 4.17: Occurrence frequencies of the tropopause heights below and above average value (~15.8 km) over the South African Highveld region

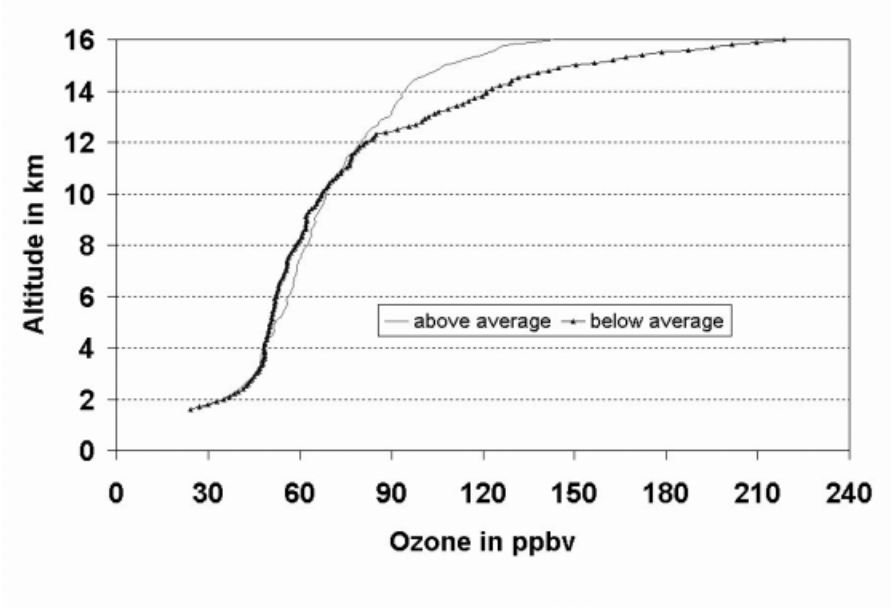


Figure 4.18: Average ozone profiles associated with the tropopause below and above average value (~15.8 km) over the South African Highveld region

It appears that the occurrence of the tropopause height below the average occurred during autumn to early summer with a maximum in September (Figure 4.17). This is in agreement with the appearance of cut-off low systems which have high frequency in April and September (Bruintjies *et al*., 1990). Activities occurring in the upper levels of the troposphere may account for the high ozone concentrations and a strong ozone gradient (as observed in a ridging high ozone profiles and discussed in the previous chapters).

Below an altitude of 4 km, both average ozone profiles displayed similar ozone concentrations (~30 to 50 ppbv) (Figure 4.18). However, ozone profiles with a height >15.8 km exhibited higher ozone concentrations between 4 and 10 km. Between 10 and 12 km, they displayed similar features and ozone concentrations. Above 12 km, ozone profiles with a tropopause height <15.8 km had higher ozone concentrations and a strong ozone gradient (with a difference of ~75 ppbv at 16 km between the two groups). This indicates that the lowering of the tropopause height is related to high ozone concentrations in the upper levels of the troposphere, suggesting the possibility of ozone-rich air from the stratosphere being injected into the troposphere.

Seasonal variability of tropospheric ozone over the South African Highveld

It was established that tropospheric ozone over the South African Highveld region follows an annual cycle, with a maximum in spring and a minimum in autumn (Thompson *et al*., 1996a). However, there are uncertainties about the origin of the spring maximum, with some authors (for example, Monks (2000)) suggesting that high ozone concentrations observed during spring could be the result of:

(a) Stratospheric injection of ozone into the troposphere;

(b) Ozone being transported from polluted countries; or

(c) Ozone produced in the troposphere by photochemical reactions involving ozone precursor gases.

Seasonally averaged tropospheric ozone profiles (with tolerance bars), together with averaged relative humidity, were constructed and plotted in Figures 4.19 and 4.20 for the two study periods, 1990 to 1993 and 1999 to 2003, respectively. The number of ozone profiles used is shown in brackets on the figures.

Ozone enhancement (as discussed previously) at <4 km is evident in some of the average ozone profiles, especially in the winter ozone profile for the period 1999 to 2003.

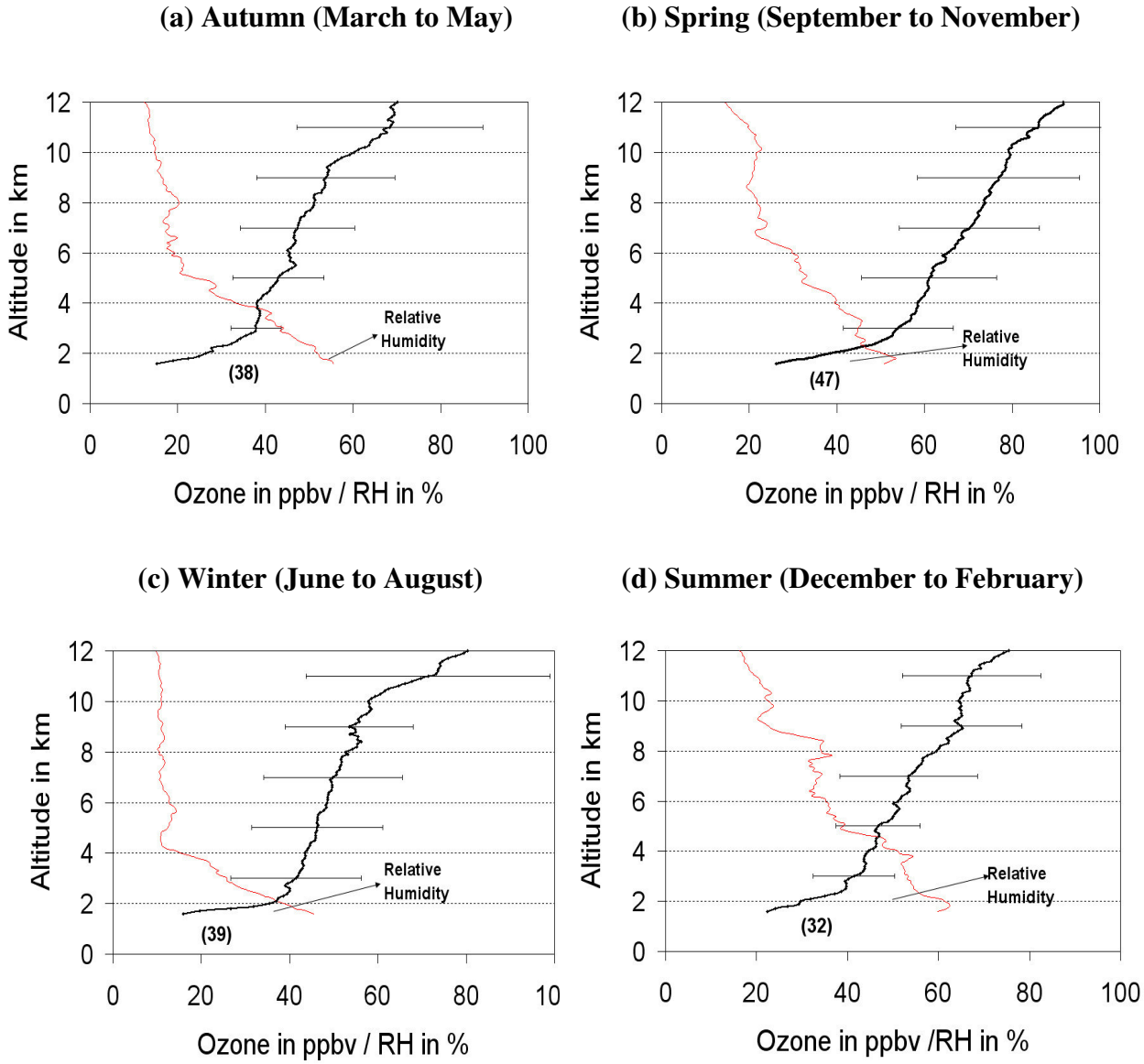
Autumn average ozone profiles showed ozone concentrations increasing steadily with height and exhibiting low ozone concentrations throughout the troposphere, with a maximum of <80 ppbv. High relative humidity (~60 %) near the earth's surface was responsible for the lower ozone concentrations observed at that altitude.

Spring ozone profiles display overall high tropospheric ozone concentrations and high variability throughout the troposphere (as indicated by the tolerance bars) especially for the period 1999 to 2003. Generally ozone concentrations increase steadily with height, leading to a strong ozone gradient at 12 km. This expected maximum can be attributed to several factors such as biomass burning, and stratospheric tropospheric exchange as previously discussed (Barsby and Diab, 1995; Diab *et al*., 2004). However, high ozone concentrations and high average relative humidity (~50 %) near the earth's surface suggests that ozone was either produced from photochemical reactions or came from the polluted boundary layer (Thouret *et al.,* 2000).

In winter, the average ozone profiles were characterised by high variability (as indicated by the tolerance bars) and display strong ozone gradients between 9 and 12 km. This suggests the possibility of stratospheric transfer of ozone into the upper levels of the troposphere. A noticeable ozone enhancement is evident at <4 km in the

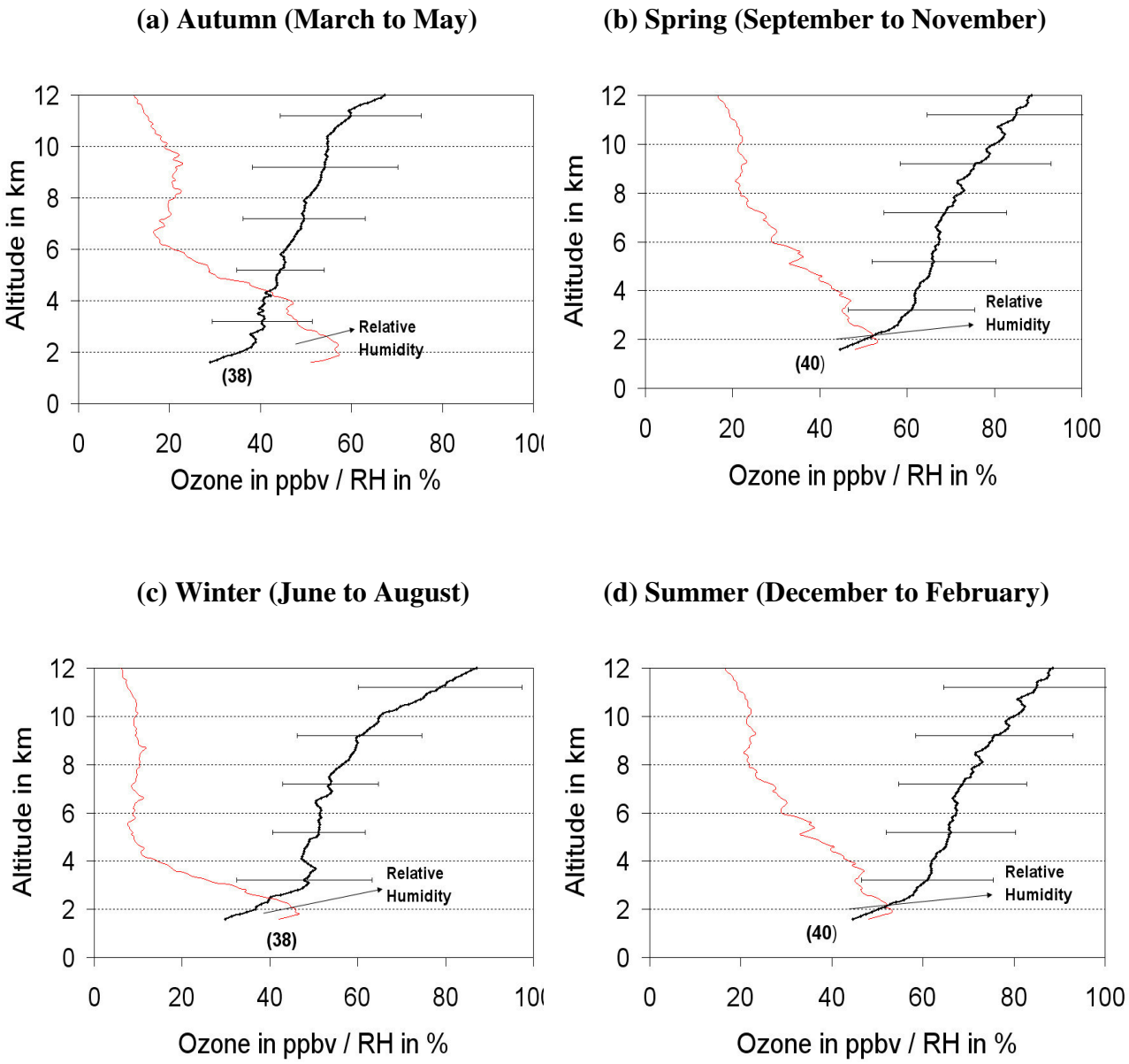
average ozone profile for the period 1999 to 2003, indicating the existence of the absolutely stable layer at 700 hPa.

Summer ozone profiles also exhibited a lower enhancement in ozone at <4 km. Ozone concentrations increased steadily with height reaching the maximum ranging from 70 to 80 ppbv. Relative humidity values in summer for both periods are higher (~60 to ~70 %), coinciding with the high concentrations of ozone at <4 km, suggesting that ozone either comes from photochemical production or convection from the polluted boundary layer (Leung *et al*., 2004; Thouret *et al*., 2000).



Legend: The tolerance bars indicate one standard deviation, above and below the average profile. The vertical line at 60 ppbv used as a reference line in each case.

Figure 4.19: Seasonally averaged tropospheric ozone profile and average relative humidity over the South African Highveld for 1990 to 1993



Legend: The tolerance bars indicate one standard deviation, above and below the average profile. The vertical line at 60 ppbv used as a reference line in each case.

Figure 4.20: Seasonally averaged tropospheric ozone profile and average relative humidity over the South African Highveld for 1999 to 2003

Seasonal variations of tropospheric ozone at different altitudes

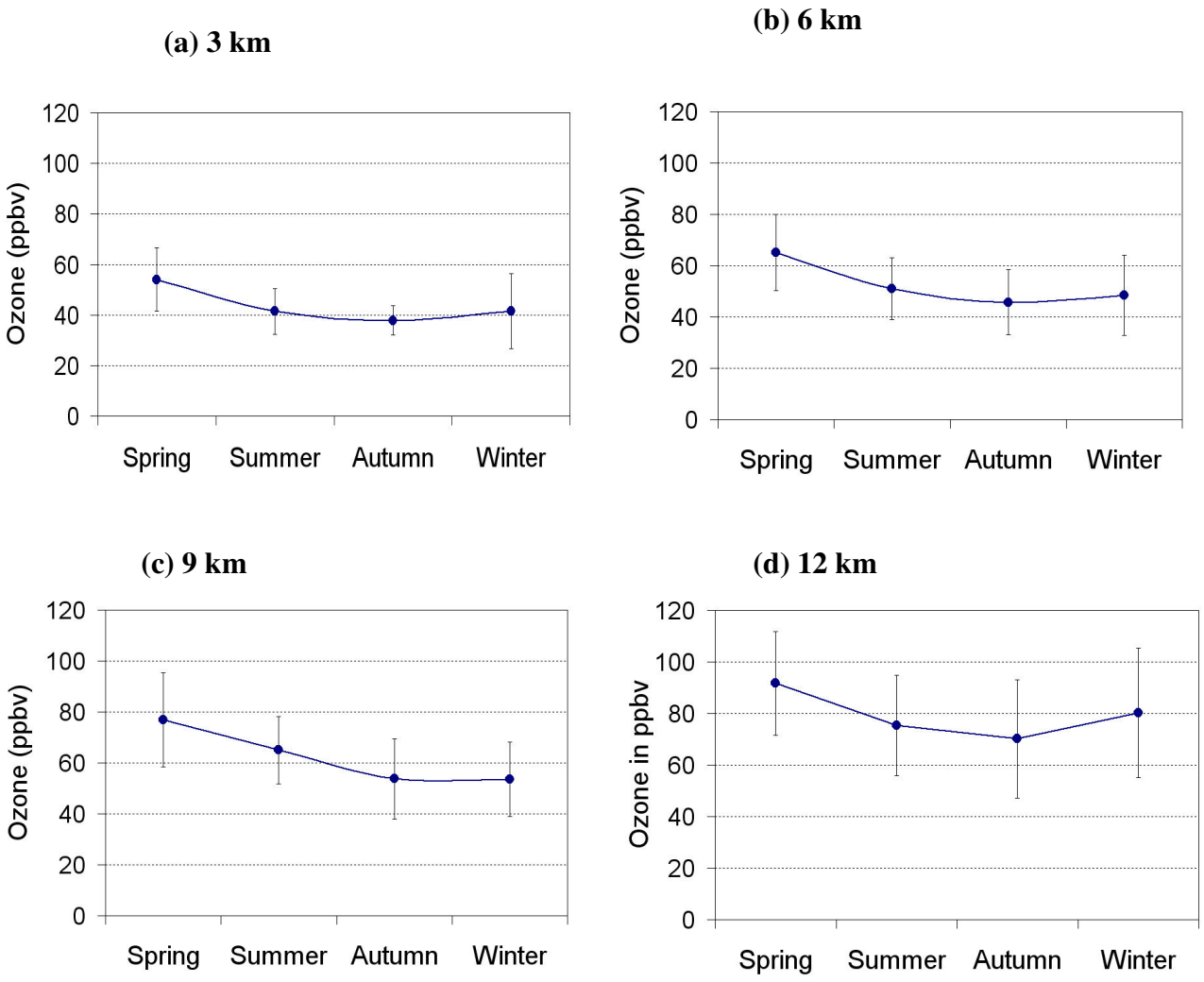
Seasonal variations of ozone concentrations within the troposphere are presented (Figures 4.21(a) to (d) and 4.22(a) to (d)) for the two study periods.

Higher ozone concentrations prevailed during spring at all heights. The ozone concentrations for both periods ranged between 50 to 60 ppbv at 3 km, with a value between 85 to 90 ppbv at 12 km. During summer, higher ozone concentrations were displayed than in winter at 3, 6, and 9 km altitudes. However, at 12 km, winter ozone profiles displayed higher values than summer ozone profiles. Ozone concentrations were found to be the lowest in autumn at all heights over the two periods.

At 3 km ozone concentrations ranged between 38 ppbv in autumn to 54 ppbv in spring over the period 1990 to 1993. During 1999 to 2003, ozone concentrations ranged from ~40 ppbv in autumn to 60 ppbv in spring at 3 km.

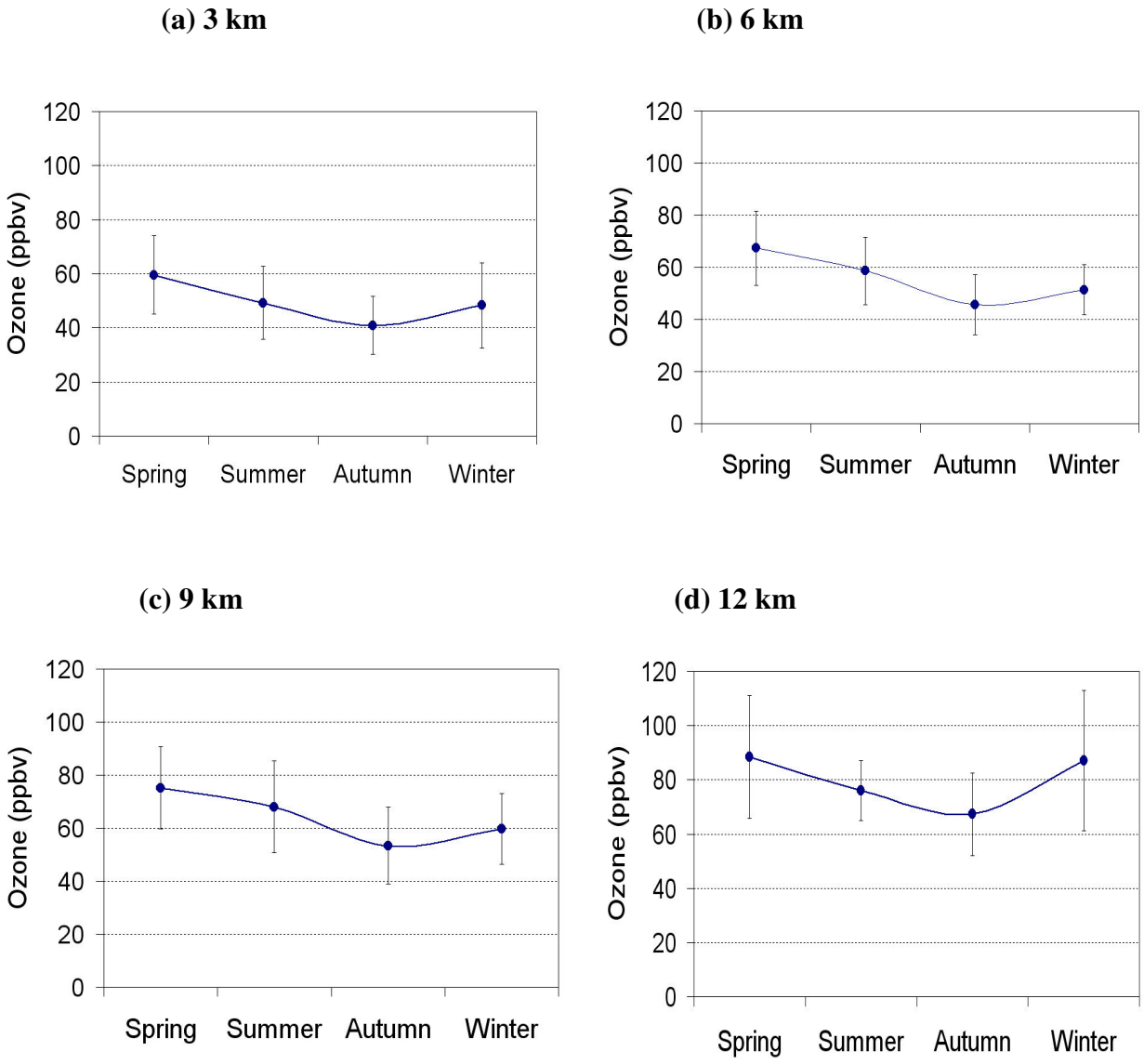
At 12 km ozone concentrations ranged from ~70 ppbv in autumn to ~92 ppbv in spring over the period 1990 to 1993. During the period 1999 to 2003, ozone concentrations ranged from ~67 ppbv in autumn to 89 ppbv in spring.

There was an increase in tropospheric ozone in the lower troposphere from the period 1990 to 1993, to 1999 to 2003 which was also observed and discussed in the previous chapters. However, at 12 km; there was a decrease in ozone concentration during the period 1999 to 2003.



Legend: The tolerance bars indicate ± one standard deviation.

Figure 4.21: Seasonal variation of tropospheric ozone at different altitudes for the period 1990 to 1993



Legend: The tolerance bars indicate ± one standard deviation.

Figure 4.22: Seasonal variation of tropospheric ozone at different altitudes for the period 1999 to 2003

Temporal variations of tropospheric ozone

Tropospheric ozone over the South African Highveld region has increased since the 1970s (Zunckel, 1992), as outlined previously. In this section, data collected during the SAFARI-92 and SAFARI-2000 field campaigns, are compared to investigate this phenomenon further. Average ozone profiles constructed for SAFARI-92 and SAFARI-2000 are presented in Figure 4.23.

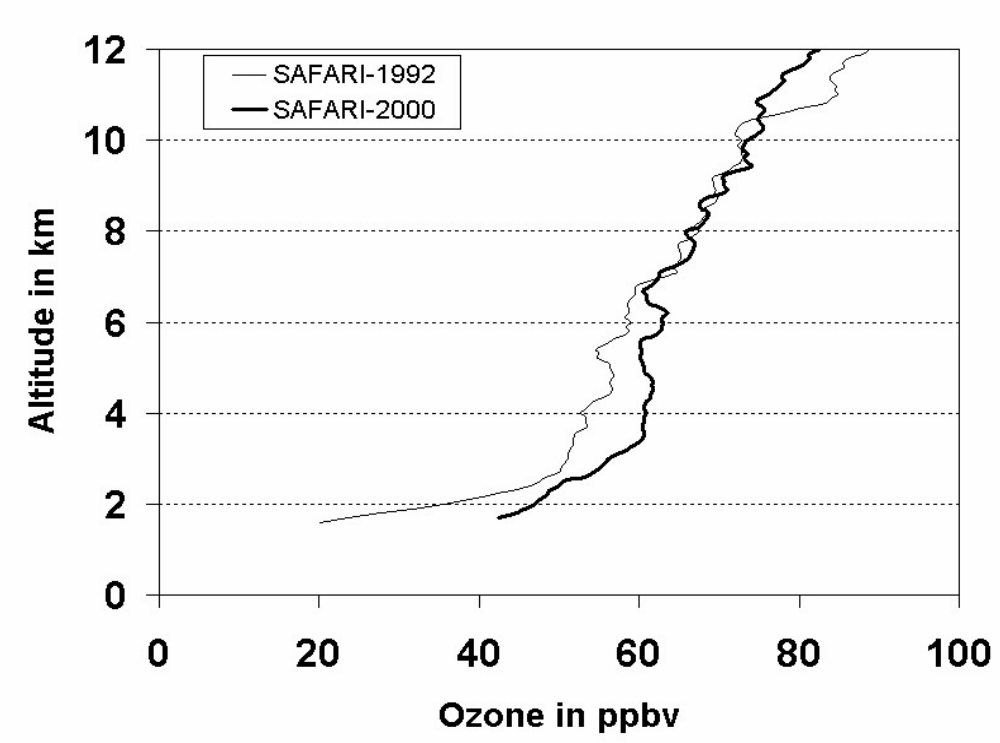


Figure 4.23: Average tropospheric ozone profiles during SAFARI-92 and SAFARI-2000

Average ozone profiles from both SAFARI campaigns showed similar features from the earth's surface to ~7 km. Both ozone profiles displayed noticeable enhancement in ozone concentrations at <7 km, with a minimum average of 20 ppbv during SAFARI-92 and a minimum average of 40 ppbv during SAFARI-2000. The

individual ozone profiles during 2000 exhibited high ozone concentrations (up to 60 ppbv) near the earth's surface, whilst individual ozone profiles during 1992 were <30 ppbv near the earth's surface. Between 7 and 10.5 km, there was not much change in ozone concentrations since 1992. However, between altitudes of 10.5 to 12 km the average ozone profiles displayed lower ozone concentrations during 2000 as compared to 1992. This indicates an increase in tropospheric ozone over the South African Highveld from the 1970s, in the lower altitudes of the troposphere, but a decrease in higher altitudes of the troposphere.

****

The effects of synoptic weather systems on the distribution of tropospheric ozone have been discussed. Ozone structures normally observed over the South African Highveld have been outlined after comparison between SOMs-derived structures and synoptic systems-related structures. Comparison of SOMs, TWINSPAN and SPSS ozone structures was done. The position of tropopause height affects the proportion of ozone in the troposphere. A low tropopause height is related to high concentrations of ozone exhibiting a strong ozone gradient which is less pronounced with tropopause height located higher in the upper levels of the troposphere. Tropospheric ozone over the South African Highveld displayed seasonal variations with high ozone concentrations in spring and low ozone concentrations in autumn. It is apparent that tropospheric ozone over this region has increased since the 1970s, especially in the lower levels.

CHAPTER 5:
SUMMARY

Despite the concern about tropospheric ozone, its contribution to climate change is uncertain in South Africa, since few studies have been undertaken on this topic. Air masses originating from southern Africa have been shown to have a great impact on tropospheric ozone over the South African Highveld. Findings for this research study will be discussed in this chapter.

Vertical Tropospheric Ozone Distribution over the South African Highveld

Different vertical structures of tropospheric ozone over the South African Highveld have been investigated using SOMs and major synoptic systems, as it is well known that ozone profiles respond differently to each major meteorological synoptic system, producing unique vertical structures. These two methods have identified similar vertical ozone structures, resulting in six major tropospheric ozone structures which normally occur over the South African Highveld (Figure 4.11).

Some of ozone structures identified in this study are similar to those identified by TWINSPAN (Two-Way Indicator Species Analysis) and SPSS (Statistical Package for the Social Science, version 11, 2001) (Diab *et al*., 2003; Diab *et al*., 2004) respectively.

All ozone profiles displayed ozone enhancement at <4 km with the exception of the easterly wave and uniformly enhanced ozone profiles (Figure 4.11). This indicates the influence of an absolutely stable layer at 700 hPa on the vertical distribution of trace gases in the troposphere. Trace gases in the troposphere are trapped below this layer

if it becomes persistent, contributing to tropospheric ozone through photochemical production.

High ozone episodes observed were investigated, to show whether El Niño or La Niña events could have an influence on ozone concentrations. The results were inconclusive.

Low-level enhancement ozone profile

This ozone structure was more pronounced in winter and autumn, exhibiting low ozone concentrations near the earth's surface. Ozone enhancement was evident at <6 km. Thereafter, ozone concentrations increased steadily at a slower rate with height, reaching a maximum of 90 ppbv.

Trajectory analysis showed air masses reaching the South African Highveld at 750 hPa were mainly continental air masses originating locally and from other African countries (such as Namibia and Botswana) and contributed to the enhancement of tropospheric ozone observed at <6 km as shown in Figure 3.3. These pollutants are then trapped between the absolutely stable layers at 700 hPa and 500 hPa that normally become persistent during winter (Kirkman *et al*., 2000; Cosijn and Tyson, 1996). Overall low ozone concentrations displayed by these ozone profiles are due to reduced anthropogenic activities (such as biomass burning) over southern Africa during autumn as established by other authors (Thompson *et al*., 1996b; Diab *et al*., 1996).

Westerly disturbance ozone profile

Ozone concentrations increased steadily with height between 4 and 12 km with a noticeable ozone enhancement displayed at <4 km. The individual ozone profiles in this group did not exceed a maximum of 90 ppbv except for a few cases. The occurrence frequencies (Figures 4.1 and 4.2) of the synoptic systems during the two

study periods had shown that westerly disturbances were more of a winter to spring phenomenon, coinciding with the burning season in southern Africa.

The enhancement at <4 km was due to the contribution of air masses originating from local sources and other African countries (such as Zambia) reaching the South African Highveld at 750 hPa (Figure 4.5(b)). At the 500 hPa level, some of the air masses originated from the local sources and other African countries (such as Botswana and Zambia), whilst the remainder originated from the west Atlantic Ocean and as far as South America (Figure 4.5(c)). The overall tropospheric ozone enhancement is due to biomass-burning emissions originating from other African countries (such as Botswana and Zambia) and South America, as these products can be transported at high altitudes via westerlies near 25°S latitude to the tropical south Atlantic Ocean (Piketh and Walton, 2004).

Uniformly enhanced ozone profile

This ozone vertical structure was only identified by SOMs as a typical spring ozone profile. Relatively high ozone concentrations were displayed uniformly from the earth's surface up to 12 km. This coincides with the southern Africa burning season which normally occurs from May to October (Scholes *et al*., 1996; Le Canut *et al*., 1996). Therefore, the high ozone concentrations observed could be the results of biomass-burning emissions being transported to the South African Highveld. Subsidence dominated most days as established from the upper-air data, which lead to build-up of these biomass-burning emissions which then became subjected to production of tropospheric ozone, thus contributing to the high ozone concentrations observed in the ozone profiles contained in this group.

This is supported by movement of air masses originating from local sources as well as from other African countries (such as Botswana and Mozambique), at 750 hPa (Figure 3.5(b). However, at 500 hPa predominantly maritime air from the west Atlantic Ocean (Figure 3.5(c)). There was no indication of possible stratospheric

injection of ozone into the upper levels of the troposphere since ozone is uniformly distributed throughout the troposphere. The coincidence of high relative humidity and high ozone concentrations near the earth's surface suggests that ozone came from either photochemical production, or convection from a polluted boundary layer (Thouret *et al*., 2000).

Ridging high ozone profile

This ozone vertical structure normally occurs during winter and autumn. Low ozone concentrations were displayed near the earth's surface, with an average minimum of <20 ppbv reaching the average maximum of ~90 ppbv. Ozone profiles displayed ozone concentrations increasing steadily with height and a strong ozone gradient between 10 and 12 km.

Ozone enhancement was also observed at <6 km. This was due to continental air masses that primarily originated from local sources and other African countries (such as Zimbabwe) reaching the South African Highveld at the 750 hPa level (Figure 4.4(b)). This could be linked to the existence of the absolutely stable layers at the 700 and 500 hPa levels, because it is during this period that absolutely stable layers are more pronounced (Cosijn and Tyson, 1996).

High ozone concentrations observed between 10 and 12 km were linked to the lowering of the tropopause associated with ozone being transferred from the lower levels of the stratosphere to the upper levels of the troposphere. In this study it was established that a low tropopause height over the South African Highveld normally occurs during winter. The average tropopause height during the days when the ridging high prevailed was ~15.1 km below the average value. Previous studies have shown that the South African Highveld is sometimes under the influence of deep, well-developed, mid-latitude cyclonic systems (known as cut-off low systems) with a maximum between April and September (Bruintjies *et al*., 1990; Bamber *et al*., 1984; Taljaard, 1985). When those systems have matured, tropopause folding might occur

with the possible stratospheric injection of ozone into the troposphere (Zunckel, 1992), explaining the high ozone concentrations observed.

Easterly wave ozone profile

This zone structure showed a steady increase of ozone concentrations from the earth's surface up to 12 km. The structure is not seasonally dependent as it occurs throughout the year with the maximum occurrence in spring, during which easterly wave systems have the highest frequency (Figure 4.1 and 4.2).

This coincides with the biomass-burning season in southern Africa, resulting in biomass-burning emissions being transported to the South African Highveld. Trajectory analysis showed some of the continental air masses reaching the South African Highveld at 750 hPa (Figure 4.6(b)) were of continental origin from local sources and other African countries (such as Namibia and Mozambique). Overall high ozone concentrations displayed by individual ozone profiles are due to easterly waves bringing air rich in ozone from the tropics.

Continental high ozone profile

This ozone structure had small, but noticeable, ozone enhancement appeared at 3 km, with low ozone concentrations near the earth's surface. Ozone profiles showed a vertical stratification with height that is facilitated by the presence of absolutely stable layers (Kirkman *et al*., 2000). Generally, continental high systems are more pronounced during winter when absolutely stable layers at 700 hPa and 500 hPa may become persistent (Cosijn and Tyson, 1996).

Overall low ozone concentrations could be the contribution of air masses primarily originating from the adjacent Atlantic and Indian Oceans at 750 hPa and from the west Atlantic Ocean at 500 hPa reaching the South African Highveld (Figure 4.3(b) and (c)). This is corroborated by previous studies which established that there is a poor relationship between anticyclonic conditions and ozone content (Barsby and

Diab, 1995). The enhancement at <4 km was supported by some of the trajectories of continental air masses reaching this region at 750 hPa (Figure 4.3(b)).

Seasonal and Temporal Variations of Ozone over the South African Highveld

Tropospheric ozone over the South African Highveld follows an annual cycle, with minimum in autumn and maximum in spring, and is in agreement with previous studies (Thompson *et al*., 1996a). In this study, analysis showed that spring ozone profiles exhibited higher ozone concentrations from the earth's surface up to 12 km and summer ozone profiles displayed high ozone concentrations at 3, 6, and 9 km altitudes. Winter ozone profiles had lower ozone concentrations as compared to both spring and summer at low altitudes – but, at 12 km, they exhibited higher ozone concentrations and a strong ozone gradient. Autumn ozone profiles had the lowest ozone concentrations throughout the troposphere. There are still uncertainties as to the origin of the spring tropospheric ozone maximum: some authors linked this maximum to stratospheric tropospheric exchange of ozone (Junge, 1962), whilst others linked it to biomass burning (Thompson *et al*., 1996b). Diab *et al*. (2004) suggested that the effect of biomass burning over this region is less significant. However, out of 64 ozonesondes launched between September and November for both study periods, 53 ozone profiles (83 %) were associated with air masses originating from other African countries (such as Mozambique, Botswana, Zambia, and Zimbabwe). Hence, air masses originating from these countries – especially during southern Africa's burning season – possibly affect concentrations of ozone in the South African Highveld troposphere, and could be responsible for the ozone enhancement observed during spring.

It was established in this study that tropopause height over the South African Highveld exhibits an annual cycle with a maximum occurring in summer and a minimum in winter with an average of ~15.8 km. It was also established that the lowering of the tropopause height to below the average value of ~15.8 km is accompanied by a strong ozone gradient and high ozone concentrations appearing

between 10 and 12 km. The deep ozone gradient observed especially during the winter period was attributed to the lower tropopause height accompanied by the injection of ozone from the low levels of the stratosphere into the upper levels of the troposphere. This could be linked to cut-off low system occurrence which has a maximum in April and a secondary maximum in September (Bruintjies *et al*., 1990; Taljaard, 1985). These systems can initiate tropopause folding, leading to the transfer of ozone from the stratosphere to the troposphere (Zunckel, 1992).

Ozone profiles for the period 1999 to 2003 showed higher ozone concentrations than ozone profiles over the period 1990 to 1993. This average increase of ~10 ppbv was also observed by Diab *et al.* (2004). When comparing SAFARI-92 and SAFARI-2000 ozonesonde data, an increase in tropospheric ozone was observed between 2 and 7 km. However, from 10.5 to 12 km ozone profiles during 1992 displayed high ozone concentrations compared to ozone profiles for 2000. These findings suggest that tropospheric ozone over the South African Highveld since the 1970s is more of tropospheric origin than stratospheric origin (and probably produced from photochemical reactions involving ozone precursor gases). This indicates that the concentrations of trace gases and other pollutants over the South African Highveld have increased – possibly due to the increasing population and industrial facilities, leading to the higher production of ozone in the troposphere (Zunckel, 2000; Diab *et al*., 2004).

****

Important findings emerged in this study, for example, major tropospheric structures occurring over the South African Highveld were highlighted. The influence of synoptic systems on tropospheric ozone has been discussed. Seasonal and temporal tropospheric ozone variations and the impacts of the location of the tropopause height on tropospheric ozone content have been discussed in detail.

CHAPTER 6:
CONCLUSIONS

Tropospheric ozone plays a crucial role in the atmosphere and affects the climate. High ozone concentration in the troposphere poses a threat to the environment and is regarded as a health hazard. In this chapter the findings of the research study are highlighted.

Vertical Distribution of Tropospheric Ozone over the South African Highveld

(1) Six vertical tropospheric ozone structures that normally occur over the South African Highveld were identified by using SOMs and major synoptic systems, some of which were seasonally dependant.

(2) The enhancement observed at lower altitudes was due to photochemical production of ozone from trace gases trapped below the 700 hPa absolutely stable layer and, in some cases, between the 700 hPa and 500 hPa absolutely stable layers.

(3) A typical spring ozone profile (uniformly enhanced ozone profile) had ozone concentrations uniformly distributed throughout the troposphere.

(4) A strong ozone gradient was evident in the some of the vertical structures, especially the ridging high ozone profiles. It was apparent that ozone has been transferred from low levels of the stratosphere to the upper levels of the troposphere.

(5) Trajectory analysis had shown that movement of air masses from local sources and other African countries were associated with the increase in ozone concentration, whereas moist maritime air primarily from the west Atlantic Ocean was associated with low ozone concentration over the

South African Highveld. It was also shown that air masses originating as far as South America, especially during the biomass-burning season, contributed in tropospheric ozone enhancement over this region.

Effects of Synoptic Systems on the Vertical Distribution of Ozone

(1) Ozone profiles associated with anticyclonic conditions exhibit stratification due to the possible appearance and persistence of absolutely stable layering as was displayed in the continental ozone profile.

(2) Ozone profiles associated with continental highs, ridging highs, westerly disturbances exhibited a noticeable ozone enhancement at <4 km.

(3) Easterly wave-associated ozone profiles exhibited high ozone concentrations and a steady increase of ozone concentrations up to 12 km.

(4) Ozone profiles during El Niño or La Niña events were analysed with no conclusive results.

Seasonal and Temporal Ozone Changes over the South African Highveld

(1) Overall low ozone concentrations during autumn and higher ozone concentrations during spring were observed throughout the troposphere.

(2) Summer ozone profiles exhibited higher ozone concentrations than winter ozone profiles up to 9 km. However, at 12 km winter ozone profiles had displayed higher ozone concentrations.

(3) Winter ozone profiles displayed a strong ozone gradient between 10 and 12 km. The conclusion was that there was a possibility of stratospheric ozone injection into the upper levels of the troposphere.

(4) Tropopause height over the South African Highveld follows an annual cycle experiencing a minimum in winter and a maximum in summer with an average of ~15.8 km.

(5) Tropospheric ozone profiles with tropopause height situated at lower altitudes below the average value had higher ozone concentrations in the upper levels of the troposphere than ozone profiles with tropopause height situated at higher altitudes.

(6) Since low tropopause height normally occurs during winter, the strong ozone gradient observed during winter was due to lowering of the tropopause height. Cut-off low systems are normally observed in winter and have the highest frequency of occurrence in April and September (Taljaard, 1985). These systems can trigger the formation of tropopause folds, lowering the tropopause and ozone-rich air is transferred from the lower levels of the stratosphere into the upper levels of the troposphere.

(7) As shown in Chapters 3 and 4, the spring ozone maximum was linked to biomass-burning emissions being transported from other African countries reaching the South African Highveld at 750 hPa.

(8) Although the spring ozone profiles exhibited a strong gradient at 12 km, there was not enough evidence to support that some of the ozone in the troposphere could have originated from the stratosphere. Therefore, it was concluded that the spring maximum was of tropospheric origin or being transported from polluted areas.

(9) Tropospheric ozone over the South African Highveld has increased since the 1970. Data collected during the SAFARI-92 and SAFARI-2000 field campaigns had shown that ozone concentrations have increased only in the lower levels. From 10 to 12 km, there was a decrease in tropospheric ozone concentrations over the South African Highveld region.

(10) The increase in tropospheric ozone over the period 1999-2003 is due to predominance of easterly waves during this period (table 4.1). The easterly waves were found to be associated with high tropospheric ozone concentrations.

(11) Tropospheric ozone over the South African Highveld was being produced photochemically in the troposphere rather than being transported from the stratosphere.

(12) Due to the increase of trace gases and ozone precursor gases over the South African Highveld region, tropospheric ozone had resulted from photochemical reactions. Therefore, photochemical production of tropospheric ozone has become a significant source of ozone in the troposphere of the South African Highveld.

The classification of ozone profiles into different dominant structures over the South African Highveld is in agreement with previous studies (Diab *et al*., 2003; Diab *et al*., 2004) in which six and four groups of ozone profiles were identified for the Johannesburg and Irene areas respectively. Four of the six structures obtained in this study are similar to ozone structures derived from those studies (Diab *et al*., 2003; Diab *et al*., 2004). Tropospheric ozone over this region is under the influence of several factors including emissions from Johannesburg and Pretoria industries, and biomass burning as highlighted previously. The increase of tropospheric ozone over the South African Highveld is due to the increase of population and industrial sources of ozone precursor gases and trace gases which eventually change the climate (Zunckel, 1992; Diab *et al*., 2004).

REFERENCES

Ancellet, G., Beekmann, M. and Papayannis A., 1994: Impact of a cut-off low development on downward transport of ozone in the troposphere, *Journal of Geophysical Research*, 99 (D2), 3451-3468.

Appenzeller, C. and Davies, H.C., 1992: Structure of stratospheric intrusions into the troposphere, *Nature*, 385, 570-572.

Bamber, D.J., Healey, P.G.W., Jones, B.M.R., Penkett, S.A., Tuck, A.F. and Vaughan, G., 1984: Vertical profiles of tropospheric gases: chemical consequences of stratospheric intrusions, *Atmospheric Environment,* 18 (9), 1759-1766.

Barsby, J. and Diab, R.D., 1995: Total ozone and synoptic weather relationship over southern Africa and surrounding oceans, *Journal of Geophysical Research*, 100 (D2), 3023-3032.

Bethan, S., Vaughan, G. and Reid S.J., 1996: A comparison of ozone and thermal tropopause heights and the impact of tropopause definition on quantifying the ozone content of the troposphere, *Quarterly Journal of the Royal Meteorological Society*, 122, 929-944.

Black, F.M., 1989: Motor vehicles as a source of compounds important to tropospheric and stratospheric ozone, *Studies in Environmental Science*, 35, 85-109.

Boyd, I.S., Bodeker, G.E., Connor, B.J., Swart, D.P.J. and Brinksma, E.J., 1998: An assessment of ECC ozonesondes operated using 1 % and 0.5 % KI cathode solutions at Lauder, New Zealand, *Geophysical Research Letters,* 25 (13), 2409-2412.

Brewer, A.W. and Milford, J.R., 1960: The Oxford-Kew ozone sonde, *Procedures of the Royal Society of London*, 256 A, 470-495.

Bruintjies, R.T., Archer, C.B. and Zunckel, M., 1990: Daily and seasonal variations in the atmospheric ozone over Pretoria between April 1964 and February 1972, *South African Journal of Science*, 86, 419-425.

Collins, W.J., Derwent, R.G., Johnson, C.E. and Stevenson, D.S., 2000: The impact of human activities on the photochemical production and destruction of tropospheric ozone, *Quarterly Journal of the Royal Meteorological Society*, 126, 1925-1951.

Collins, W.J., Derwent, R.G., Garnier, B., Johnson, C.E. and Sanderson, M.G., 2003: Effect of stratosphere-troposphere exchange on the future tropospheric ozone trend, *Journal of Geophysical Research*, 108 (D12), 8528, doi: 10.1029/2002JD002617.

Cosijn, C. and Tyson, P.D., 1996: Stable discontinuities in the atmosphere over South Africa, *South African Journal of Science*, 92, 381-386.

Crane, R.G. and Hewitson, B.C., 2003: Clustering and upscaling of station precipitation records to regional patterns using self-organizing maps (SOMs), *Climate Research*, 25, 95-107.

Cristofanelli, P., Bonasoni, P., Collins, W., Feichter, J., Forster, C., James, P., Kentarchos, A., Kubik, P.W., Land, C., Meloen, J., Roelofs, G.J., Siegmund, P., Sprenger, M., Schnabel, C., Stohl, A., Tobler, L., Tositti, L., Trickl, T. and Zanis, P., 2003: Stratosphere-to-troposphere transport: A model and method evaluation, *Journal of Geophysical Research*, 108 (D12), 8525, doi: 10.1029/2002JD002600.

Crutzen, P.J. and Zimmermann, P.H., 1991: The changing photochemistry of the troposphere, *Tellus*, 43AB, 136-151.

Crutzen, P.J., Lawrence, M.G. and Poschl, U., 1999: On the background photochemistry of tropospheric ozone, *Tellus*, 51A-B, 123-146.

D'Abreton, P.C. and Tyson, P.D., 1996: Three-dimensional Kinematic trajectory modelling of water vapour transport over southern Africa, *Water South Africa*, 22 (4), 297-306.

D'Abreton, P.C., 1996: Lagrangian kinematic and isentropic trajectory models for aerosol and trace gas transport studies in southern Africa, *South African Journal of Science*, 92, 157-160.

Danielsen, E.F., 1968: Stratospheric-Tropospheric Exchange Based on Radioactivity, Ozone and Potential Vorticity, *Journal of the Atmospheric Science*, 25, 502-518.

Davies, T.D., Kelly, P.M., Low, P.S. and Pierce, C.E., 1992: Surface Ozone Concentrations in Europe: Links with Regional-Scale Atmospheric Circulation, *Journal of Geophysical Research*, 97 (D9), 9819-9832.

De Backer, H., De Muer, D. and De Sadelaer, G., 1998: Comparison of ozone profiles obtained with Brewer-Mast and Z-ECC sensors during simultaneous ascents, *Journal Geophysical Research*, 103 (D16), 19641-19648.

Diab, R.D., Thompson, A.M., Zunckel, M., Coetzee, G.J.R., Combrink, J., Bodeker, G.E., Fishman, J., Sokolic, F., McNamara, D.P., Archer, C.B. and Nganga, D., 1996: Vertical ozone distribution over southern Africa and adjacent oceans during SAFARI-92, *Journal of Geophysical Research*, 101 (D19), 23823-23833.

Diab, R.D., Raghunandan, A., Thompson, A.M. and Thouret, V., 2003: Classification of tropospheric ozone profiles over Johannesburg based on MOZAIC aircraft data, *Atmospheric Chemistry and Physics*, 3, 713-723.

Diab, R.D., Thompson, A.M., Mari, K., Ramsay, L. and Coetzee G.J.R., 2004: Tropospheric ozone climatology over Irene, South Africa, from 1990-1994 and 1998-2002, *Journal of Geophysical Research*, 109, D20301, doi: 10.1029/2004JD004793.

Fishman, J. and Crutzen, P.J., 1978: The origin of ozone in the troposphere, *Nature*, 274, 855-858.

Fishman, J., Solomon, S. and Crutzen, P.J., 1979: Observational and theoretical evidence in support of significant in-situ photochemical sources of tropospheric ozone, *Tellus,* 31, 432-446.

Fishman, J., Fakhruzzaman, K., Cros, B and Nganga, D., 1991: Identification of widespread pollution in the southern hemisphere deduced from satellite analyses, *Science*, 252, 1693-1696.

Fishman, J., Brackett, V.G. and Fakhruzzaman, K., 1992: Distribution of tropospheric ozone in the tropics from satellite and ozonesonde measurements, *Journal Atmospheric and Terrestrial Physics*, 54 (5), 589-597.

Freiman, M.T., Jury, M.J. and Medcalf, S., 2002: The state of the atmosphere over South Africa during the Southern African Regional Science Initiative (SAFARI 2000), *South African Journal of Science*, 98, 91-96.

Garstang, M., Tyson, P.D., Swap, R., Edwards, M., Kallberg, P. and Lindesay, J.A., 1996: Horizontal and vertical transport of air over southern Africa, *Journal Geophysical Research*, 101 (D19), 23721-23736.

Germano, T., 1999: Self Organizing Maps, http://davis.wpi.edu/~matt/courses/soms/ Website accessed: 12 March 2006.

Gettelman, A. and Foster, P.M.de F., 2002: A climatology of the tropical tropopause layer, *Journal of the Meteorological Society of Japan*, 80 (4B), 911-924.

Halenka, T., Laštovička, J. and Radicella, S., 1994: The effect of the passage of cold fronts on the vertical distribution of ozone at the CHMI observatory at Prague-Libuš, *Quarterly Journal of the Royal Meteorological Society*, 120, 1415-1423.

Harris, G.W., Wienhold, F.G. and Zenker, T., 1996: Airborne observations of strong biogenic No_x emissions from the Namibian Savanna at the end of the dry season, *Journal of Geophysical Research,* 101 (D19), 23707-23711.

Hoerling, M.P., Schaack, T.K. and Lenzen, A.J., 1991: Global objective tropopause analysis, *Monthly Weather Review*, 119, 1816-1831.

Hoinka, K.P., 1998: Statistics of the global tropopause pressure, *Monthly Weather Review*, 126, 3303-3325.

Hoinka, K.P., 1999: Temperature, humidity, and wind at the global tropopause, *Monthly Weather Review*, 127, 2248-2265.

Holton, J.R., Haynes, P.H., McIntyre, E.M., Douglass, A.R., Rood, R.B and Pfister, L., 1995: Stratosphere-troposphere exchange, *Review of Geophysics*, 33, 403-439.

James, P., Stohl, A., Forster, C., Eckhardt, S., Seibert, P. and Frank, A., 2003a: A 15-year climatology of stratosphere-troposphere exchange with a Lagrangian particle dispersion model: Mean climate and seasonal variability, *Journal of Geophysical Research*, 108 (D12), 8522, doi: 10.1029/2002JD002639.

James, P., Stohl, A., Forster, C. and Eckhardt, S., 2003b: A 15-year climatology of stratosphere-troposphere exchange with a Lagrangian particle dispersion model: Methodology and validation, *Journal of Geophysical Research*, 108 (D12), 8519, doi: 10.1029/2002JD002637.

Johnson, B.J., Oltmans, S.J., Vömel, H., Smit, H.G.J., Deshler, T. and Kröger C., 2002: Electrochemical Concentration Cell (ECC) ozonesonde pump efficiency measurements and tests on the sensitivity to ozone of buffered and unbuffered ECC sensor cathode solutions, *Journal of Geophysical Research*, 107 (D19), 4393, doi: 10.1029/2001JD000557.

Junge, C.E., 1962: Global ozone budget and exchange between stratosphere and troposphere, *Tellus*, XIV, 363-377.

Kentarchos, A.S. and Roelofs, G.J., 2003: A model study of stratospheric ozone in the troposphere and its contribution to tropospheric OH formation, *Journal of Geophysical Research*, 108 (D12), 8517, doi: 10.1029.2002JD002598.

Kiladis, G.N., Straub, K.H., Reid, G.C. and Gage, K.S., 2001: Aspects of inter-annual and intra-seasonal variability of the tropopause and lower stratosphere, *Quarterly Journal of the Royal Meteorological Society*, 127, 1961-1983.

Kim, K., Jung, E., Campistron, B. and Heo, B., 2001: A physical examination of tropopause height and stratospheric air intrusion, A case study, *Journal of the Meteorological Society of Japan*, 79 (5), 1093-1103.

Kirkman, G.A., Piketh, S.J., Andreae, M.O., Annegarn, H.J. and Helas, G., 2000: Distribution of aerosols, ozone and carbon monoxide over southern Africa, *South African Journal of Science*, 96, 423-431.

Kleinman, L.I., 2005: The dependence of tropospheric ozone production rate on ozone precursors, *Atmospheric Environment*, 39, 575-586.

Komhyr, W.D., 1964: A carbon–iodide (CI) ozone sensor for atmospheric soundings, *Proceedings of the Atmospheric Ozone Symposium*, Albuquerque, 1964.

Komhyr, W.D. and Harris, T.B., 1971: Development of an ECC Ozonesonde, *NOAA Technical Report* ERL 200-APCL 18, U.S. Department of Commerce, Boulder, Colorado, 54 pp.

Komhyr, W.D., 1986: Operations handbook-Ozone measurements to 40 km altitude with model 4A-Electrochemical Concentration Cell (ECC) ozonesondes (used with 1680 MHz radiosondes), *NOAA Technical Memorandum* ERL-ARL-149, Boulder, Colorado., 49 pp.

Le Canut, P., Andreae, M.O., Harris, G.W., Wienhold, F.G. and Zenker, T., 1996: Airborne studies of emissions from savanna fires in southern Africa: Aerosol emission measured with laser optical particle counter, *Journal of Geophysical Research*, 101 (D19), 23615-23630.

Lacaux, J.P., Delmas, R., Jambert, C. and Kuhlbusch, T.A.J., 1996: NO_x emissions from African savanna fires, *Journal of Geophysical Research*, 101 (D19), 23585-23595.

Lelieveld, J. and Dentener F.J., 2000: What controls tropospheric ozone? *Journal of Geophysical Research*, 105 (D3), 3531-3551.

Leung, Y.K., Chang, W.L. and Chan, Y.W., 2004: Some characteristics of ozone profiles above Hong Kong, *Meteorology and Atmospheric Physics*, 87, 279-291.

Levy, H., 1972: Photochemistry of the lower troposphere, *Planet Space Science*, 20, 919-935.

Levy, H., 1973: Photochemistry of minor constituents in the troposphere, *Planet Space Science*, 21, 575-591.

Lindesay, J.A., Andreae, M.O., Goldammer, J.C., Harris, G., Annegarn, H.J., Garstang, M., Scholes, R.J. and van Wilgen, B.W., 1996: International Geosphere-Biosphere Programme/International Global Atmospheric Chemistry SAFARI-92 field experiment: Background and overview, *Journal of Geophysical Research,* 101 (D19), 23, 521-530.

Lindesay, J.A., 1997: *African savanna fires, global atmospheric chemistry and the southern tropical Atlantic regional experiment: Fire in southern African savannas ecological and atmospheric perspectives*, Witwatersrand University Press, Johannesburg.

Liu, S.C., Trainer, M., Fehsenfeld, F.C., Parris, D.D., Williams, E.J., Fahey, D.W., Hübler, G. and Murphy, P.C., 1987: Ozone Production in the rural troposphere and the implications for the regional and global ozone distributions, *Journal of Geophysical Research,* 921 (D4), 4191-4207.

Marsland, S., 2003: *Novelty detection in learning systems*, Division of Imaging Science and Biomedical Engineering, University of Manchester, UV, available on, http://www.icsi.berkeley.edu.~jagota/NCS, volume 3.

Marufu, L., Dentener, F., Lelieveld, J., Andreae, M.O. and Helas, G., 2000: Photochemistry of African troposphere: Influence of biomass-burning emissions, *Journal Geophysical Research*, 105 (D11), 14513-14530.

Merrill, J.T. and Moody, J.L., 1996: Synoptic meteorology and transport during the North Atlantic Regional Experiment (NARE) intensive: Overview, *Journal of Geophysical Research*, 101 (D22), 28903-28921.

Monks, P.S., 2000: A review of the observations and origins of the spring ozone maximum, *Atmospheric Environment,* 34, 3545-3561.

Newchurch, M.J., Ayoub, M.A., Oltmans, S., Johnson, B. and Schmidlin, F.J., 2003: Vertical distribution of ozone at four sites in the United States, *Journal of Geophysical Research*, 108 (D1), 4031, doi: 10.1029/2002JD002059.

O'Hare, A., 1997: The synoptic control of tropospheric ozone pollution during 24-28 June 1994, *Weather*, 52, 378-382.

Otter, L.B., Marufu, L. and Scholes, M.C., 2001: Biogenic, biomass and biofuel sources of trace gases in southern Africa, *South African Journal Science*, 97, 131-138.

Piketh, S.J., 2000: *Transport of aerosols and trace gases over southern Africa*, Unpublished PhD Thesis submitted to the University of the Witwatersrand, Johannesburg.

Piketh, S.J., and Walton, N.M., 2004: Characteristics of atmospheric transport of air pollution for Africa, *The handbook of environmental chemistry*, volume 4, part G, 173-195.

Preston-Whyte, R.A. and Tyson, P.D., 1988: The atmosphere and weather of southern Africa, Oxford University Press, Cape Town.

Preston-Whyte, R.A. and Tyson, P.D., 2000: The weather and climate of southern Africa, second edition, Oxford University Press, Cape Town.

Price, J. and Vaughan, G., 1993: The potential for stratosphere-troposphere exchange in cut-off low systems, *Quarterly Journal of the Royal Meteorological Society*, 119, 343-365.

Regener, V.H., 1960: On a sensitive method for the recording of atmospheric ozone, *Journal of Geophysical Research*, 63, 3975-3977.

Reid, G.C. and Gage, K.S., 1981: An annual variation in height of the tropical tropopause, *Journal of the Atmospheric Sciences*, 38, 1928-1937.

Scholes, R.J., Kendall, J. and Justice, C.O., 1996: The quantity of biomass burned in southern Africa, *Journal of Geophysical Research*, 101 (D19), 23667-23676.

Seo, K. and Bowman, K.P., 2001: A climatology of isentropic cross-tropopause exchange, *Journal of Geophysical Research*, 106 (D22), 28159-28172.

Shea, R.W., Shea, B.W. and Kauffman, J.B., 1996: Fuel biomass and combustion factors associated with fires in savanna ecosystems of South Africa and Zambia, *Journal of Geophysical Research*, 101 (D19), 23551-23568.

Staehelin, J., Harris, N.R.P., Appenzeller, C. and Eberhard, J., 1999: Ozone trends: A review, *Reviews of Geophysics*, 39, 231-290.

Steinbrecht, W., Claude, H., Köhler, U. and Hoinka, K.P., 1998: Correlation between tropopause height and total ozone: Implications for long term changes, *Journal of Geophysical Research*, 103 (D15), 19183-19192.

Stohl, A., Bonasoni, P., Cristofanelli, P., Collins, W., Feichter, J., Frank, A., Forster, C., Gerasopoulos, E., Gäggeler, H., James, P., Kentarchos, T., Kromp-Kolb, H., Krüger, B., Land, C., Meloen, J., Papayannis, A., Priller, A., Seibert, P., Sprenger, M., Roelofs, G.J., Scheel, H.E., Schnabel, C., Siegmund, P., Tobler, T., Trickl, T., Wernli, H., Wirth, V., Zanies, P. and Zerefos, C., 2003: Stratosphere-troposphere exchange: A review, and what we have learned from STACCATO, *Journal of Geophysical Research*, 108 (D12), 8516, doi: 10.1029/2002JD002490.

Swap, R.J., Annegarn, H.J., Suttles, J.T., Haywood, J., Helmlinger, M.C., Hely, C., Hobbs, P.V., Holben, B.N., Ji, J., King, M.D., Landmann, T., Maenhaut, W., Otter, L., Pak, B., Piketh, S.J., Platnick, S., Privette, J., Roy, D., Thompson, A.M., Ward, D., and Yokelson, R., 2002: The Southern African Regional Science Initiative (SAFARI 2000): overview of the dry season field campaign, *South African Journal of Science*, 98, 125-130.

Taljaard J.J., 1985: Cut-off-lows in South Africa region, South African Weather Bureau, Technical paper, 14, 153pp.

Tennant, W.J. and Hewitson, B.C., 2002: Intra-seasonal rainfall characteristics and their importance to the seasonal prediction problem, *International Journal of Climatology*, 22, 1033-1048.

Tennant, W., 2003: An assessment of intraseasonal variability from 13-yearr GCM simulation, *Monthly Weather Review*, 31, 1975-1991.

Tennant, W.J. and Reason, C.J.C., 2005: Associations between the global energy cycle and regional rainfall in South Africa and Southwest Australia, *Journal of Climate*, 18, 3032-3047.

Thompson, A.M., Diab, R.D., Bodeker, G.E., Zunckel, M., Coetzee, G.J.R., Archer, C.B., McNamara, D.P., Pickering, K.E., Combrink, J., Fishman, J. and Nganga D., 1996a: Ozone over southern Africa during SAFARI-92/TRACE A, *Journal of Geophysical Research*, 101 (D19), 23793-23807.

Thompson, A.M., Pickering, K.E., McNamara, D.P., Schoeberl, M.R., Hudson, R.D., Kim, J.H., Browell, E.V., Kirchhoff, V.W.J.H. and Nganga, D., 1996b: Where did tropospheric ozone over Southern Africa and the tropical Atlantic come from in October 1992? Insights from TOMS, GTE TRACE A, and SAFARI 1992, *Journal of Geophysical Research*, 101 (D19), 24251-24278.

Thompson, A.M., Tao, W., Pickering, K.E., Scala, J.R. and Simpson, J., 1997: Tropical deep convection and ozone formation, *Bulletin of the American Meteorological Society*, 78, 1043-1054.

Thompson, A.M., Hudson, R.D., Frolov, A.D., Witte, J.C., and Kucsera, T.L., 2001: Tropospheric ozone from space: Tracking pollution with the TOMS (Total Ozone Mapping Spectrometer), Geoscience and Remote Sensing Symposium, IGARSS apos;01. IEEE 2001 International, Volume 3, Issue, 2001, 1035-1037.

Thompson, A.M., Witte, J.C., McPeters, R.D., Oltmans, S.J., Schmidlin, F.J., Logan, J.A., Fujiwara, M., Kirchhoff, V.W.J.H., Posny, F., Coetzee, G.J.R., Hoegger, B., Kawakami, S., Ogawa, T., Johnson, B.J., Vömel, H. and Labow, G., 2003: Southern Hemisphere Additional Ozonesonde, 1998-2000 tropical climatology: Comparison with Total Ozone Mapping Spectrometer (TOMS) and ground-based measurements, *Journal of Geophysical Research*, 108 (D2), 8238, doi: 10.1029/2001JD000967.

Thouret, V., Cho, Y.N., Newell, R.E., Marenco, A. and Smit, G.J., 2000: General characteristics of tropospheric trace constituent layers observed in the MOZAIC program, *Journal of Geophysical Research*, 105, 17379-17392.

Tyson, P.D., Garstang, M., Swap, R., Kalleberg, P. and Edwards, M., 1996: An air transport climatology for subtropical southern Africa, *International Journal of Climatology*, 16, 265-291.

Tyson, P.D., Garstang, M., Thompson, A.M., D'Abreton, P., Diab, R.D. and Browell, E.V., 1997: Atmospheric transport and photochemistry of ozone over central southern Africa during the Southern Africa Fire-Atmosphere Research Initiative, *Journal of Geophysical Research*, 102 (D9), 10623-10635.

Vaisala, Oy., 1991: *Ozonesonde user's guide*, Edition OES-T05331-1.3, 93pp.

Varotsos, C., Cartalis, C., Vlamakis, A., Tzanis, C. and Keramitsoglou, I., 2004: The long-term coupling between column ozone and tropopause properties, *Journal of Climate*, 17, 3843-3854.

Ward, D.E., Hao, W.M., Susott, R.A., Babbitt, R.E., Shea, R.W., Kauffman, J.B. and Justice, C.O., 1996: Effect of fuel composition on combustion efficiency and emission factors for African savanna ecosystems, *Journal of Geophysical Research*, 101 (D19), 23569-23576.

Watson, C.E., Fishman, J. and Reichle Jr, H.G., 1990: The significance of biomass burning as a source of carbon monoxide and ozone in the southern hemisphere tropics: A satellite analysis, *Journal of Geophysical Research*, 95 (D10), 16443-16450.

WMO (World Meteorological Organization), 1986: *Atmospheric ozone*, WMO report, No. 16.

WMO (World Meteorological Organization), 1995: *The changing ozone layer*, written by Bojkov, R.D, and joint publication with the United Nations Environment Programme (UNEP).

WMO (World Meteorological Organization), 1998: *Jülich Ozone Sonde Intercomparison (JOSIE)*, edited by Smit, H. and Kley, D., report No. 130, WMO Global Ozone Research and Monitoring Project, Rep. No. TD926, Geneva.

Zängl, G. and Hoinka, K.P., 2000: The tropopause in the polar regions, *Journal of Climate*, 14, 3117-3139.

Zhang, J., and Rao, S.T., 1999: The role of vertical mixing in the temporal evolution of ground-level ozone concentrations, *Journal of Applied Meteorology*, 38, 1674-1691.

Zunckel, M., 1992: *Ozone profile changes above Pretoria, 1965 to 1991*, Unpublished MSc dissertation submitted to the University of Pretoria, Pretoria.

Zunckel, M., Robertson, L., Tyson, P.D. and Rodhe, H., 2000: Modelled transport and deposition of sulphur over southern Africa, *Atmospheric Environment*, 34, 2797-2808.